Microstructural Evolution and Physical Properties of Polymer-Modified Mortars

Inauguraldissertation

der Philosophisch-naturwissenschaftlichen Fakultät

der Universität Bern

vorgelegt von

Andreas Jenni

von Escholzmatt (LU)

Leiter der Arbeit:

Dr. M. Herwegh

Institut für Geologie der Universität Bern

Microstructural Evolution and Physical Properties of Polymer-Modified Mortars

Inauguraldissertation

der Philosophisch-naturwissenschaftlichen Fakultät

der Universität Bern

vorgelegt von

Andreas Jenni

von Escholzmatt (LU)

Leiter der Arbeit:

Dr. M. Herwegh

Institut für Geologie der Universität Bern

Von der Philosophisch-naturwissenschaftlichen Fakultät angenommen.

Bern, 27.03.2003 Der Dekan:

Prof. Dr. G. Jäger

Table of Contents

Abstract

Polymer-modified cementitious materials provide the base for building materials commonly used on modern construction sites. By adding polymers, the properties of cementitious materials can be extended to suit a variety of applications. With respect to adhesion properties, for example, the first patent of latex-modified hydraulic cement systems was issued in 1924 (Lefebure 1924). In the field of tile adhesives, latex-modification allowed thin-bed application, a technique that is still standard because of its economic advantages with respect to application time and resource costs. Before invention of redispersible powders, the appropriate latex was only available in the form of dispersions. Mortar mixing was an important issue, which when improperly performed, often caused cases of damage at construction sites. The development of latex in the form of redispersible powders drastically reduced this problem, because it allowed the production of one-component systems or so-called “dry mortars”, which only require the appropriate amount of water to be added before application.

Mortar properties were continuously improved by optimising the formulation or enhancing the system's components. Empirical approaches dominated, in which numerous formulations were compared with each other, in terms of physical properties of the resultant mortars. To further improve these properties at the present stage, an extended understanding of the mechanisms active during mortar evolution is required. Many of these mechanisms leave characteristic marks on the mortar microstructures, which, once recognised and related to the corresponding mechanism, can be linked with the physical properties. Therefore, the microstructure represents a major key to an improved understanding of the highly complex system of polymer-modified mortars.

The cementitious, mineralic microstructures can be investigated by methods commonly applied in earth and material sciences. In contrast, organic compounds like polymers can form delicate and fragile structures requiring specific techniques that originated in the field of organic chemistry and biology. Therefore, the investigation of tile adhesive requires an interdisciplinary approach, in which methods from different fields of research are adapted and combined.

As is common in applied research, the investigation of polymer-modified mortars is a tightrope walk between the complex, commercial system and model systems usually based on crude simplifications. The combination of both approaches might result in large forward steps in understanding, and new insights.

The present study on polymer-modified, cementitious mortars tries to incorporate the previously mentioned requirements and is organised in the following manner: (a) methods of quantitative investigations, (b) influence of polymers on microstructure and physical properties, (c) changes of microstructures and physical properties during wet storage.

a) The first chapter describes the new methods developed to quantitatively investigate microstructures in polymer-modified mortars. A combination of digital light, fluorescence and electron microscopy allowed the visualisation of different mortar components such as specific polymer components, air voids, cement phases, and filler minerals. In a second step, their occurrence and spatial distribution was quantified by image analysis requiring appropriate program routines, whose use and functionality is explained. To demonstrate the power of the new quantitative approach in the field of polymer-modified tile adhesives, a selected mortar formulation was analysed as an example. The results show that the mortar fractionated during application and hardening, inducing a variety of phase enrichments or depletions. The occurrence of these microstructural heterogeneities suggests the major influence that the microstructure has on the physical properties of the mortar system.

b) In the second chapter, the microstructural evolution of the mortar and the mechanisms involved were investigated by using the methodology developed above. It is shown that water flux, induced by evaporation

and capillary forces of the porous substrate, played the most important role in mortar fractionation. It transported cellulose ether, polyvinyl alcohol, and cement ions to the mortar interfaces, where they became accumulated. In contrast, latex components did not migrate and remained homogeneously distributed within the microstructure. Combination of quantitative with qualitative investigations allowed a reconstruction of the mechanisms forming the microstructure during the different mortar stages. By correlating microstructural observations with physical properties (e.g., adhesive strength), skinning on the mortar surface of the applied fresh paste was found to decrease adhesion strength to the tile. As a consequence, it is the mortar-tile interface that dominates the properties of the entire hardened substrate-mortar-tile system.

c) In chapter three the influence of wet storage on the microstructure and its physical properties are investigated. Wet storage represents an important test criteria on the durability of polymer-modified systems exposed to wet conditions in case of outdoor or bath room applications. Tests on individual polymer structures revealed that cellulose ether and polyvinyl alcohol redissolved in the pore water, whereas latices were water-resistant. Consequently, latex distributions in the mortar measured before and after wet storage were identical because latex remained immobile, but cellulose ether and polyvinyl alcohol distributions changed. By combining these observations with microstructural investigations of the failure surfaces, pore size, shrinkage and physical test data, we were able to show that changes in the mortar volume and reinitiated cement hydration caused a decrease of the mechanical properties during wet storage. Although they remained immobile, the latex films also weakened due to water uptake and swelling, which was shown to be a reversible mechanism.

The appendix A includes non-published studies in a short and descriptive form. The corresponding database is available upon request after consultation with the author and Elotex AG. Appendix B includes extended abstracts of the given talks.

Zusammenfassung

Polymer-modifizierte, zementäre Baustoffe kommen heutzutage auf jeder grösseren Baustelle zum Einsatz. Durch Zugabe von Polymeren können die Eigenschaften von zementären System erweitert und somit an verschiedenste Anwendungen angepasst werden. Das erste Patent für ein Zementsystem, dessen Vergütung durch Latex eine Verbesserung der Adhäsionseigenschaften bewirkte, wurde 1924 ausgestellt (Lefebure 1924). Im Bereich der Fliesenkleber konnte durch Latexvergütung das Dünnbettverfahren eingeführt werden, das sich bis heute dank den damit verbundenen Zeit- und Geldeinsparungen durchsetzt. Vor der Erfindung des Dispersionspulvers war der entsprechende Latex nur in Form einer Dispersion erhältlich, was das Mörtelmischen auf der Baustelle komplizierte und deshalb oft fehlerhafte Anwendung inklusive der daraus resultierenden Schadensfälle nach sich zog. Die Entwicklung von Latex-Dispersionspulvern ermöglichte den Verkauf von Einkomponenten-Systemen, sogenannten Trockenmörteln, denen auf der Baustelle nur noch Wasser zugegeben werden muss, was die Anwendung deutlich erleichtert.

Durch Optimierung der Mörtelformulierung oder Verbesserung der einzelnen Komponenten wurden seither die Mörteleigenschaften kontinuierlich verbessert. Dabei überwiegte die empirische Forschung, bei der die physikalischen Endeigenschaften von Mörteln mit verschiedenen Formulierungen miteinander verglichen wurden. Heutzutage erfordern weitere Produkteverbesserungen ein vollumfängliches Verständnis der Mechanismen, die während der Mörtelevolution ablaufen. Viele dieser Mechanismen hinterlassen ihre Spuren in Form von Mikrostrukturen im Mörtel, die, einmal erkannt und den Mechanismen zugeordnet, mit den physikalischen Mörteleigenschaften verbunden werden können. Somit stellen Mikrostrukturen den Schlüssel zu einem umfänglichen Verständnis der polymervergüteten Mörtel dar.

Das Zementgefüge kann mit Methoden untersucht werden, die in Erd- und Materialwissenschaften gebräuchlich sind. Im Gegensatz dazu bilden Polymere instabile Gebilde, die anfällig auf verschiedenste Einwirkungen sind, und darum spezifisch angepasste analytische Methoden aus der organischen Chemie und Biologie erfordern. Zur Untersuchung von Fliesenklebern müssen also Methoden aus verschiedensten Forschungsbereichen kombiniert und allenfalls angepasst werden.

Die Erforschung von polymervergüteten Mörteln ist, wie in jeder angewandten Forschung, eine Gratwanderung zwischen dem komplexen realen System und Modellsystemen, die auf Vereinfachungen beruhen. Die Kombination beider Arbeitsweisen bringt uns am ehesten einen Schritt weiter im Verständnis dieser Systeme.

Die vorliegende Arbeit ist folgendermassen aufgebaut: (a) Quantitative Untersuchungsmethoden, (b) Einfluss von Polymeren auf Mikrogefüge und physikalische Eigenschaften, (c) Veränderung des Mikrogefüges und der physikalischen Eigenschaften während der Nasslagerung.

a) Das erste Kapitel beschreibt die neu entwickelten Methoden, die eine quantitative Charakterisierung des Mikrogefüges erlauben. Mittels digitaler Licht-, Fluoreszenz- und Elektronenmikroskopie konnten die verschiedenen Mörtelkomponenten wie die einzelnen Polymere, Luftporen, Zementphasen und Füllstoffe sichtbar gemacht werden. In einem zweiten Schritt wurden das Auftreten und die räumliche Verteilung dieser Phasen mittels Bildanalytik quantifiziert. Die dafür verwendeten, neu entwickelten Programmroutinen werden vorgestellt und erläutert. Eine Fallstudie, durchgeführt an einem ausgewählten Fliesenkleber, zeigt die Schlagkraft der entwickelten quantitativen Methoden auf. Die Resultate bezeugen eine Reihe von An- und Abreicherungen innerhalb des Mörtelgefüges, die auf Fraktionierung während seiner Evolution hindeuten. Das Auftreten solcher mikrostruktureller Heterogenitäten impliziert, dass das Mörtelgefüge massgeblich die physikalischen Eigenschaften des ganzen Systems beeinflusst.

b) Im zweiten Kapitel wurden die Evolution des Mörtelgefüges und die damit verbundenen Mechanismen mittels den zuvor vorgestellten Methoden untersucht. Es konnte gezeigt werden, dass Wasserströmungen im Mörtel, verursacht durch Verdunstung und Kapillarkräfte im Substrat, den Hauptantrieb der Fraktionierung darstellen. Sie transportieren Celluloseether, Polyvinylalkohol und Zementionen zu den Mörtelgrenzflächen hin, wo sie angereichert werden. Im Gegensatz dazu migrieren Latexpartikel nicht und bleiben homogen im Gefüge verteilt. Solche Erkenntnisse wurden mit Resultaten aus qualitativen Experimenten kombiniert, was die Rekonstruktion der Mechanismen, die während den verschiedenen Mörtelstadien das Mikrogefüge formen, erlaubte. Durch das Verknüpfen von Mikrogefüge und physikalischen Mörteleigenschaften konnte des Weiteren gezeigt werden, dass die Hautbildung auf der Oberfläche des frisch aufgetragenen Mörtels die Adhäsion zur Fliese hin deutlich verringert. Daraus folgt, dass die mechanisch schwache Grenzfläche zwischen Mörtel und Fliese die physikalischen Endeigenschaften des Substrat-Mörtel-Fliesen-Systems dominiert.

c) Kapitel drei behandelt den Einfluss der Nasslagerung auf das Mikrogefüge und auf die physikalischen Eigenschaften. Nasslagerung ist ein wichtiges Testkriterium der Beständigkeit von polymervergüteten Systemen, die häufig im Aussenbereich oder in Nasszellen im Einsatz stehen. Versuche an den einzelnen Polymeren zeigten, dass sich Celluloseether und Polyvinylalkohol in der Porenlösung des Mörtels auflösen. Im Gegensatz dazu ist Latex wasserbeständig. Dadurch erklärt sich, dass die Latexverteilungen im Mörtel vor und nach der Wasserlagerung identisch sind, die Latexphase also immobil ist. Die Verteilungen des mobilen Celluloseethers und Polyvinylalkohols aber ändern sich während der Nasslagerung. Durch Verknüpfung dieser Resultate mit Erkenntnissen aus Gefügeuntersuchungen an Haftzugbruchstellen, Schwund-, Poren- und Festigkeitsmessungen, konnte nachgewiesen werden, dass Volumenänderungen des Mörtels und wiederbeginnende Zementhydratation den Nasshaftabfall bewirken. Obwohl immobil, können die Latexfilme dieser Degradation nur beschränkt entgegenwirken: sie sind während der Nasslagerung einer reversiblen Schwächung unterworfen, bewirkt durch Wasseraufnahme und Quellen.

Der Appendix A beschreibt nicht publizierte Studien in Kurzform. Die entsprechenden Daten sind nach Absprache mit dem Autor und Elotex AG erhältlich. In Appendix B sind die erweiterten Vortragszusammenfassungen zusammengestellt, welche in den entsprechenden Begleitbänden der Kongresse enthalten sind.

Acknowledgements

First of all, I would like to thank my supervisors Marco Herwegh and Roger Zurbriggen for their professional support of the entire scientific work. We spent hours and hours discussing the complexity that lurks behind a simple ceramic tile in our bathrooms, whereby they passed their knowledge on to me. It was a great pleasure for me to work together with them.

Certainly, this was also the case for Lorenz Holzer, who initiated me into the environmental scanning electron microscopy. Thank you for the thrilling days we spent working with this tricky machine, and for all the other help you provided based on your experience in the cement business.

Thomas Aberle developed cellulose ether and polyvinyl alcohol staining, which provided the base for the method, and resulted in probably the most important findings of this study. Thank you very much for your perfect work.

The new methods used in this study required elaborate sample preparation techniques, which were developed and carried out carefully by Verena Jakob and Jürg Megert on dozens of samples prepared by Dominique Schaub. Their excellent work is gratefully acknowledged.

At any time, I was relieved to know that Adrian Pfiffner supported the whole project and I would like to thank him for his confidence in my work.

Karl Ramseyer always helped me with word and deed, which I appreciate.

I like to thank Robert Kölliker for giving me an understanding of polymer chemistry through many valuable discussions and for reviewing the manuscripts.

The cooperation with Elotex AG was very enriching and showed me, what science in "real life", outside of university, looks like. I was always cordially received by the whole Elotex staff and had valuable discussions, which are gratefully acknowledged.

Although my field of research was quite exotic for my colleagues at the Institute of Geological Sciences, they never made me feel like this. Special thanks are dedicated to Edwin Gnos and Thomas Burri, who explained to me the functions of the electron microprobe as far as possible. The excellent facilities and services provided by this institute are available because of many people working behind the curtain. Especially, I thank Ulrich Linden, Werner Zaugg, Barbara Grose, Ruth Mäder, Heidi Haas, Adrian Liechti, and Hanspeter Bärtschi.

I would also like to thank Frank Winnefeld for his help with the Raman spectroscopy experiments, Beatrice Frey for showing me the transmission electron microscope, Bernard Grobéty for the x-ray powder diffraction analysis, Philipp Steinmann for the water analysis, Hans Imboden for entrusting "his" laser scanning microscope to me and Monique Y. Hobbs for final language corrections.

Financial support from Elotex AG and KTI for project Nr. 4551.1 KTS is gratefully acknowledged. The electron microprobe used in this study was financed by the Swiss National Science Foundation (Credit 21-26579.89).

I am very grateful to my parents, who always supported whatever I did in my life.

As man cannot live on science, mountains, and food alone, I thank Gisela Michel for everything she gave to me, and, hopefully, always will.

Chapter 1

Quantitative Microstructure Analysis of Polymer-Modified Mortars

A. Jenni, M. Herwegh, R. Zurbriggen, T. Aberle, L. Holzer

(submitted to:

Journal of Microscopy)

Abstract

Digital light, fluorescence and electron microscopy in combination with wavelength dispersive spectroscopy were used to visualise individual polymers, air voids, cement phases, and filler minerals in a polymer-modified cementitious tile adhesive. In order to investigate the evolution and processes involved in formation of the mortar microstructure, quantifications of the phase distribution in the mortar were performed including phase-specific imaging and digital image analysis. The required sample preparation techniques and imaging related topics are discussed.

In form of a case study, the different techniques are applied to obtain a quantitative characterisation of a specific mortar mixture. The results indicate that the mortar fractionates during different stages ranging from the early fresh mortar till the final hardened mortar stage. This induces process-dependent enrichments of the phases at specific locations in the mortar. In sum, the presented approach proved to provide important information for a comprehensive understanding of the functionality of polymer-modified mortars.

1.1 Introduction

Polymer modified mortars exist in a broad variety of applications, e.g., tile adhesives. They are commercially available as premixed dry compounds, so-called dry mortars, which can basically be grouped into binders, fillers and additives (see Table 1). Typical additives are cellulose ether (CE) and redispersible powder (RP). CE acts as thickener and air entraining agent providing appropriate fresh mortar properties. RP is a polymeric powder typically gained by spray-drying of a polyvinyl alcohol (PVA) containing latex emulsion. The purpose of RP is the improvement of fresh mortar properties and increase in flexibility and strength of the hardened mortar. Ordinary Portland cement (OPC) is the most typical mineral binder, which is added in the amount of 20-40 wt.%. 60-80 wt.% of the mortar are composed of filler materials, typically siliceous and/or carbonate sand and finer grained fractions (<100 µm).

At the construction site dry mortar has to be mixed with a pre-defined amount of water to gain a ready-to-use fresh mortar resulting in a creamy and homogeneous mass with a considerable amount of entrained air (15-30 vol.%). This so-called fresh mortar is applied by a trowel onto the substrate (wall or floor) and then covered by the tiles. Curing of the mortar during the following days and weeks is strongly dependent on the availability and migration of the added water involving three main processes (Table 2): (1) cement hydration, (2) drying, and (3) polymer film formation.

1) Water reacts with anhydrous clinker phases and forms various cement hydrates. With the growth of these hydrates the mineral grains (clinker and fillers) are cemented together (Taylor 1997).
2) Pore water which is not consumed by the hydration of the cement evaporates and leaves capillary pores (Taylor 1997).
3) Polymer film formation occurs which depends primarily on loss of water and curing time (Routh & Russel 1999).

The finally cured mortar consists of mineral grains (cement clinker and fillers) which are bound by the interstitial cement hydrates and polymer films. The bulk porosity of a cured mortar is between 30 and 50 vol.% (Table 2). Despite of the low polymer level, the application performance is strongly dependent on the functionality of the polymers and their distribution in the mortar. The dynamic evolution of the mortar results in distinct sizes, shapes, spatial distributions and degree of connectivity of the different phases, i.e. a typical microstructure, which defines the mortar's final physical properties. Therefore, the characterisation of this microstructure is the essential key for a profound

[wt.%] of Dry mix	Component	Details
35.0	Ordinary Portland cement	CEM I 52.5 R, Jura Cement Fabriken, Wildegg, CH
40.0	Quartz sand	0.1-0.3 mm, Zimmerli Mineralwerke AG, Zürich, CH
22.5	Carbonate powder	Durcal 65, average grain size 57.5 µm, Omya AG, Oftringen, CH
0.5	Cellulose ether	MHEC 15000 PFF, Aqualon GmbH, Düsseldorf, D
2.0	Redispersible powder	VC: lab sample, Elotex AG, Sempach Station, CH or SA: lab sample, Elotex AG, Sempach Station, CH
25.5	Water	deionised

Table 1. Typical formulation for ceramic tile adhesive, which is used for all samples of this study. As common in the construction business the percentages relate to 100 wt.% of the dry mix.

knowledge of both evolution and final properties. Related to the different phases, however, four major problems arise: (1) identification, (2) variations in size ranges, (3) variations in concentration ranges, and (4) quantification.

1) Some phases can already be identified by light or electron optical methods (e.g., fillers, voids, cement phases, Yang & Buenfeld 2001). As far as the authors know, no methods for the identification and localisation of different polymer types in the mortar exist. An additional problem related to this subject is an appropriate sample preparation.

2) The size of the mortar's phases range from several 100 µm down to the nano-scale. Hence, different visualisation methods are required for the different scales.

3) The concentrations of the different phases vary drastically ranging from 0.5 up to 50 vol.% (see Table 2). In particular the polymers show very low bulk concentrations, which even become reduced locally due to their small sizes and spatial distribution.

4) So far, microstructures of polymer modified mortars were generally investigated by studying fracture surfaces (e.g. Su 1995, Zurbriggen 1998a, Fig. 1a). However, it has to be considered that no reliable quantitative information about phase distribution can be obtained because fractures through inhomogeneous materials always follow inherent zones of weakness like air voids. In case of polymer enriched regions, this problem can even become worse because especially these parts are characterised by their high strength. In other words, such parts rarely will be exposed along fracture surfaces. As a consequence, planar surfaces (Fig. 1b) are required which enable a more reliable quantitative approach similar to those already practised for mineral phases in case of concretes (Scrivener et al. 1986, Kjellsen & Detwiler 1992).

In sum, strategic sample preparation and analysis techniques are necessary to solve the aforementioned problems.

This study presents a multi-method approach combining different light and electron microscopy techniques. In the following chapters we will demonstrate the preparation and analysis techniques, show which technique is appropriate for the individual phases and what the associated errors are. Finally the results of all methods are combined to achieve a

complete spatially resolved mortar quantification. Based on the new findings we will highlight some applications and show fundamental results with respect to the mortar's microstructural evolution.

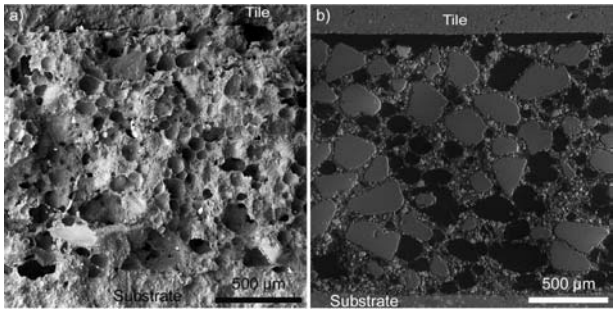

Fig. 1. (a) Secondary electron micrograph (scanning electron microscopy) of a fractured section through tile, mortar (VC-modified, see Table 1) and substrate. Air voids, separated by thin cement-polymer walls or polymer films, dominate the mortar structure. Filler grains are generally covered with cement-polymer matrix and therefore rarely visible. (b) Backscattered electron SEM micrograph of the same mortar as (a) but on an impregnated, cut and polished section: e.g. quartz grains (dark grey), air voids (black), and the cement-polymer matrix consisting of cement minerals, polymers, capillary and gel pores.

Fresh mortar [vol.%]		Hardened mortar [vol.%]
14	Portland cement → Unhydrated Portland cement	10
	Portland cement → Cement hydrates & gel pores	6
32	Water → Capillary pores	30
22	Air voids → Air voids	22
	2.5 Redispersed powder → Latex film & 2.5 PVA film	
	0.5 Cellulose ether → Cellulose 0.5 ether film	
19	Quartz sand → Quartz sand	19
10	Powdered calcite → Powdered calcite	10

Table 2. The mortar components used in this study before and after completed reactions. The system is open with respect to water (evaporating) and air (penetrating).

1.2 Materials and experimental set-up

The compounds and content of the dry instant mortar are listed in Table 1. This mortar formulation is close to ceramic tile adhesives commercially available. Of special interest in the context of this study are the two major polymer additives, CE and RP. In this study, we used two different types of RP: VC (vinyl-acetate/ethylene/vinyl-chloride) and SA (styrene/acrylic).

Starting from initial dry mixing to the finally hardened mortar the instructions of the European standard CEN prEN 1348 are followed. Water is added to the dry mortar and mixed for 1 minute. During mixing air is entrained and stabilised by the dissolved CE. Simultaneously the redispersible powder is redispersed and turns, together with CE, the mortar into a creamy paste with good workability characteristics. Three minutes after mixing, the fresh mortar is applied as a first contact layer onto a concrete substrate (dimensions of the concrete plate are 10x40x3 cm, Gehwegplatte, Gebr. Müller AG, Triengen, Switzerland; water uptake is approximately 3.0 wt.%.). In a second step, a toothed trowel (teeth 6x6x6 mm) is used to apply the mortar in a constant thickness creating ripples. After 5 min (open time) the tiles are laid in and loaded with 2 kg for 30 seconds. We used fully vitrified ceramic tiles (5x5x0.5 cm; Winkelmanns weiss unglasiert lose, SABAG Bauhandel AG, Rothenburg, Switzerland). Samples were stored for 28 days at 23°C and 50% relative humidity.

Based on this geometric configuration the area of interest, i.e., the mortar layer, is situated in between the concrete substrate and the ceramic tile. Thus vertical sections through the centre of the tile and perpendicular to the ripple direction will reflect representative microstructures (Fig. 1). The vertical sectioning is problematic: the samples cannot be sawed because the delicate mortar microstructures would be destroyed and the air voids filled with sawing residues. This could be improved by cleaning the air voids in an ultrasonic bath, which again can destroy the polymer structures. Therefore, the most promising way to produce a fresh surface is to break the sample along pre-cut notches within the ceramic tile and the concrete substrate. The

ceramic tiles used in this study do not absorb water and an influence of pre-cutting on water movement in the adjacent mortar can be excluded. On the other hand, pre-cutting the very porous concrete plate would change the sucking behaviour of the substrate and thus create artefacts during curing. For that reason the notch in the concrete substrate has to be carefully cut under dry conditions after hardening of the mortar. After breaking, the resulting fracture surface sample provides the base for the specific preparations required for the different analysis methods described in the following chapters.

1.3 Methods and results

1.3.1 Conventional light microscopy and slide scanning

Conventional light microscopy and slide scanning are used in this study for the quantification of relatively large microstructural elements such as mineral fillers, air voids and the cement-polymer matrix. In the following we will use the latter term for all fine-grained areas consisting of unhydrated and hydrated cement minerals, polymers, capillary and gel pores. The preparation of thin sections for the investigation of a common cementitious matrix with air voids and aggregates is widespread in cement and concrete research (Chen et al. 2002) including impregnation, cutting and polishing. Thereby impregnation of the porous material with resin is an inevitable prerequisite in order to achieve planar surfaces.

Sample preparation

We applied the following impregnation procedure to the fractured surfaces:

1) Samples are exposed to a vacuum of approximately 10^{-3} bar which takes up to 12 hours depending on the free water content of the sample
2) Intrusion of epoxy-based, coloured resin
3) Hardening at 12 bars for 24 hours (room temperature)
4) Heat treatment at 80°C for 2 hours
5) Final hardening at room conditions for at least 3 days

Depending on the pore structure, the sample is only partly intruded by the resin, but goes at least as deep as 4 mm for all samples.

Based on the impregnated samples thin sections (20-30 µm) are cut and polished according to conventional preparation techniques.

Image acquisition

Coloured digital images can be captured on any conventional light microscope equipped with a digital camera. In addition to this well-known method, we also applied slide scanning (Nikon Coolscan II) which is an easy and fast technique for image acquisition. In addition to the provided scan-equipment, a metal frame for the insert of thin sections was constructed. For digital imaging on the microscope and the slide scanner, respectively, resolutions of 8636 dpi and 2700 dpi were used. In case of slide scanning an area of 4 cm x 1.5 mm can be acquired at once.

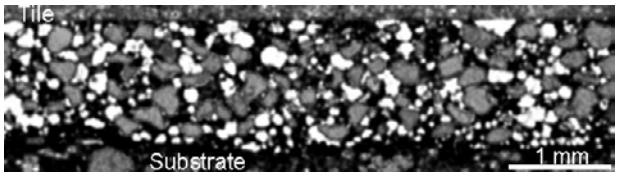

Fig. 2. Part of filtered micrograph of a VC-modified mortar microstructure. The image was acquired with the slide scanner. Air voids (white), quartz filler (grey) and cement-polymer matrix (black).

Digital image analysis

Image processing was done in Adobe PhotoShop 6.0 and includes autoleveling of the three RGB colour channels, blurring, contrast/brightness adjustment, and conversion of the processed colour image into a greyscale image. In this image (Fig. 2), bright areas correspond to air voids filled with impregnation resin, grey areas to the translucent mineral fillers (quartz and calcite), and black areas to the very fine-grained cement-polymer matrix. In the grey value histogram,

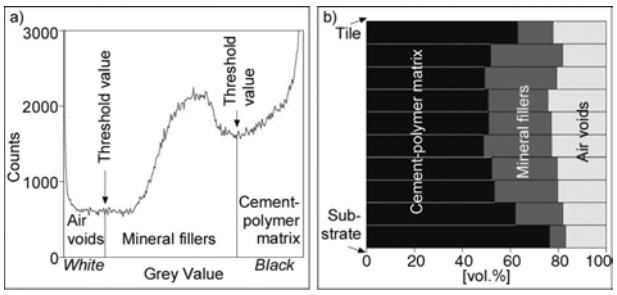

Fig. 3. (a) Grey value histogram of a slide scan performed on a VC modified mortar. Note the phase specific grey value ranges in the entire grey value spectrum (0-255). (b) Distribution diagram of the segmented phases collected along stripes (vertical axis) within the mortar between substrate and tile.

these three textural phases show distinct peaks and can therefore be segmented by setting the appropriate threshold values (Fig. 3a). The three resulting binary images are quantified by a macro running on the software Image SXM (Rasband & Barret 1997), which calculates the area percentage of each phase in a stripe (Fig. 3b). These stripes are chosen layer-wise from top (contact to tile) to bottom (contact to substrate) such that their lengths are sub-parallel to the contacts and their widths correspond to a fraction of the mortar thickness. Based on statistical arguments the stripe widths depend on the size of the measured phases and the total area imaged. Ten stripes were calculated to cover the entire mortar cross section. The macro basically consists of a double loop, which counts the number of segmented pixels of a stripe:

$$Stripe_i = \sum_{y=(i-1)\frac{W}{S}}^{i\frac{W}{S}} \left(\sum_{x=0}^{L} SegmentedPixel(x,y) \right) \qquad (1)$$

where S is the number of stripes, i is the stripe position, W and L the width and length of the mortar layer, respectively. In addition the macro takes rounding problems and the non-rectangular geometry of the measured mortar layer in account. The area percentage of each phase in each stripe equals to the sum of segmented pixels over the total number of pixels in the stripe times 100. The sum of all three phases in one stripe has to equal 100%. Because none of the imaged phases show shape preferred orientations within the xz-plane, i.e. parallel to the mortar interfaces, the area percentages equal to volume proportions. As a consequence a diagram results which shows the concentration of the phases as a function of the distance from the substrate (Fig. 3b).

1.3.2 Fluorescence microscopy of stained polymers

The identification of CE and PVA on planar surfaces is difficult because CE- and PVA-phases are either densely intergrown with the cement-matrix or they form very thin sail-like films in air voids. For both types the resolution of light microscopy is not sufficient for their identification. In addition, they show no distinct optical contrast to the other phases. Also with scanning electron microscopy (SEM), CE- and PVA-components can not be distinguished from the impregnation resin because they have similar backscattered coefficients and for element mapping CE and PVA do not contain characteristic elements. In order to circumvent these problems we developed an improved method for fluorescence microscopy which includes an appropriate staining technique.

Sample preparation

CE and PVA can be stained with fluorescein-5-isothiocyanate isomer I (FITC) prior to mortar mixing, following a similar procedure described by De Belder & Granath 1973. 5 g CE is dissolved in 200 ml DMSO (dimethyl sulfoxyde) at 95°C. After the CE is completely dissolved, 250 mg of FITC are added. The mixture is stirred for 4 hours at 95°C and then cooled down to room temperature. Stained CE is precipitated in THF (tetra-hydro furane), isolated, dried at room temperature and then re-dissolved in 250 ml of water. To prevent bacterial decomposition of CE, 5 drops of biozid (Metatin 907; Acima, Rohm and Haas, Buchs, Switzerland) are added. The CE solution is dialysed against deionised water to remove FITC that has not reacted with CE. The molecular weight cut-off (MWCO) of the membrane is 5000 (Zellutrans E917.1; Roth AG, Switzerland). The highest possible degree of FITC substitution is DS=0.006 (calculated for 100% yield). This low degree of FITC substitution should not change CE properties too much, but is sufficient high to obtain good fluorescence. In order to prove that FITC

remains bound to the CE or PVA even under cementitious high pH conditions, the stained CE or PVA was dissolved for 24 hours in cement water (Jenni et al. 2001a), i.e., water showing a similar ionic composition as in the cement's pore water. Afterwards, the pH of the solution was neutralised and a dialysis was performed using a membrane passable for FITC but not for CE or PVA. No FITC passed the membrane, which shows that the FITC remains bound to the CE or PVA under high pH conditions.

Stained CE or PVA was used to prepare mortar samples and thin sections in the same manner as described above. In general, the properties of fresh mortar paste containing stained CE or PVA did not change except that a slightly lower viscosity was observed in case of CE.

Image acquisition

For fluorescence microscopy two major sources of artefacts have to be considered: a) Depending on the optical properties of the mortar phases, the incident light can penetrate the sample and thus FITC covered by translucent phases (quartz, impregnation resin) show fluorescent light emission. Therefore, the resulting micrograph contains both the required surface plus inhomogeneous three dimensional informations. The latter can be minimised by using ultra thin sections. b) A second source of artefacts is photobleaching (Song et al. 1995), i.e., FITC loses its ability to fluoresce due to exposure to excitation light. In this study, a laser scanning microscope (LSM, ZEISS 410) was used to minimise these two artefacts. In this way, the photobleaching effect can be ignored because of the extremely short dwell time of the laser beam. In addition, micrographs taken in confocal mode with the focus point situated on the sample surface contain only limited three dimensional information (Fig. 4). Acquisition parameters for all LSM micrographs were held constant. Size: 1024x1024, pixel size: 1.666 µm, zoom: 1.5, lens: 5x, attenuation: 1, bandwidth: 0, scantime: 0.7, laser: 488 nm, emission filter: bandpass 515-565 nm, pinhole: 20, confocal mode, contrast: 222, brightness: 9810, frames averaged: 4.

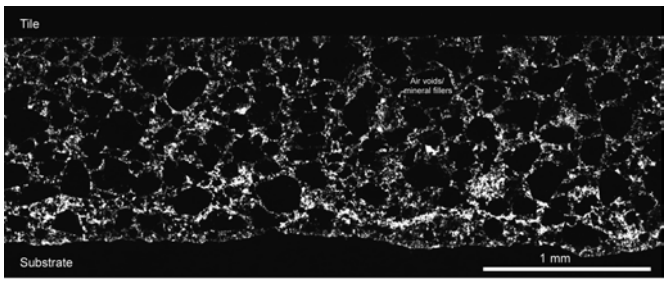

Fig. 4. Part of a filtered micrograph acquired with a laser-scanning microscope from a VC-modified mortar: FITC stained CE (bright areas), air voids and mineral filler (black areas). Note the CE enrichment at the first contact layer (approximately 0.2 mm above the substrate).

Digital image analysis

For low amounts, the FITC concentration is directly proportional to the fluorescence intensity (Rost 1991) which again is directly proportional to the grey value in the final digital image. Therefore, the CE/PVA concentration area can be related to the grey value of the corresponding pixel in the micrograph. The CE grey value histogram (Fig. 5a) shows no specific peak corresponding to the stained polymer phases, i.e., the intensity of the emitted light is spread over a wide range. This is explained by two closely linked factors: a) The variable size of the polymer structures which can be smaller or larger than the beam interaction area on the sample surface inducing higher or lower emitted light intensities. b) No size interval of the polymer structures predominates. The greyscale image is quantified in a similar way as described above using a macro running on Image SXM (Rasband & Barret 1997). In contrast to the light microscopy approach, a background level (Bkd) has to be defined as mean grey value on polymer free phases like fillers, impregnation resin and tile. In equation 2 this background level has to be subtracted from the measured value to obtain the true CE induced fluorescence on a pixel:

$$Stripe_i = \sum_{y=(i-1)\frac{W}{S}}^{i\frac{W}{S}} \left(\sum_{x=0}^{L} Greyvalue(x,y) - Bkd \right) \qquad (2)$$

where S is the number of stripes, s is the stripe position, W and L the width and length of the mortar layer, respectively. Because the grey value is directly

proportional to the CE concentration, the total sum of all measured grey values is then related to the known amount of CE normalised to the cement-polymer matrix:

$$CE_{TOT} = \sum_{i=1}^{S} \frac{Stripe_i}{\phi_i^{cem}} \quad (3)$$

where the CE_{TOT} is the CE volume fraction [vol.%] known from the formulation and ϕ_i^{cem} is the percentage of the cement-polymer matrix in the analysed region *i* (Table 2). Normalisation to the cement-polymer matrix has the advantage to check for polymer fractionations between the different analysed regions *i*, i.e. prevents that enrichments of fillers and/or air voids influence the CE distribution pattern (Fig. 5b). CE enrichments are equally distributed in the z-axis, i.e. perpendicular to the image plane, therefore area percentages equal volume percentages. The same procedure was applied for PVA. The error related to this approach is in the range of 4.4%-5.2% in case of CE and in the range of 10.1%-12.1% in case PVA. It is calculated via the standard deviation of the mean grey value of the tile (8 samples).

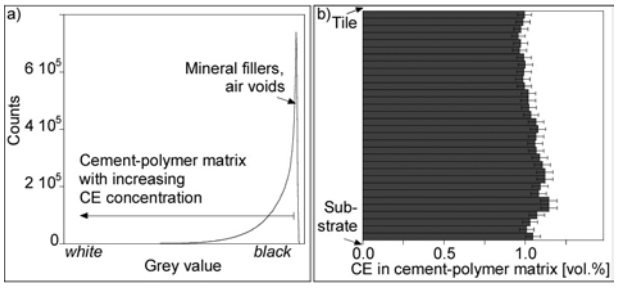

Fig. 5. (a) Grey value histogram of an image acquired with a laser scanning microscope. (b) Distribution diagram of stained CE collected along stripes (vertical axis) within the mortar between substrate and tile: note the enrichments and depletions between tile-mortar and mortar-substrate interface.

1.3.3 Electron microscopy of polymers

Latex films can be visualised by element distribution maps for polymers containing characteristic elements with a significant concentration difference with respect to other mortar phases. For example, areas with increased chlorine concentrations can be linked with the distribution of VC in a mortar texture. Other polymers without characteristic elements (e.g. SA, PVA) can be stained selectively so that they are marked with heavy elements such as osmium or iodine. This paragraph describes the identification and quantification of VC in polymer-modified mortars.

Sample preparation

Experimental tests on isolated polymer films showed that common impregnation resins attack the films from latex polymers (Jenni et al. 2001b). Additionally, the appropriate physical impregnation parameters had to be evaluated in order to avoid any kind of physical damaging. Impregnation with Polyfin (mixture of different paraffins, Polysciences, Inc., Warrington, USA, http://www.polysciences.com/) proved to preserve original polymer films (Jenni et al. 2001b) applying the following procedure: fractured sample surfaces prepared as described above, and Polyfin resin chips were exposed to a vacuum of 16 mbar and heated up to 75°C to achieve a viscosity suitable for penetration. After melting, the samples must be immersed completely in the Polyfin with fractured sample surface facing upwards. Vacuum and temperature are hold constant for 1 h, then pressure is raised to 1 bar within approximately 5 minutes. The resin penetrates only several mm into the sample, but within this range, fragile structures are not destroyed. Cooling to room temperature takes approximately 2 hours. Caution concerning impregnation artefacts is still required because the elevated temperatures can provoke an improved latex film formation, although the original distribution of latex will not be changed by this process.

The hardened resin is non-transparent, rather soft and therefore not suitable for the manufacturing of ordinary thin sections. For that reason, this technique is only used for the preparation of polished sections. During polishing significant material contrasts between soft (Polyfin and polymers) and rigid phases (mineral filler, clinker and cement hydrates), can create topography which is unfavourable for quantitative electron microscopy. Best results are achieved by polishing on wet diamond discs (granulation up to 3000). After polishing, the surface is cleaned carefully by a hexane

saturated wipe from Polyfin smears. The prepared surface is then coated with a 300 nm thin carbon layer (Balzers carbon coater).

Image acquisition

The Cl wavelength dispersive spectroscopy (WDX) mapping is acquired on a electron microprobe (EMPA) Cameca SX-50 (Cl $K\alpha_1$: PET on SP1; acceleration voltage: 20 kV, beam current: 30 nA, pixel time: 50 ms, pixel step: 2 µm, image size: 750x750 pixels, stage movement mode, 1 frame). Note that the small Cl concentration requires such a long pixel time leading to a total image acquisition time of about 8 hours.

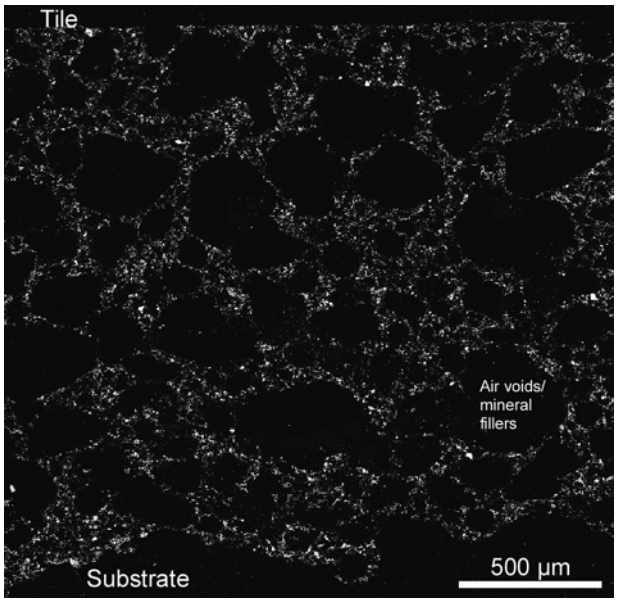

Fig. 6. WDX chlorine mapping of a VC-modified mortar: Elevated chlorine concentrations (bright) in the polymer-cement matrix, air voids and mineral fillers (black).

Digital image analysis

The pixel step was adapted to the interaction volume of the electron beam lying in the range of 1-2 µm. Similar to the LSM approach, the sizes of the polymer films can be much smaller than the interaction volume inducing the same problems already treated above. In other words, also for the WDX approach the grey value of a pixel on the element mapping (Fig. 6) is proportional to the number of X-ray counts. They are approximately proportional to the Cl concentration and therefore to the VC concentration. For this reason, the same image analysis technique used for quantification of LSM micrographs, including the same treatment for background correction, can be applied to WDX element mappings (Fig. 7). The mean error related to the WDX approach is around 15.2%.

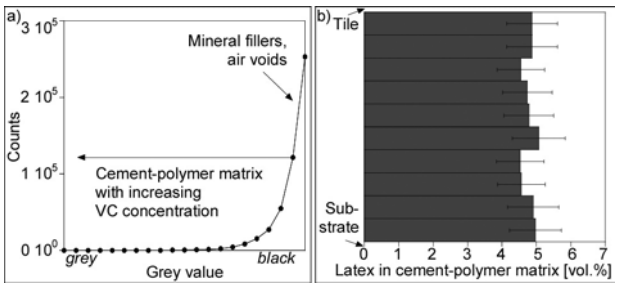

Fig. 7. (a) Grey value histogram (only darker end 235-255 displayed) of a chlorine mapping. (b) Distribution diagram of latex containing chlorine collected along stripes (vertical axis) within the mortar between substrate and tile.

1.4 Discussion

1.4.1 Methods

The three presented methods allow to solve the four problems outlined in the introduction (Table 3). Planar sections are inevitable for microstructure quantification requiring specific sample impregnation procedures (epoxy-based and Polyfin impregnation). In terms of phase identification, particularly CE, PVA and latex require complementary approaches to conventional light microscopy as there is polymer specific staining or WDX combined with the appropriate visualisation technique (LSM, EMPA). The problems related to the drastic variations in size and concentration of the distinct phases can be circumvented by (a) applying methods with different resolutions, (b) measuring bulk concentrations within the interaction volume limited by the method's resolution and (c) using highly sensitive acquisition methods (fluorescence microscopy, WDX). Each method has advantages but also limitations which both are discussed in the following section. Subsequently, the phase distribution patterns resulting from these different methods are compiled leading to a complete quantification of the mortar. In terms of the

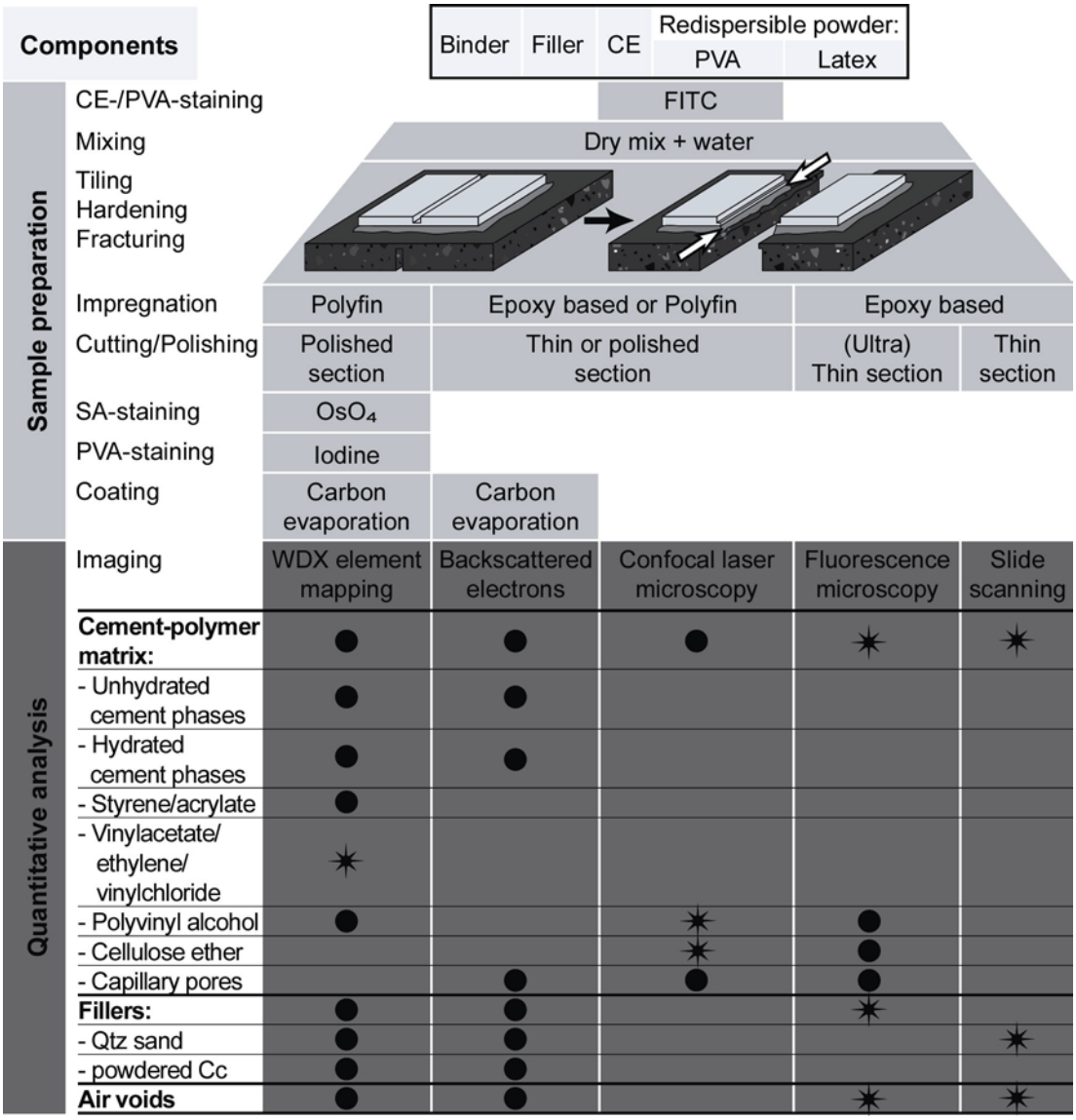

Table 3. Overview showing the acquisition methods and sample preparation techniques required for the quantification of the mortar phases. The methods presented in this paper are marked with a star.

microstructure evolution, we will finally highlight some implications inferred from the generated distribution patterns.

Slide scanning

The advantage of slide scanning is the fast and easy imaging of almost the entire section across the entire mortar bed. Consequently a large data set is obtained providing an excellent statistical base. Figs. 3b and 8 (upper row) show distribution patterns generated via slide scanning and light microscopy, respectively, analysed in the identical sample area. It becomes obvious that for slide scanning (Fig. 3b) the volume proportion of the cement-polymer matrix is larger, i.e., overestimated compared to the original mortar formulation (Table 2). This is attributed to the limitation in resolution preventing the identification of fine-grained filler particles with sizes in the range of 10-30 µm which are therefore measured together with the cement-polymer matrix. Thus, the slide scanning approach can be applied for the quantification of air

voids, large-sized filler particles and cement-polymer matrix including small-sized filler.

Fluorescence microscopy of stained polymers

By using a LSM, the common artefacts of fluorescence microscopy, i.e., photobleaching and three-dimensional effects, can be minimised. The striking advantage of fluorescence microscopy is the high sensitivity, which allows the allocation of stained polymers present in concentrations less than 0.1 vol.% within a total acquisition time of less than 1 second per image (LSM). FITC staining of latex (VC, SA), as third polymer type, is not suitable due to the lack of hydroxyl groups on the copolymer.

Electron microscopy of polymers

Comparable to LSM, the interaction volume of the electron beam and the sample is 1-2 µm and therefore larger than most of the VC structures. Again, VC bulk concentrations in the interaction volume are measured. These low concentrations are close to the detection limit of WDX requiring long acquisition times.

Alternatively to polymer specific element mapping, the polymers can also be stained after sectioning. For this purpose, for example, Osmiumtetroxide (OsO_4) and Iodine can be used because Os is built in latices like SA containing C-C double bonds (Hayat 1993) and Iodine is caught in helix structures of the PVA (West 1948). In this way, Osmium and Iodine are mapped as characteristic elements. Tests performed on isolated polymer films confirmed this behaviour. In the mortar microstructure, however, Osmium and Iodine are not exclusively restricted to the polymers indicating that, to a lesser extent, cement minerals also can adsorb these reagents. Thus, OsO_4 and Iodine staining are not applicable in this study due to the low polymer concentration and the adsorbent surfaces of the cement phases.

To summarise the results, the different phase specific analysis methods can now be combined to quantitatively investigate the phase distributions within a mortar sample. The next chapter shows such a quantification approach and the resulting inferences in terms of the mortar's evolution.

1.4.2 A case study

In Fig. 8, the distribution patterns resulting from the methods presented above are joined to obtain a quantification of all phases of interest.

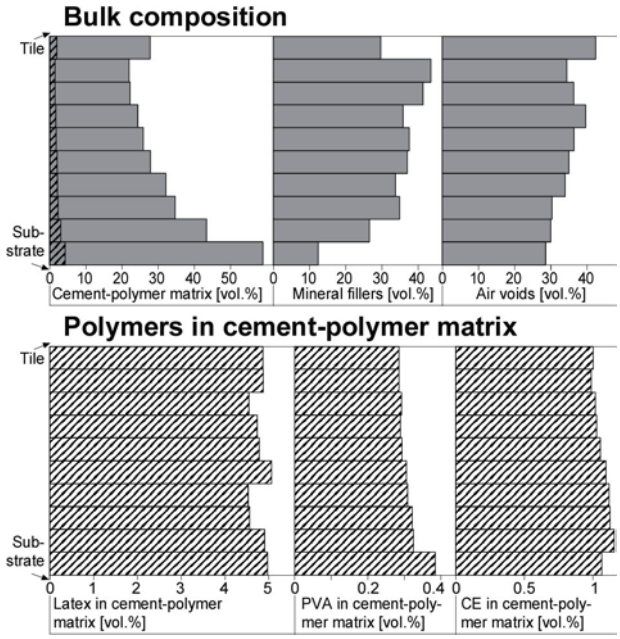

Fig. 8. Combination of distribution diagrams: cement-polymer matrix (polymers shaded), mineral fillers and air voids (based on micrograph acquired with light microscopy); VC latex (based on WDX chlorine mapping), polyvinyl alcohol and cellulose ether (based on laser scanning micrographs, polymers stained with FITC). Horizontal axes on the upper and lower row indicate volume percents of the whole mortar and the cement-polymer matrix, respectively.

The cement-polymer matrix is enriched directly adjacent to the tile and substrate interfaces, while the mineral filler shows the opposite distribution, i.e., distinct depletions adjacent to both interfaces. The air void content is enhanced adjacent to the tile interface. The distributions of the polymers within the cement-polymer matrix are depicted in the second row of Fig. 8 and are on a first view homogenous. The concentration variations of VC are within the error range and therefore show no significant enrichments. In contrast, the PVA concentration diminishes slightly towards the tile, while CE is enriched at about one fifth of the

mortar layer above the substrate and decreases towards both interfaces.

Based on these data, the following new inferences about the mortar evolution outlined in the introduction can be drawn:

1) The first order fractionation of cement-polymer matrix, air voids and filler occurs directly during tiling and is induced by a geometric effect. Here, both tile and substrate prevent a dense package of coarse-grained spheroidal filler. As a consequence, cement-polymer matrix and air voids have to fill the resulting wedges in between interface and grain surfaces. Fracturing during adhesive strength tests occurs mainly along an interface (adhesive failure) indicating that the microstructure at this contact can have a considerable influence on the final adhesive strength of the whole system.

2) Two kinds of air voids can be entrapped while the ceramic tile is applied onto the mortar surface: a) During the open time, a skin forms on the mortar surface where the larger sand grains induce an uneven mortar surface. As the tile is applied, this roughness leads to entrapment of air voids, resulting in the enrichment right underneath the tile (Fig. 8). In addition to 1), this microstructural component also weakens the final strength of the system. b) The application of the mortar by a toothed trowel generates mortar ridges and valleys. During inlaying of the tile, most of the air in the valleys escapes laterally. Entrapped air leads to voids 4-15 times larger than the average air void size, which can have a considerable influence on the air void distribution.

3) After application of the mortar, pore water starts to migrate towards the sucking substrate. In this way, both the dissolved PVA and CE are transported. Filtering at the substrate surface and the top of the first contact layer results in an accumulation of PVA and CE above the specific filter horizon, respectively. This means that these polymers can migrate through the pore system and are therefore not or only partly adsorbed on cement particles under wet conditions.

4) In contrast, the latex particles are too large to pass the smallest capillary pores and/or are partly adsorbed on mineral surfaces. Therefore, VC is evenly distributed in the mortar.

1.5 Conclusions

The methods specified allow to visualise and quantify air voids, mineral fillers, the cement matrix and the polymers (VC latex, PVA, CE) present in common tile adhesives (Table 3). Based on these results inferences about the mortar evolution and the processes involved can be obtained but further improvements of the methodology are possible:

1) Apart from VC and SA, different latices are used in the field of tile adhesives to improve their properties. However, latices containing no specific element or no double bonds cannot yet be visualised for quantification.

2) The low concentrations of Cl in VC or Os in stained SA lead to very high acquisition times of the WDX element mappings. Therefore, the number of mappings is limited. Alternatively, fluorescence staining of latices without changing their properties is very demanding, but would allow to image the latices as fast as done for CE and PVA.

3) No methods exist to quantify the spatial phase distribution within the cement-polymer matrix on the submicron scale because the methods specified are restricted to resolutions of >1-2 µm.

4) The mechanisms controlling the microstructure evolution are inferred from the hardened end product. Complementary methods for in-situ investigations of the wet mortar exist (environmental scanning electron microscopy, in-situ light microscopy of polymer film formation) and additionally provide time dependent data.

Nevertheless, our approach combined with previously used techniques in the field of cement and concrete research allows to investigate several polymer-specific topics. Especially in tile adhesives, the investigated polymers increase considerably the adhesive strength,

which is one of the most important parameters of these products. In this sense, particularly the polymer distribution is the controlling feature. Applying our new approach, the adhesive strength can be studied in function of the complete microstructure including polymers. Furthermore, polymers like CE, PVA and latex occur in a broad variety of composites used in industrial applications. In this context the presented approach might represent a useful tool not only in cementitious materials.

Chapter 2

Influence of Polymers on Microstructure and Physical Properties of Cement Mortars

A. Jenni, L. Holzer, R. Zurbriggen, M. Herwegh

(to be submitted to:
Cement and Concrete Research)

Abstract

The impact of polymer-modification on the physical properties of cementitious mortars is investigated using a multi-method approach. Special emphasis is put on the identification and quantification of different polymer components within the cementitious matrix. With respect to thin-bed applications, particularly tile adhesives, the spatial distributions of latex, cellulose ether, polyvinyl alcohol and cement hydration properties can be quantified. It is shown that capillary forces and evaporation induce water fluxes in the interconnected part of the pore system, which transport cellulose ether, polyvinyl alcohol, and cement ions to the mortar interfaces. In contrast, the distribution of latex remains homogeneous. In combination with results from qualitative experiments, the quantitative findings allow reconstruction of the evolution from fresh to hardened mortar, including polymer film formation, cement hydration and water migration. The resulting microstructure and the failure modes can be correlated with the final adhesive strength of the tile adhesive. The results demonstrate that skinning prior to tile inlaying can strongly reduce wetting properties of the fresh mortar, lowers final adhesion strength, and therefore dominates bulk strength.

2.1 Introduction

Commercially available tile adhesive mortars consist of a binder, mineral fillers and are usually modified with cellulose ether (CE) and redispersible polymer powder (RP). These additives fulfil different tasks during the evolution from fresh to hardened mortar. The main purposes of CE are thickening, air entrainment and water retention in order to establish proper workability properties. RPs further improve fresh mortar rheology, but mainly provide flexibility and tensile strength. The powder is usually manufactured by spray drying of a polyvinyl alcohol (PVA) containing latex emulsion. The most typical binder is ordinary Portland cement, used in combination with different types of mineral fillers. The simultaneous existence of binder and polymers provokes the interaction of two fundamental processes: film formation and cement hydration. In comparison to common concrete technology, polymer-modified, thin-bed mortars are characterised by high water/cement ratios of about 0.8, but due to their high surface/volume ratios, they dry out more quickly. As a result, the cement is only partly hydrated (20%, instead of >90% as in concrete). Tile adhesive mortars typically also contain a much higher air void content (25 vol.%, instead of <5% in concrete; see Fig. 1a).

To date, the influence of polymers has generally been investigated in an empirical manner by comparison of physical properties (compressive, flexural and adhesive strength) from different mortar formulations (e.g., Afridi et al. 1995, Ohama 1987, Ohama 1995, Schulze 1985, Schulze 1999, Schulze & Killermann 2001). In general, these studies document that the increase of strength can be correlated with the concentration and type of latex polymers. Furthermore, Larbi & Bijen 1990 measured the pore solution chemistry of different polymer-modified mortar formulations in function of time, and concluded that latices interact with ions in pore solution. Changes in covalent latex bond occurrences due to chemical interactions with cement ions are also documented by infrared spectroscopy (Rodger et al. 1985, Silva et al. 2002). A review of such interaction processes, mainly based on studies of ion measurements in aqueous systems, is given in Chandra & Flodin 1987.

In this paper, we focus on the fundamental relationship between the microstructure and the macroscopic properties of modified mortars. It is generally accepted that physical properties of cementitious materials are strongly dependent on microstructural aspects. For example, several studies correlate pore size distributions and polymer modification (e.g., Silva et al. 2001). However, only few studies are carried out on

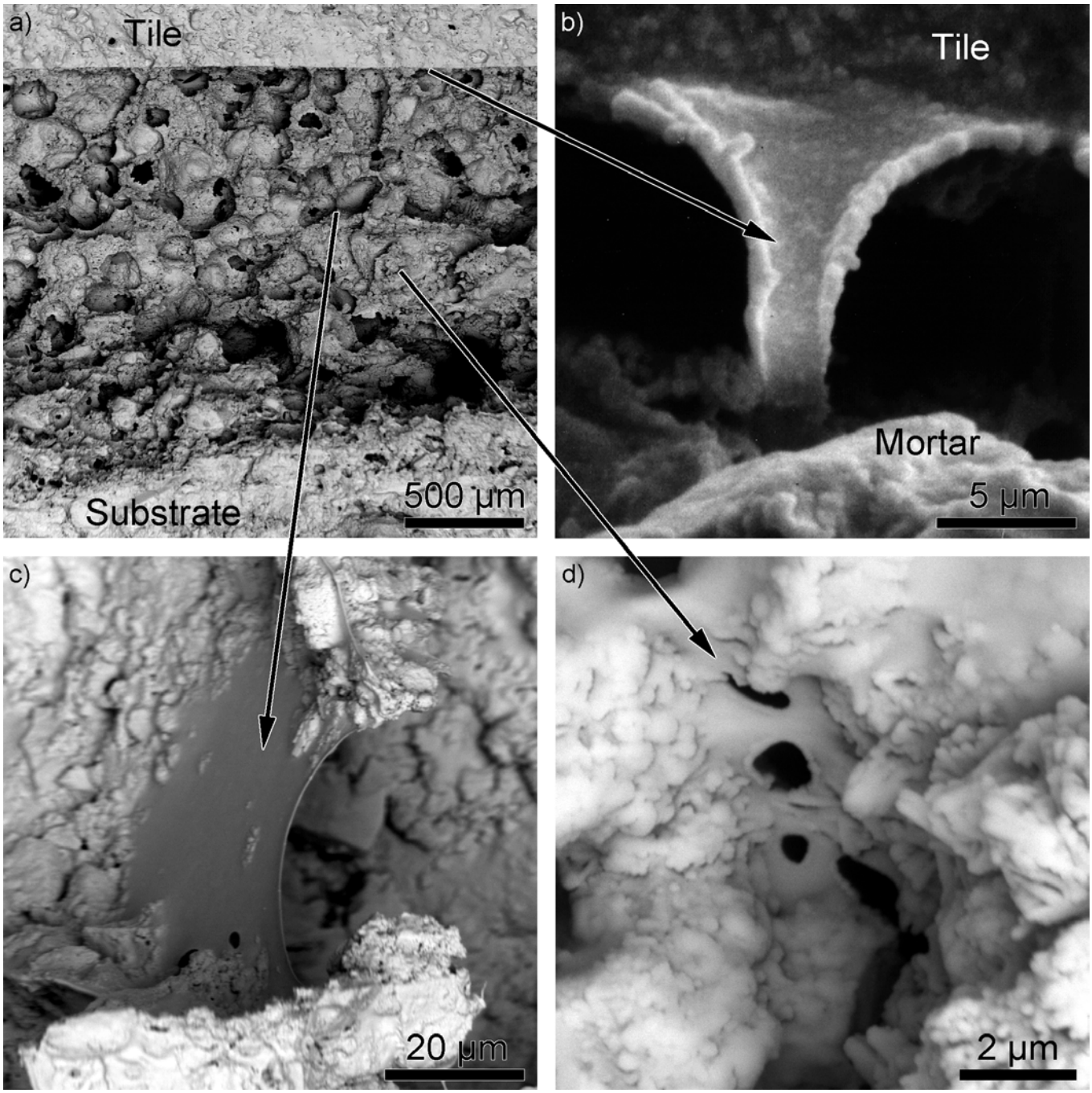

Fig. 1. SEM images showing the microstructure of a tile adhesive (fracture surfaces coated by Au evaporation technique). The mortar formulation is given in Table 1, but with 3 wt.% EVA. (a) Overview showing a cross-section through the mortar bed. The microstructure is typically dominated by a large number of air voids. Details: (b) polymer film bridging a shrinkage crack at the mortar-tile interface. (c) polymer structure at the air void interface and (d) polymer film in a capillary pore of the cement-polymer matrix.

the role of polymers in modified mortars as manifest by their morphology and distribution within the microstructure (e.g., Stark et al. 2001, Tubbesing 1993). Su 1995, Su et al. 1996) describe the adsorption of styrene acrylate polymer on cement grains immediately after mixing, resulting in early film-formation and reduced hydration rates. The remaining part of the polymers, which is presumably dispersed in

the pore water, undergoes film-formation during the subsequent drying period.

In all microscopic investigations, the identification of polymers within the cementitious matrix is a major problem, especially for commercial formulations with low polymer concentrations of 1-4%. More severe polymer modifications in mortar generally are based on a variety of different polymer types, requiring the identification of these different phases in the mortar microfabric (various latices, CE, PVA, the latter as a component in many commercial RPs).

For a profound understanding of the phase distributions in the mortar microstructure, which influence the physical properties of mortar thin-bed applications, the role of inhomogeneities has to be taken into account. Mortar-tile and mortar-substrate interfaces in particular represent inherent zones of weakness, which may dominate the final adhesive strength of the entire system. Further local inhomogeneities may form within the matrix by mechanical (e.g., application), physical (e.g., evaporation and associated water flux) or chemical processes (e.g., local precipitation). Water transport is a potential mechanism for efficient mass transfer, i.e., redistribution of dissolved chemical species. Schweizer 1997 and Zurbriggen 2001, for example, have documented enrichment and depletion of CE and inorganic phases at mortar interfaces. In-situ investigations in an environmental scanning electron microscope (ESEM) revealed that CE and PVA may become mobile during wetting and drying cycles, whereas latices generally tend to remain immobile (Holzer et al. 2001). However, the general distribution patterns of these polymer types in thin-bed applications and the associated fractionation processes have not yet been elaborated. For this purpose, the different polymer components and their spatial distribution within the mortar bed have to be visualised and quantified by different approaches (Jenni et al. 2001b and chapter 1). In addition, the study of potential fractionation mechanisms during mortar evolution requires a time-resolved microanalysis. Unfortunately, it is impossible to continuously follow microstructure evolution in-situ during the entire time ranging from fresh mortar stage to the final hardened mortar. Consequently, it is necessary to complement quantitative studies on the end product with selected experiments to analyse a particular stage, and to trace critical periods of the microstructural evolution.

Until now, no straightforward method existed for microscopic identification and quantification of different polymer components within the mortar. The major goal of this study is to describe the general morphology of different polymer-types within the mortar in order to distinguish them, to identify potential local enrichments and to correlate them with the associated fractionation processes. The mutual interpretation of the microstructural evolution, mechanisms involved and resulting material properties, is an important step toward a better understanding of polymer-cement composites and the development of new products.

2.2 Methods

The microstructural evolution of tile adhesives was investigated by a multitude of qualitative and quantitative methods, carried out a) on the hardened mortar and b) during mortar evolution.

a) The general sample preparation resulted in a specimen composed of three layers, the concrete substrate, the mortar bed, and the tile. Depending on the analytical method used, specific preparation steps were performed. The film morphologies in hardened mortar were investigated by scanning electron microscopy (SEM) on fracture surfaces. Concentration profiles across the mortar bed were measured by wavelength dispersive x-ray spectroscopy (WDX) element mappings and fluorescence microscopy, both acquired on polished sections. Combined thermogravimetric and differential thermo analysis (TGA) of layer-wise sample series across the mortar bed resulted in the distribution pattern of portlandite and provide a rough idea on the spatially resolved degree of cement hydration.

b) ESEM freeze-dry experiments on fresh mortar pastes revealed the CE behaviour during the early

stages of mortar evolution. Light microscopy on polymer films in model systems outside the mortar illustrated film formation mechanisms.

2.2.1 General sample preparation

With two exceptions (film formation experiments in model systems, and freeze-drying in ESEM), all samples were prepared according to the following procedure: The general mortar formulation was similar to commercial ceramic tile adhesives (Table 1), but not optimised to further improve the final mortar properties, e.g. adhesion strength. In order to identify the functionality of specific polymer types, formulations containing only one polymer type have also been investigated. In these samples, mineral fillers replaced the quantity of polymer omitted, and the percentages of all other components were kept constant. After mixing, fresh mortar was applied on a concrete plate in two steps: as a first contact layer with a thickness corresponding to the coarsest grain size of the filler components (approximately 0.3 mm), which then was trowelled repeatedly with a toothed trowel (profiled 6x6x6 mm, Fig. 2). After 5 min (Open Time) the fully vitrified ceramic tiles (5x5x0.5 cm) were laid in and loaded with 2 kg for 30 seconds. Then, the samples shown in Fig. 2 were stored for 28 days at 23°C and 50% relative humidity.

[wt.%] of Dry mix	Com-ponent	Details
35.0	Ordinary Portland cement	CEM I 52.5 R, Jura Cement Fabriken, Wildegg, CH
40.0	Quartz sand	0.1-0.3 mm, Zimmerli Mineralwerke AG, Zürich, CH
22.5	Carbonate powder	Durcal 65, average grain size 57.5 µm, Omya AG, Oftringen, CH
0.5	Cellulose ether	MHEC 15000 PFF, Aqualon GmbH, Düsseldorf, D
2.0	Re-dispersible powder	VC, SA, EVA: lab samples with different latex compositions, containing PVA, Elotex AG, Sempach Station, CH
25.5	Water	deionised

Table 1. Typical formulation for ceramic tile adhesive used for all samples in this study, unless otherwise indicated. As common in mortar business, the percentages relate to 100 wt.% of the dry mix.

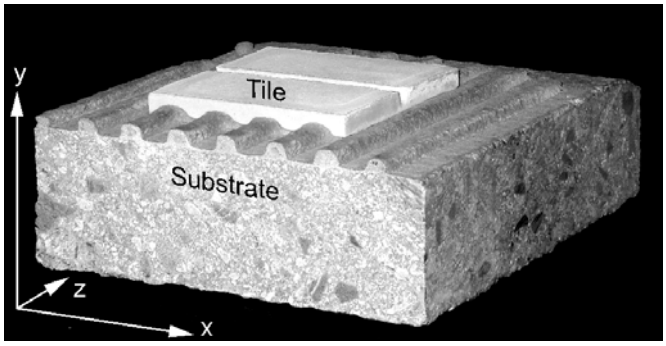

Fig. 2. The hardened mortar sample. Between tile and substrate, the mortar ripples are deformed to a continuous mortar layer, shown in Fig. 1a.

All results presented below are based on the chosen experimental set-up and may deviate for different substrate and tile materials or dimensions (e.g., Schweizer 1997).

2.2.2 Light microscopy: film formation in model systems

Polymer films were produced outside the mortar using two different experimental set-ups: a) film formation on metal grids and b) film formation between two glass plates.

a) As described in Jenni et al. 2001a, Zurbriggen 1998b, films were produced from polymer suspensions using grids with 86 µm x 86 µm sized square voids (TEM grids), which were dipped into diluted polymer dispersions. The RP polymer concentration in the dispersion was about 10%, CE concentration 2%, and PVA concentration 2.2%. This procedure resulted in the formation of films, which were attached to the grid and typically contained a hole in the centre of the former grid void (Fig. 3b). The existence of the hole indicated a

small film thickness, similar to the sail-like films observed at air void interfaces in mortars (Fig. 1). The polymer films were then investigated with transmitted light microscopy.

b) Following the description of Zurbriggen & Jenni 2002, agglomeration and film formation can be observed under the light microscope, where the polymer redispersion/solution, or the fresh mortar paste is prepared between two glass slides. Due to evaporation, the waterfront retreats provoking the formation of polymer films between the glass slides parallel to the light beam (Fig. 3a and 3d). In case of PVA and CE, the optical anisotropy induced by polymer chain ordering causes birefringence colours, a clear indication for PVA and CE films.

2.2.3 Fluorescence laser scanning microscopy (LSM): PVA and CE distribution patterns

In order to identify PVA and CE under the microscope, these polymers were stained with a fluorescent dye prior to mortar mixing. The hardened mortar samples were impregnated and polished (chapter 1), in order to obtain a mortar cross-section along the xy-plane (Fig. 2). For subsequent investigations a laser scanning microscope ZEISS 410 was used. Because PVA and CE did not occur within large voids or in the interior of unhydrated cement and filler grains, the resulting signals from the polymer were normalised to the area occupied by the cement-polymer matrix using digital image analysis. The cement-polymer matrix is defined as the total of all cement and polymer phases and gel/capillary pores (chapter 1). In this manner, the polymer distributions in the cement-polymer matrix were obtained. Due to this normalisation, an eventual inhomogeneous distribution of air voids and fillers did not affect the polymer distribution. Variations of PVA- and CE-concentrations as a function of the distance from the substrate interface were obtained by segmentation of the LSM image into horizontal stripes oriented parallel to the aforementioned interface and lying in the xy-plane (Fig. 2). The substrate was analysed with the same methods. An extensive description of polymer staining, sample preparation, sample measuring, image processing, quantification, and calculation of errors is given in chapter 1.

2.2.4 Electron microscopy

Qualitative SEM investigations of polymer films on fracture surfaces

Fracture surfaces of mortar samples were investigated using a CamScan CS4 scanning electron microscope equipped with a Robinson back-scattered electron (BSE) detector and a Voyager 4 digital image acquisition system for energy dispersive spectroscopy. Samples were coated by evaporation either with carbon or with gold (C: Balzers Carbon Coater; Au: Edwards E12E2). Distance between target and sample was around 25 cm. It is important to note that evaporation coatings with smaller distances can heat up the sample considerably and may destroy the polymer structures.

Polymer structures in the mortar microfabric are characterised by smooth surfaces. Unfortunately, this observation is also valid for cement gels, requiring additional identification criteria for polymer microstructures:

- Polymers have a much lower average atomic number (Z) compared to mineral components. The backscattering coefficient and the grey value on BSE images is a function of the Z-value (Goldstein et al. 1992). Therefore, polymer microstructures are transparent or dark on BSE images, in contrast to mineral phases, which have a significantly higher Z-value. The comparison between BSE and SE (secondary electron) images is thus a reliable way to distinguish between polymer films and cementitious gels.
- Polymer phases are prone to be damaged under the electron beam (Simmons & Thomas 1998) whereas gel-like mineral phases are much more resistant. Structural changes due to beam interactions can thus be used as criteria for the distinction between polymer and mineral components. Structural changes on the surface of polymer films in carbon coated or in non-coated samples, e.g., in an ESEM, can be induced using high magnification,

acceleration voltage and beam current as well as an extended dwell time.

ESEM freeze-dry experiments on fresh mortar

To study the distribution of CE in fresh mortar, pastes with CE as the only polymer component were used (see chapter 2.2.1 and Table 1). Immediately after mixing, small pieces of the fresh paste were shock frozen in liquid nitrogen. Fracture surfaces of shock frozen samples were then studied in an ESEM-FEG XL30. The sample was inserted under the presence of liquid nitrogen into the sample chamber, where the liquid nitrogen was evaporated and the sublimation of the frozen pore solution was followed using N_2 as imaging gas. After sublimation of the pore solution, distribution of CE in fresh mortars became visible (Fig. 3c). Polymer and mineral phases were distinguished according to the criteria given above.

Latex distribution patterns based on WDX element mapping

VC latex contains Cl, which allowed the localisation of this latex type by chlorine mapping done by WDX. Element distribution maps were measured on impregnated and polished samples using an electron microprobe (Cameca SX-50). The mortar formulation is given in Table 1. Similar to CE and PVA quantification, an identical normalisation procedure was applied to the element distribution maps in order to obtain the VC latex distribution in the cement-polymer matrix. The complete description of sample preparation, data acquisition, image processing, quantification, and calculation of errors is given in chapter 1. The substrate was analysed by the same method. Ca, Si and BSE were mapped simultaneously with Cl. Calcium and Si mappings were used in order to discriminate and quantify calcite and quartz fillers, air voids and the cement-polymer matrix. In addition, anhydrous clinker was distinguished from the rest of the matrix based on BSE images. According to Scrivener et al. 1986, the fraction of anhydrous clinker was used as a measure for the degree of hydration.

2.2.5 Thermogravimetric analysis

In general, the samples were prepared and measured after Zurbriggen 2001. More specifically, the tile (5x5 cm) was removed from the hardened sample after a normal dry storage following chapter 2.2.1 (formulation according to Table 1). In order to receive a plane failure surface at the tile-mortar interface, a PE (polyethylene) foil was inserted between tile and mortar. A zone of about 1.5 cm width was then removed from the mortar rim to avoid carbonation artefacts from the mortar edges, leaving a quadratic analysis region of 2 cm length and about 1.4 mm height. Sequential profiles through the analysis volume were obtained by scratching of layers of 0.2 mm thickness using a variety of distance holders. Each layer was measured by TGA on a TGA/SDTA 851^e from Mettler Toledo. The following experimental parameters were used: 150 µl platinum crucible, 30-1000°C, 10°C/minute, 50 ml air/minute.

Based on the weight loss of the endothermic dehydration step at about 450°C, the $Ca(OH)_2$ was stochiometrically quantified. The $Ca(OH)_2$ concentrations of each layer were then plotted vs. the vertical distance. Corrections with respect to 3-D pore and filler distribution were required for a transformation from the measured wt.% into modal composition. For this purpose, the measured values are normalised by the weight of fine filler and cement, where the amount of carbonate fine filler is estimated by thermal decarbonation between 550 and 800°C. Using the formulation percentages (22.5 g $CaCO_3$ on 35 g of cement), a bulk weight of fine filler and cement was calculated. The required assumption that both fine filler and cement are homogeneously distributed throughout the matrix was confirmed by element mapping.

Furthermore, TGA allows an estimation of the degree of cement hydration. Most dry stored tile adhesives of test samples show a total dehydration weight loss indicating a water/cement ratio of 0.12. Assuming a minimum water/cement ratio required for full cement hydration of about 0.38 (Taylor 1997), the TGA data indicate that only about one third of the cement is hydrated.

2.2.6 Adhesive strength tests and failure surface analysis

The adhesive strength was measured on substrate-mortar-tile systems by standard tensile tests according to EN 1348. The errors based on the standard deviations are in the range of ±10%. The structure of the failure surface was then macro- and microscopically investigated. Most surfaces showed criteria of mixed adhesion and cohesion fracturing. In a first approach, macroscopic images of the failure surface on the tile side were acquired by a common colour flat bed scanner (Paragon Mustek 1200 A3 PRO). The area percentages of adhesion and cohesion failure were evaluated by image analysis (failure mode distribution after Afridi et al. 1995). Due to the strong colour contrast between the light tile and dark mortar, adhesion and cohesion fractures were easily distinguished. The microstructure of the failure surface from tile and substrate are investigated by SEM in the same manner as described for fracture surfaces.

2.3 Results

2.3.1 Appearance of polymers in model systems

Investigations on polymers in simplified model systems, e.g., latex films outside the mortar, are generally straightforward in terms of preparation and reveal time-dependent information about redispersion and film formation. Fig. 3a shows a cross-section of alternating latex and PVA segments formed from an RP dispersion between two glass plates during water evaporation. The optical resolution was insufficient to study the presence of unordered PVA within or on the latex film. Fig. 3b shows latex and PVA films that formed due to drying of an RP dispersion on a grid. Whereas latex and PVA form at the evaporation front that moves within the mortar from substrate to tile during hardening, CE films can form along air pore walls during the wet fresh mortar stage, right after or even during mixing (Fig. 3d). The latter inference was additionally confirmed by in-situ ESEM experiments, where CE also was present at air void interfaces (Fig. 3c).

2.3.2 Appearance of polymers in the hardened mortar

Depending on their occurrence within the mortar, three different types of polymer domains can be distinguished (Fig. 1): polymer domains at the interface between mortar and tile (Fig. 1b), polymer domains at air void interfaces (Fig. 1c) and polymer domains within the cementitious matrix (Fig. 1d). The second type was easily recognised in SEM-investigations by its large size and smooth surface. However, in the case of the third and partly also for the first type of polymer films, no morphological criteria are available to properly distinguish them from mineral components because of a dense intergrowth with cement minerals. Therefore, additional criteria such as density contrast (comparison of BSE- and SE-images) and the affinity of polymers to beam damage (as described above) were used for discrimination. Nevertheless, in microstructural investigations the first and third types of polymer domains are usually underestimated because of the difficulties in identification. Therefore, we focus on the second type of polymer domains at air void interfaces. Based on their characteristic appearance, several film types consisting of different polymer components can be identified.

Fig. 4 shows latex, CE and PVA structures in non-commercial lab mortars modified only with one specific polymer. Though rare, latex films were found, which form thick films (>4 µm) between two adjacent air voids (Fig. 4a). The film edges are rounded. Towards the contact with the matrix, the intergrowth with cement grains gradually increases, creating a rough surface. Pure polymer domains without cement intergrowth generally have a smooth surface, which indicates an advanced latex film formation (Fig. 5a, lower left corner).

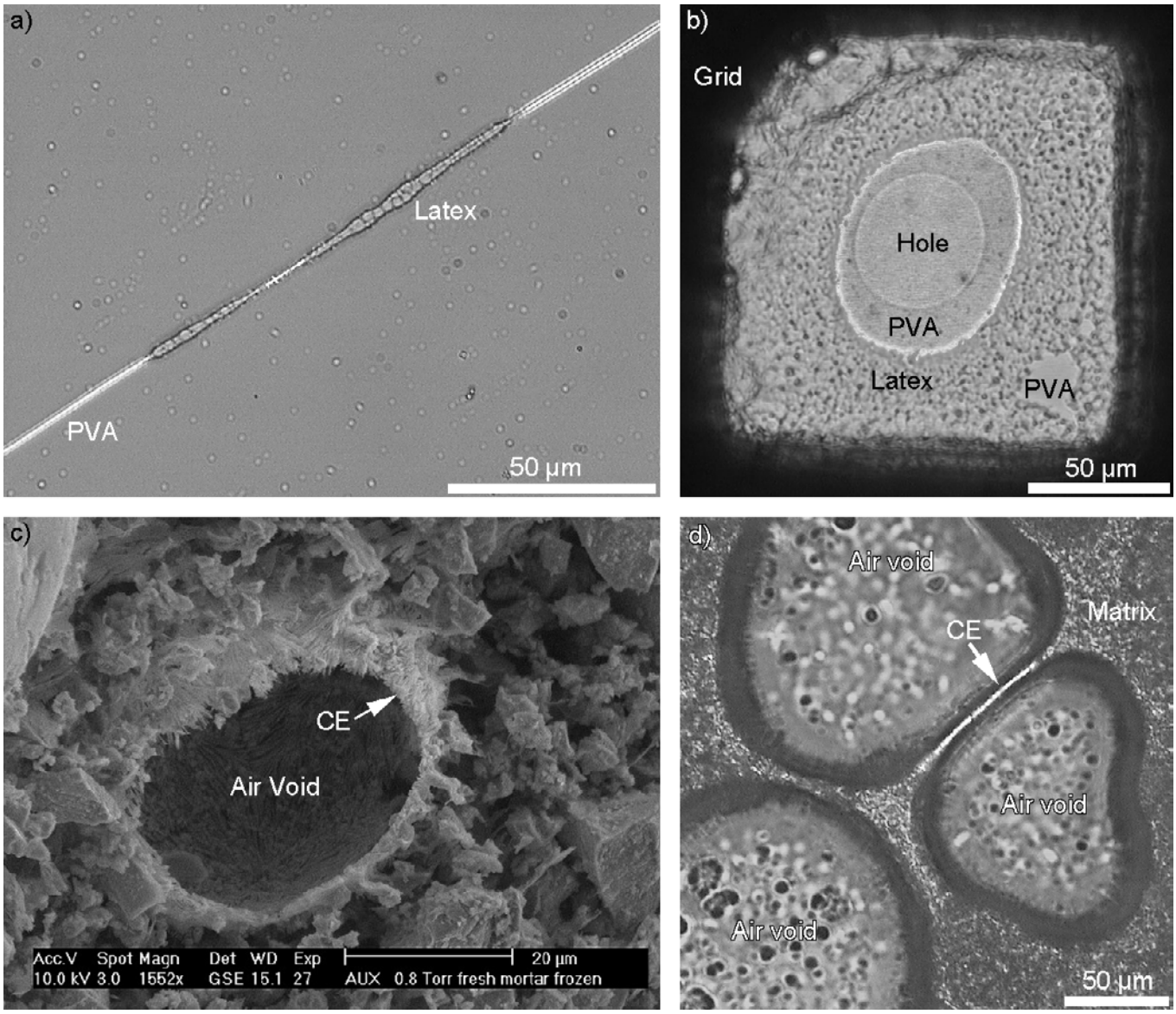

Fig. 3. Early polymer film formation in model systems (a, b) and in the fresh mortar (c, d). (a) Alternating sequences of polarising PVA (bright) and structured latex films formed at the evaporation front of a drying redispersion between two glass slides. The films formed parallel to the light beam of the polarisation light microscope, perpendicular to the glass slides. (b) Front view (transmitted light microscopy) of a situation similar to a), but formed in the void of a grid. There are clearly two phases formed, an inner PVA and an outer latex film. (c) shows a fracture surface of a previously shock-frozen fresh mortar with an air void whose surface is covered with CE (water sublimated), ESEM in-situ cryo-experiment. (d) Filler, CE and water were mixed, applied as thin layer between two glass slides, and observed by polarisation light microscopy. Note that CE films had already formed between two air voids 15 min. after mixing.

CE films are frequently observed between two juxtaposed air voids and also within them, where the film spans the inner surface of a single air void. These sail-like CE films are characterised by a thickness of less than 1 µm. The low thickness and density lead to electron transparence in C-coated samples (Fig. 4b). The surfaces of CE films are smooth and cement inclusions are rare. Locally, CE-films are detached from the cementitious substrate, which may be caused by vacuum drying or sample fracturing.

PVA films closely resemble CE structures with respect to thickness and electron transparance (Fig. 4c). However, PVA domains are rarely observed on the µm-

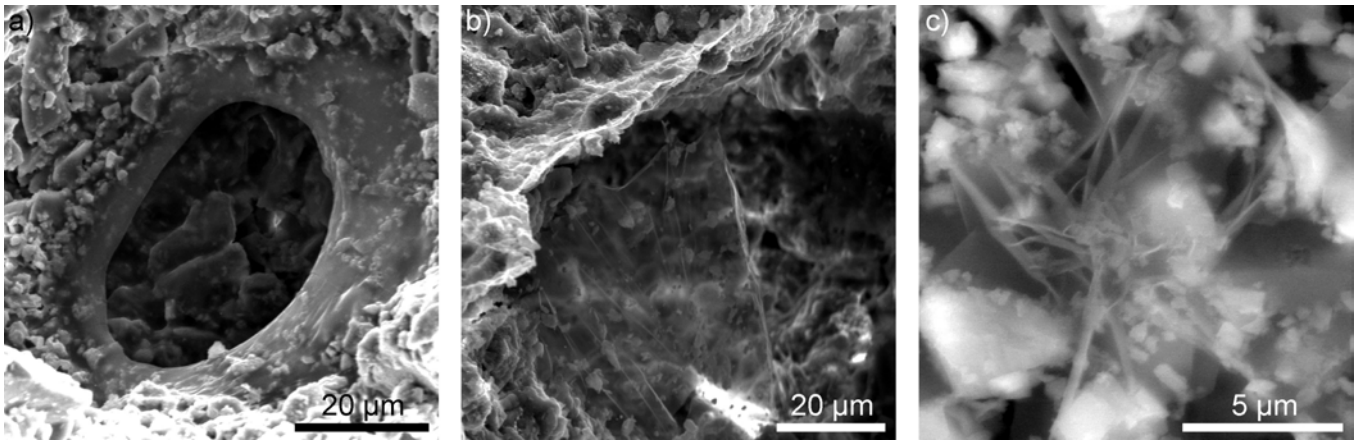

Fig. 4. SEM images of different types of polymeric microstructures on C-coated fracture surfaces in model mortars containing only one polymer type: (a) Latex, (b) CE, (c) PVA.

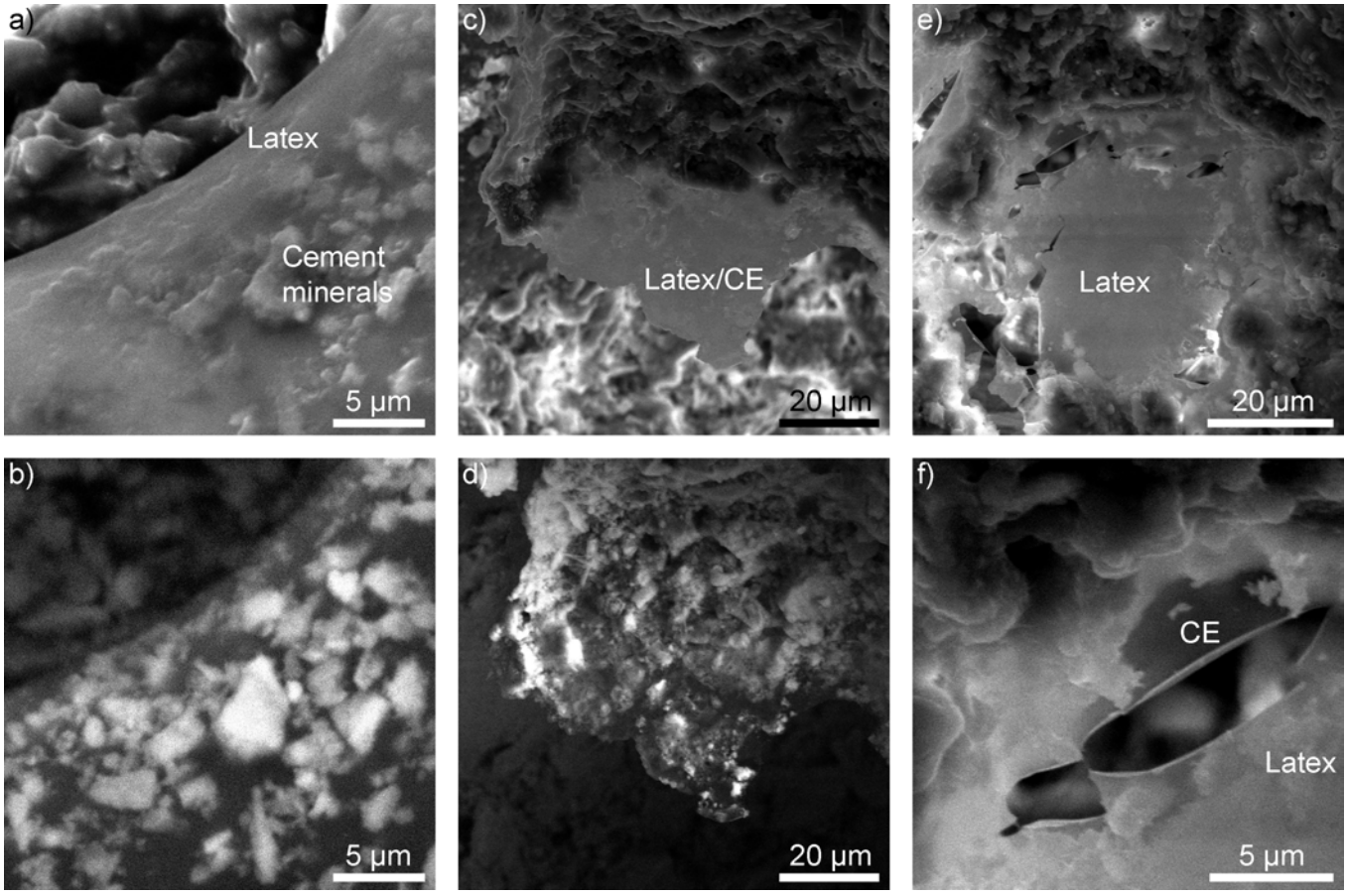

Fig. 5. Composite structures in mortars with several polymer components (SEM images of C-coated fracture surfaces). (a) SE and (b) BSE image of VC latex-cement composite microstructures. (c) SE and (d) BSE image of SA latex-CE-cement composite microstructures. SE image of EVA latex intergrown with CE in the overview (e) and a close up view from the area in the upper left corner (f).

scale. Consequently, they are thought to be mainly integrated in the cement-polymer matrix at the submicron scale.

As documented by a comparison between SE and BSE images (Figs. 5a and b), latex films may contain a high quantity of cement minerals. On the SE image, the latex domain appears as a relatively smooth and plain film (Fig. 5a, lower left corner), whereas the BSE image, which reveals more depth information, shows cement minerals that are embedded within the latex-film (Fig. 5b). Such massive latex-cement composites are typical for all types of latex films in samples without CE. In real tile adhesive formulations containing both RP and CE, composite structures of the two polymers are frequent, but the resulting composite morphology differs from the massive latex films shown in Figs. 4a and 5a/b. In mortars modified with SA and CE, no electron transparent CE-films can be observed. Therefore, the polymer structures are considered to represent CE-latex composites. These composite films are thin and plain (Fig. 5c). Frequent occurrence of fractures as well as sutured edges indicates a brittle behaviour. Again, intense intergrowth with cement phases is documented in the BSE image (Fig. 5d). In mortars modified with EVA and CE, composite polymer structures also differ drastically from pure EVA latex structures. The composite films are thinner, have a plain surface and are often cracked (Fig. 5e). They partly consist of electron transparent domains, probably composed of pure CE (Fig. 5f). In contrast to samples with SA and CE, the EVA- and CE-modified mortar contains also pure CE films.

In summary, the different polymer components can be distinguished based on distinct morphological characteristics. However the qualitative identification is mainly restricted to large polymer domains at air void interfaces. In order to link microstructural information with data from physical tests (e.g., strength), the spatial distribution of different polymer components needs to be quantified, also incorporating small-scale polymer domains within the cement-polymer matrix and/or polymer components at the mortar-tile interface.

2.3.3 Distribution patterns

Water transport in fresh mortar may lead to a redistribution and fractionation of polymer and mineral components, which can influence final physical properties such as adhesive strength. Distribution patterns of mortar components reveal important information about their spatial occurrence, and a comparison of the patterns with final failure surfaces helps to detect the zones of weakness in the microstructure, linking microstructural and physical properties.

A representative example for the distribution of VC latex is given in Fig. 6, indicating that within the analytical error, the latex is evenly distributed within the cement-polymer matrix along the y-axis (Fig. 2). A comparison of measurements performed on former grooves and ripples (application stage) also reveals homogeneous VC latex distribution. In all cases, no latex was measured within the underlying porous concrete substrate or the tile.

Analogously, representative diagrams for the distribution of CE and PVA are shown in Fig. 7. In the case of CE in VC-modified mortar, a slight but continuous CE increase towards the substrate is observed (Fig. 7a). However, in the lowermost part of the mortar bed, the CE concentrations decrease. Maximum CE concentrations are observed at the first contact layer.

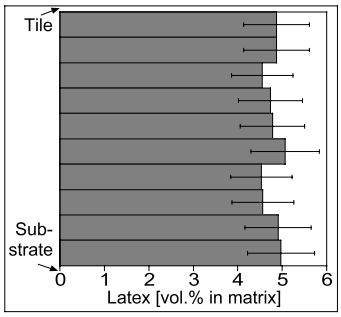

Fig. 6. Concentration profile of VC latex in the cement-polymer matrix sampled across the mortar bed on a xy-section (Fig. 2). Data is collected by electron microprobe analysis (Cl distribution maps) and then processed with image analysis. The area analysed is 1.5 mm wide and the thickness of the mortar bed is about 1.3 mm. Average concentrations are determined for 10 stripes parallel to the mortar bed. Each stripe represents an area of approximately 1.5 mm x 0.13 mm.

In the SA-modified mortar sample, the CE distribution is more heterogeneous (Fig. 7c). Again, the CE concentrations decrease towards the underlying concrete substrate. In analogy to Fig. 7a, a local maximum occurs in the region of the first contact layer surface. For all distribution diagrams a slight but reproducible enrichment of CE is observed directly at the contact between mortar and tile. These results are consistent with Zurbriggen 2001, who measured CE enrichments in tile adhesives towards the porous substrate and the porous tile.

In both VC- and SA-modified mortars, PVA is homogeneously distributed in the upper mortar part. Only in the region of the first contact layer a slight, but reproducible enrichment occurs (Figs. 7b and d). Furthermore, a slight enrichment of PVA exists directly above the mortar-substrate interface.

About 2% of total CE and 7% of total PVA can penetrate to a maximum distance of 300 µm the concrete substrate along microcracks. In contrast, latex was never found in the concrete substrate.

In general, the volume fraction of anhydrous cement phases is systematically 0.05 higher for latex- and CE-modified mortars compared to mortars without latex. For all samples, the local variations in the volume fraction of anhydrous phases are smaller than 0.1 and no identical distribution patterns can be observed in different samples. Further differentiation of the cement hydration products by more precise TGA indicates a $Ca(OH)_2$ depletion towards the substrate (Fig. 8).

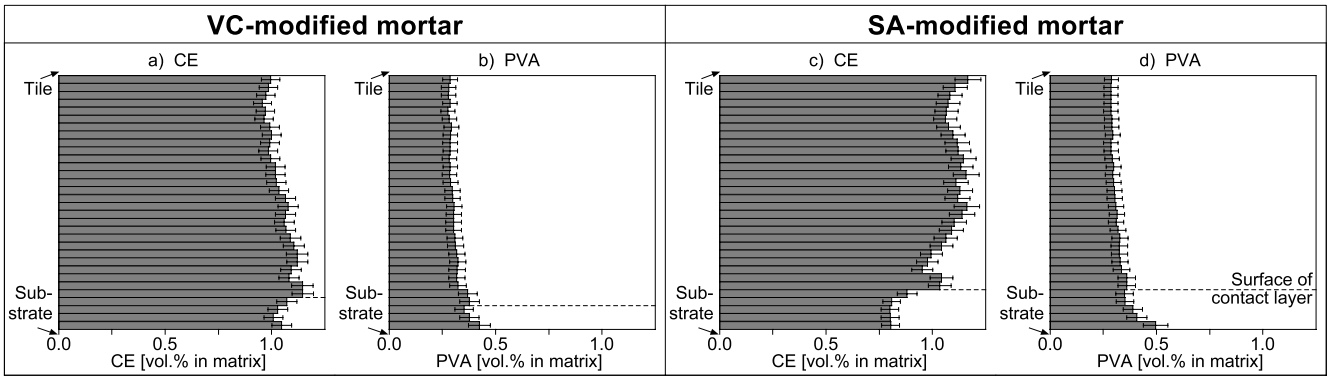

Fig. 7. Concentration variations of CE and PVA in the cement-polymer matrix as a function of the distance from the mortar-substrate interface (y-axis in Fig. 2). (a, b) VC-modified mortar. (c, d) SA-modified mortar. Data is collected by confocal laser scanning microscopy on a xy-section (Fig. 2), and then processed with image analysis. One half of the mortar was analysed (25x1.3 mm).

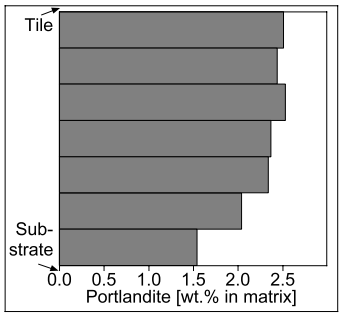

Fig. 8. Distribution diagram of portlandite $Ca(OH)_2$ in mortar as a function of the distance from the mortar-substrate-interface (y-axis in Fig. 2). Data are based on TGA bulk analysis of a measurement series sampled across the mortar bed. Each sample corresponds to a layer in the xz-plane (Fig. 2) of about 0.2 mm thickness.

2.3.4 Adhesive strength and failure surface analysis

A general relationship of adhesive strength as function of different polymer components (CE, PVA, and several types of latex) is shown in Fig. 9, where six mortar formulations with different polymer components have been tested. Each of the six data bars represents the average value obtained from five measurements on identical samples. In each sample, the quantity of polymers corresponds to the amount used in commercial tile adhesives (Table 1).

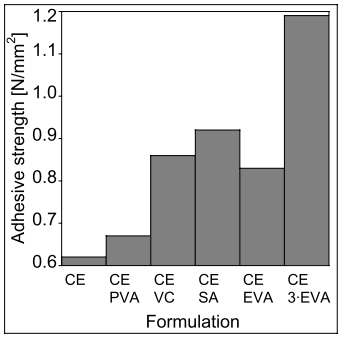

Fig. 9. Adhesive strength of mortars modified with different polymer combination (Table 1). The content of RP in formulation "CE/3·EVA" is 6 wt.%, three times higher than the standard mortar.

In latex-free samples, the addition of PVA leads to a slight increase of adhesive strength (see also Kim & Robertson 1998), while different latex modifications (VC, SA, and EVA) lead to a strong increase in adhesive strength. Note that the measurements of RP-modified mortars are situated within the error range of ± 10%. A higher latex concentration clearly increases adhesion strength.

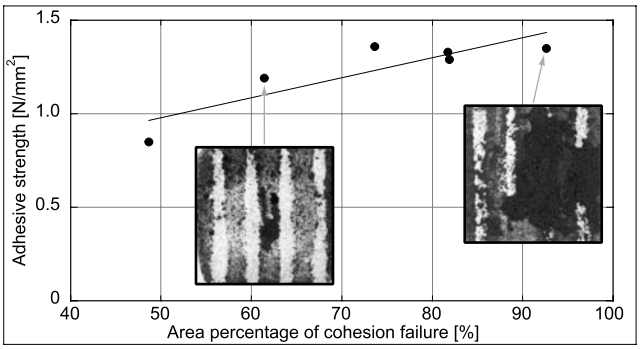

Fig. 10. Adhesive strengths plotted versus the area percentage of cohesion fractures. Data represent 6 identical mortar samples modified with SA and CE. The two micrographs document the mixed failure patterns on the tile side. The dark and bright areas represent cohesion and adhesion fractures, respectively.

Studies of the failure surfaces document important structural variations, which can be linked with the measured adhesive strength. On the macroscopic scale, adhesion failure occurs more frequently at former mortar ripples, whereas cohesion failure is mostly restricted to former grooves (Fig. 10). Adhesion fractures are exclusively localised at the tile-mortar interface. Failure at the mortar-substrate interface is not observed, but cohesion failure occurs rarely at the first contact layer surface. In Fig. 10, the values of the adhesive strength tests are plotted against the area percentages of cohesion fracturing observed on the failure surfaces. All data are collected from identical samples (SA- and CE-modified mortar). The linear trend indicates a positive correlation between cohesion failure and adhesive strength.

SEM investigations on failure surfaces point out microstructural differences between former ripples and grooves. The lower part of the inset of Fig. 11 depicts the ripple area with a smooth failure surface (adhesion failure), which shows significantly fewer air voids than the interior of the mortar bed. Unusually large air voids with irregular shape correspond to air voids which were entrapped during tile inlaying (see also chapter 1). The upper part of the inset reflects the area of a former groove region, which is characterised by a low proportion of adhesion fracturing. In contrast to the ripple domains, the size of air voids in the groove domains is comparable to those within the mortar's interior. Deeper structural domains are exposed due to cohesion failure within the mortar bed.

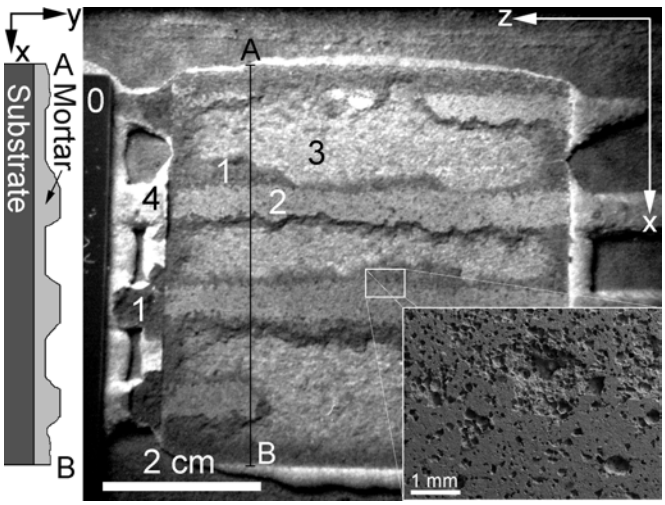

Fig. 11. Schematic cross-section and top view of the failure surface of a mortar sample illuminated with ultraviolet light to excite the stained CE within the mortar. The relative amounts of CE are represented by different light intensities (increasing from 0 to 4), which correspond with specific mortar domains: 0=tile, 1=cohesion fracture, 2=adhesion fracture at the mortar-tile interface, 3=fracture at the contact layer surface, 4=surface outside tile coverage. The inset (bottom right) represents a SE SEM image of a failure surface at the ripple-groove transition.

Based on fluorescence microscopy, CE and PVA distributions on failure surfaces can be monitored. This is shown in Fig. 11 where the brightest domains (4) represent surfaces which were not covered by a tile. The enrichments at the mortar-tile interface and at the contact layer surface (domains 2 and 3) exposed due to adhesion fracturing are weaker. Darkest areas reflect surfaces of cohesion fractures (1), which correspond with the internal mortar fraction.

2.4 Discussion

Based on numerous micro- and macroscopic observations, the structural evolution of polymer modified mortars can be reconstructed. The associated mechanisms such as film formation, drying due to evaporation and hydration are summarised schematically in Fig. 12. Although the mechanisms described below occur in similar applications, the resulting microstructures can change depending on the experimental set-up. The following discussion focuses particularly on the role of polymers during the microstructural evolution and their influence on the physical and macroscopic properties of the investigated mortars.

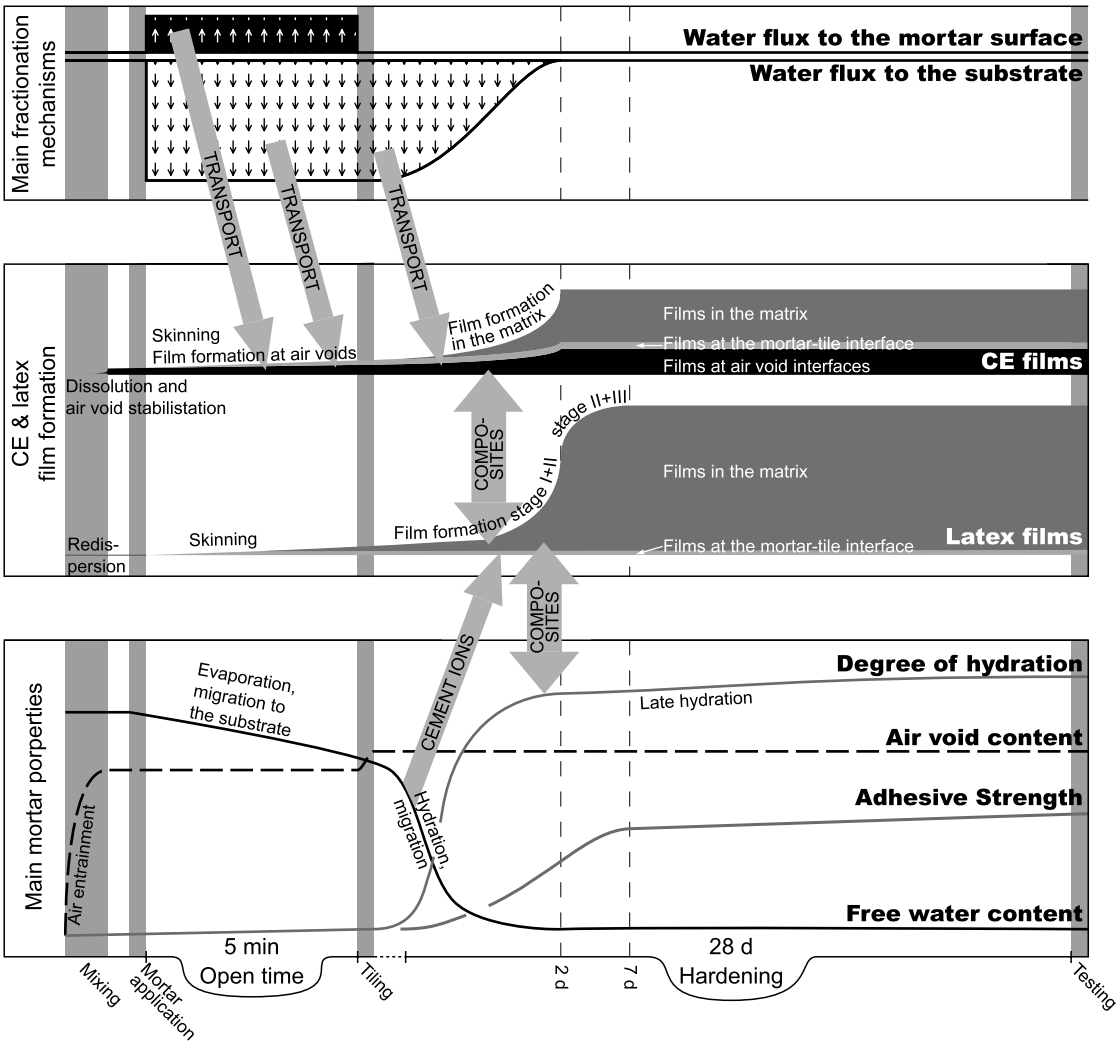

Fig. 12. Schematic synthesis of the mortar evolution. The non-linear horizontal time axis highlights the major mortar stages.

2.4.1 Mixing

During mixing, several important, polymer-related mechanisms occur: a) air entrainment, b) redispersion/dissolution of RP and c) initiation of CE film formation.

a) The air void content of mortars modified exclusively with CE is about 20 vol.%, whereas non-modified mortars contain only a few vol.% (standard pycnometer measurements). This implies that the air voids entrained during mechanical mixing are stabilised by CE. This inference is confirmed by ESEM in freeze-dried samples of fresh mortar (Fig. 3c), where the stabilisation is associated with a slight enrichment of CE at the interface between air void and wet cement paste. This enrichment can be assigned to the properties of CE as surface-active agent with a strong affinity to the gas-water interface. During mechanical mixing, the air voids are moved through the mortar and hence CE, which is dissolved in the pore solution, becomes attached at the air void interface. The air improves the workability during trowelling and tiling by influencing the mortar's rheology and compressibility during the fresh mortar stage.

b) RP can also influence the mortar's bulk rheology by slight air entrainment, mortar plasticising and stabilising, and the efficiency of RP with respect to these processes is strongly dependent on its redispersion rate. A homogeneous RP distribution also requires redispersion, and is important to prevent the formation of zones with unfavourable properties in both fresh and hardened mortar. The process of redispersion can be observed in model experiments (Fig. 3a; Zurbriggen & Jenni 2002), where the agglomerates of the RP disperse into the single latex particles. Proper redispersion is driven by the latex stabilising systems, redispersion aids and mechanical shearing. The PVA component can separate and form individual microstructures (PVA films). This separation is assumed to start very early, probably during mixing. With respect to the real mortar, a perfect redispersion of RP in cement pastes is indicated by the homogeneous distribution patterns for latex throughout the cement matrix (Fig. 6).

c) CE films are observed in fresh pastes (Fig. 3d). This is a clear indication for their formation during the mortar's wet stage, and the film formation driving force must therefore be their surface activity (Fig. 12).

With respect to cement hydration, the mixing time corresponds to the so-called induction period, which is dominated by a rapid exothermal dissolution of ions and the coeval formation of hydrate shells around the anhydrous clinker grains. This process starts immediately after water contact. As a result, the pore solution reaches a high ionic strength and pH-values of about 13. A review of hydration processes is given for example by Holzer et al. 2003 and Stark et al. 2000.

2.4.2 Mortar application and Open Time

Inhomogeneous phase distributions within the mortar bed and at the mortar-tile interface are partly related to the method of mortar application and to the duration of the Open Time (time interval between application of mortar until tiling). First, the fresh mortar is applied as a contact layer (approximately 0.3 mm thickness) onto the concrete substrate. In a second step, a toothed trowel is used to generate an alternating pattern of ripples and grooves, providing a constant mortar thickness after tiling. As the toothed trowel runs several times over the contact layer, the positions of the ripples can shift laterally, which may create cavities as observed in Fig. 13b. At this stage, water migration due to evaporation induces mortar fractionation, which invokes compositional gradients within the mortar ripples. Open Time may lead to skinning, which considerably reduces the wettability of the tile by fresh mortar and may reduce adhesion properties. The term skinning describes the sum of all mechanisms that change the composition of the mortar surface during the Open Time.

The mobility of polymer components was investigated in case of mortar ripples, which remained uncovered until fully dried and hardened. Fig. 13a shows a strong enrichment of PVA at the interfaces towards both air

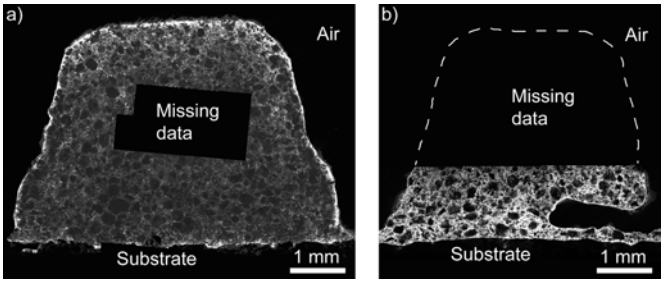

Fig. 13. LSM image showing cross-sections of hardened mortar ripples without inlaid tile. Evaporation induced water flux to the mortar surface was therefore active from mortar application to the end of the drying period. Note that this differs to the standard samples, where this mechanism acts only during the Open Time of 5 minutes. CE and PVA enrichments are bright. (a) PVA enrichment at the mortar-substrate interface and at the mortar surface. (b) CE enrichment at the contact with an internal cavity.

and substrate, where evaporation and capillary forces in the porous substrate, respectively, induce migration of the pore water and dissolved species to the mortar periphery. A similar transport and accumulation pattern occurs for CE. This accumulation geometry can be complicated by the occurrence of cavities, where an additional enrichment of CE or PVA at the surface of the cavity leads to an internal inhomogeneity, further increasing the CE/PVA concentration on top of the contact layer as the ripple is compressed during tiling. In samples with a standard Open Time of 5 minutes, the enrichment at the mortar-tile interface is small for CE and even below the detection limit for PVA (Fig. 7). Furthermore, dissolved inorganic components are migrating with the pore solution towards the surface and the substrate. However, associated processes such as cement hydration and capillary transport towards the substrate persist after the tile inlaying. The distribution patterns of inorganic phases are therefore not exclusively related to the Open Time fractionation and are discussed in relation with the progressive drying during the hardening process. Nevertheless it is important to note that the enrichment of inorganic phases at the surface may also contribute to skinning. Preliminary measurements revealed an increased concentration of $CaCO_3$ formed during Open Time at the surface. This is explained by portlandite efflorescence immediately followed by fast carbonation. As observed on common failure surfaces (e.g., Fig. 11), mortars predominantly fail along surfaces where skinning occurred. Therefore, these areas represent the weakest zones of the entire mortar bed.

2.4.3 Tiling

The moment of tiling is an important step because the 6 mm high ripples become squeezed to a continuous mortar bed of 1-2 mm thickness, inducing a considerably mass flow. Particularly, the associated mortar flux was studied in an experiment using a calcite-free mortar formulation, where parts of the ripple and groove surfaces were marked with powdered calcite. The final location of the markers in a cross-section was investigated using optical light microscopy. By comparison of initial and final position of the markers inferences about the flow pattern in the mortar can be drawn.

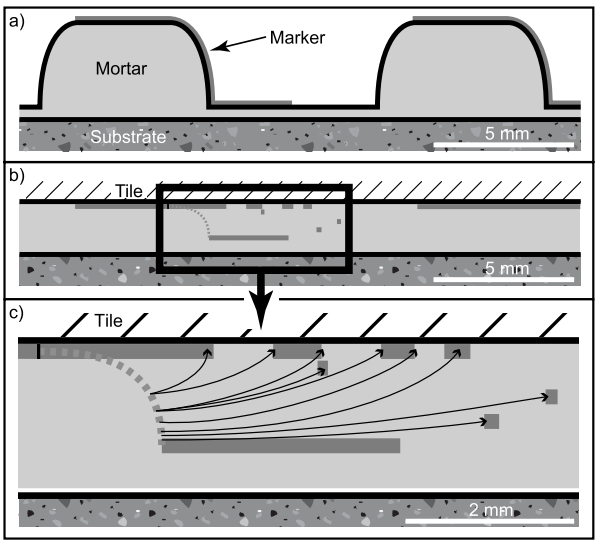

Fig. 14. Simplified diagram showing experiments on mortar flow caused by tile inlaying. (a) Parts of the ripple and groove surfaces have been covered with a marker. (b) After tile inlaying, the markers are redistributed over the mortar layer. (c) Arrows indicate inferred mortar flow during tiling.

At the mortar-tile interface, the initial surfaces at the top of the ripples are preserved, whereas the ripple flanks are completely disrupted. In the latter case, some parts are moved towards the tile interface in an area corresponding to a previous groove, while other parts are now embedded within the mortar matrix. In the experiment, the markers can be used to study the

mechanical redistribution of the mortar surface previously affected by skinning. As shown in Fig. 14, skins are mainly preserved on top of former ripples and on the bottom of former grooves. This geometry dominates the failure locations (Fig. 11): adhesion fracturing is prevalent at ripple surfaces, whereas cohesion fracturing occurs within the mortar matrix, predominantly in former groove domains (Fig. 10 and 11).

2.4.4 Hardening

During the hardening process, cement hydration and latex film formation continuously increase the strength of the bulk system. One critical parameter during hardening is the water concentration gradient, which is generated by capillary transport into the concrete substrate, by evaporation at the tile grouts and by chemical drying due to cement hydration. The water retention ability of CE and the amount of the finest-sized pores retard drying.

The vertical water flux into the underlying substrate results in a redistribution of organic and inorganic components. Figs. 6 and 7 indicate that the mobility is different for each of the three polymer types. PVA concentrations markedly increase towards the substrate interface. This enrichment can be attributed to a filtering effect associated with carbonation in the uppermost layer of the substrate. Carbonation leads to a general reduction of the pore size preventing the polymers from penetrating the concrete substrate. This is confirmed by the observation that PVA and CE in the substrate are exclusively found within micro cracks and not within the cementitious matrix. Analogously, the contact layer surface itself undergoes a pore size reduction due to smoothing by the trowel and skinning. Therefore, this horizon filters the downward migrating pore water, inducing PVA and CE enrichments. This accumulation enhances the skinning-related primary enrichment. In general, the distribution of CE is much more heterogeneous compared to PVA. Due to the high surface activity, CE occurs at air-paste interfaces in air voids and capillary pores, which are influenced by water fluxes. In contrast, the less surface active PVA is strongly intergrown with the cement-polymer matrix, suggesting that it is partly out of reach of migrating water.

In contrast to CE and PVA, latex distribution is homogeneous (Fig. 6) because latex was evenly distributed during mixing, and not transported during later mortar stages. The immobility of latex can be attributed to a) particle size, b) adsorption on cement particles, and c) wet sintering.

a) Latex particles have a size between 400 nm up to a few microns, whereas the capillary pores range down to 10 nm. Therefore, latex particles are not able to migrate through the capillary pore system.

b) Stark et al. 2001, Su et al. 1996 observed styrene acrylate latex adsorption on mineral surfaces, a process which also reduces the mobility of latex.

c) Routh & Russel 1999 describe latex film formation under wet conditions (wet sintering). This type of film formation generates cement-polymer composites, which become immobile during an early stage.

The redistribution of inorganic components due to water migration can barely be detected by means of element distribution mappings in the hardened mortar. Nevertheless, compositional gradients detected by TGA suggest portlandite depletion towards the concrete substrate (Fig. 8). As the drying front is progressing from grout to centre and from substrate to tile, hydration is stopped earlier in the peripheral grout region and near the substrate. The overall degree of hydration (reflected by the anhydrous volume fraction determined by image analysis of BSE SEM) seems to be uniform from substrate to tile, as this method is less sensitive than TGA profiling. Based on the overall uniform degree of hydration, local strength variations within the mortar bed are not expected.

Film formation occurs over an extended period and is also strongly related to the water content. For solution polymers (i.e. CE and PVA), film formation is mainly driven by evaporation and the water content of the film. Additionally, adsorption behaviour, surface activity, cross-linking, complexation, coagulation, and reduced solubility are further driving mechanisms for the accumulation of polymers and the formation of films.

More specifically, CE is already present at the air void interfaces during the mixing stage (Figs. 3c and d), where the oversaturation of water films induces CE film formation. Further dehydration leads to a closer entanglement of the CE chains, and film contraction. In advanced stages, CE films may detach from the air void interface, forming sail-like structures in the void (Fig. 4b).

Compared to CE, PVA is less surface active and therefore, the enrichment at air void interfaces is less effective. In addition, the PVA content in the mortar is generally much lower. Hence, PVA films predominantly occur within the cement-polymer matrix on a submicron scale, because local concentrations are too low to form structures comparable to the large CE films in voids.

In this context, it is important to note that most of our qualitative observations are restricted to relatively large polymer films at air void interfaces and large capillaries (Figs. 1, 4 and 5). However, small-scale domains within the finer capillaries and the submicron-scaled intergrowth of polymers and minerals in composite microstructures may be even more important for the overall material properties. However, it is suggested similar driving forces to those described for the larger films would also act at the submicron-scale.

The formation of latex films is even more complex as the polymer forms latex particles. Latex film formation starts with agglomeration (stage I) and deformation of these particles into hexagonal shapes (stage II). Routh & Russel 1999 describe a variety of different film formation mechanisms during stage I and II, which can be used to explain skinning and particle deformation during wet and dry mortar conditions. Four independent arguments lead to the conclusion that latex film formation, at least partly reaches the advanced stage III of particle coalescence, where polymers diffuse across initial particle boundaries. (1) A major strengthening of latex-modified mortars occurs well after the free water is used up, cement hydration stops and capillary latex deformation mechanisms after Routh & Russel 1999 are assumed to slow down significantly (Fig. 12). (2) Latex films in mortars show very smooth surfaces, relict particle structures are rare (Fig. 5a). (3) Latex films in mortars do not redisperse during water immersion (Holzer et al. 2001, Jenni et al. 2001a). As capillary latex deformation is principally a reversible mechanism dependent on the humidity, particle coalescence is a possibility to explain the water resistance. (4) Prolonged hot storage at 70°C or even around 100°C does not enhance adhesion properties. If the latex forms films by capillary deformation only under normal storage conditions, then increased diffusion rates during hot storage should significantly improve strength properties by such thermal treatments.

Cement phases and cement ions in the pore water influence the latex film formation (Jenni et al. 2001a, Larbi & Bijen 1990). These cement-latex interactions induce a strong intergrowth at the submicron scale between the two phases, leading to the formation of the cement-polymer matrix. As this is the main occurrence of latex in the microstructure, the latex-cement composite matrix is thought to have a major influence on the final properties of latex-modified mortars.

Comparison of latex structures in RP-modified mortars with and without CE indicates that the latex morphology changes (Figs. 4 and 5) pointing to latex-CE interaction. Thus, sail-like CE structures are absent in SA-/CE-modified mortars while they are still present in CE-/VC- and CE-/EVA-modified mortars. Therefore, the latex type influences the CE-latex interaction. Additionally, the difference in the CE distribution patterns between VC-/CE- and SA-/CE-modified suggests an influence of these latex-specific interactions on the CE mobility in the mortar (Fig. 7).

2.4.5 Adhesive strength and failure modes

Latex modification leads to an increase of the hardened mortar's adhesive strength (Fig. 9). Consistently, neither failure surfaces nor fracture surfaces parallel to the xy-plane in Fig. 2 intersect latex films (Fig. 4a). In contrast, many CE films are fractured (Fig. 4b). Consequently, CE films are weaker than latex structures and contribute less to the total adhesive strength than latex films (also shown by Fig. 9).

A major difference in fracture behaviour is observed in relation to the trowelling pattern of ripples and grooves. Above ripples, the tile contacts a surface that

underwent skinning, where adhesion fracturing predominates. Whereas in the region of former grooves, mortar flow during tiling forces fresh paste to wet the tile properly, and cohesion fracturing is more frequent (Figs. 10 and 11). Therefore, skinning on a future interface area can reduce adhesion properties drastically.

Entrapped air voids at the mortar-tile interface (inset Fig. 11) are a direct consequence of an uneven mortar surface and a stiff skin, because it prevents entrapped air to be mixed and sheared into the paste while tiling. Instead, the entrapped air remains at the interface with the tile and decreases the contact area between tile and mortar, which reduces adhesion properties (chapter 1).

To summarise, adhesive strength varies within the same formulation (Fig. 10). However samples with higher adhesive strength show increased percentages of cohesion fracturing, a correlation that is observed for all latex-modified tile adhesives. Hence, the mortar-tile interface is the weakest element of the substrate-mortar-tile system and therefore dominates failure behaviour.

2.5 Conclusions

The influence of polymers on microstructure and physical properties of mortars can be described as follows:

- The addition of latex increases adhesive strength of a tile adhesive mortar. Microstructural investigations confirm that latex is dispersed homogeneously in the cement-polymer matrix, which causes an improvement of both final cohesion and adhesion properties.
- Latex films with a width of 10-100 µm are observed at air void interfaces. These films usually include CE as a second polymer component and tend to be intergrown with cement phases. The composite latex-CE films represent the predominant occurrence of latex in the matrix. Therefore, they are considered to be responsible for the observed increase of adhesive strength. The affinity to form composite latex-CE films and their morphology is dependent on the type of RP latex (SA, EVA, and VC). Further investigations are needed to evaluate the influences of this latex-CE interaction on the mortar properties.
- Both, PVA and CE are dissolved in the pore solution and can form isolated films upon drying.
- During the Open Time, evaporation induces a water flux to the surface, whereas capillary forces pull the water to the porous substrate, a process that continues after tiling. The migration of pore water leads to a fractionation of soluble species, resulting in a distinct enrichment of PVA and CE above the substrate. With respect to the inorganic components, fractionation associated with water migration leads to a depletion of portlandite towards the mortar-substrate-interface.
- Investigation of failure surfaces reveals that mortar-tile interfaces represent the weakest part in the system. The adhesive strength of the entire system is dominated by the properties of this interface. In this context, skinning in particular induces a pronounced weakening of the interface strength. For that reason, future developments and research should focus on improvement of the interface properties.

Chapter 3

Changes in Microstructures and Physical Properties of Polymer-Modified Mortars During Wet Storage

A. Jenni, R. Zurbriggen, L. Holzer, M. Herwegh

(to be submitted to:
Cement and Concrete Research)

Abstract

The decrease in strength of tile adhesive mortars during wet storage was investigated. In a first approach, the water resistance of the polymer phases was tested in model and in-situ experiments. It was observed that cellulose ether and polyvinyl alcohol structures are water-soluble. Subsequent investigations on polymer mobility within the mortar showed that the migrating pore water transports cellulose ether and polyvinyl alcohol during periods of water intrusion and drying. In combination with filtering, this leads to enrichments above the mortar-substrate interface. In contrast, latices interacting with the cement are water-resistant, and therefore, immobile in the mortar. Further experiments revealed that the mortar underwent considerable volume changes depending on the storage condition. Simultaneous with the resulting cracking, cement hydrates grew within these shrinkage or expansion cracks. Combining the different data revealed that the strength decrease of wet stored tile adhesives is, on the one hand based on differential volume changes in the cement matrix, and on the other hand on the reversible swelling and resulting softening of the latex films.

3.1 Introduction

Polymer-modification is widespread in cementitious applications to improve the physical properties of building materials. As many of these materials are exposed to wet conditions during service life, numerous studies investigated the influence of water storage on their physical properties.

In the case of ceramic tile adhesives, material performance is tested by several strength tests after defined storage conditions and duration according to standard EN1348. The standard dry storage requires four weeks at 23°C and 50% relative humidity. Typically, after one week of dry storage microstructural evolution virtually stops and final strength is reached (chapter 2). The standard water storage procedure requires one week of dry storage followed by three weeks of immersion in water. Consequently, a comparison of physical properties between a dry and wet stored mortar sample corresponds to a comparison of properties right before and after the water immersion period of the specimen. The development of the material properties is strongly related to the evolution of the microstructures. For this reason, we focus on water-induced changes of polymer-related microstructures in case of a cementitious tile adhesive. These products are commonly modified with cellulose ether (CE) and redispersible powder (RP), the latter containing latex and polyvinyl alcohol (PVA, for mortar formulation see Table 1). Each of these polymers fulfils different tasks during the mortar evolution. CE thickens the fresh mortar, entrains air during mixing and retains water. RPs mainly provide flexibility and tensile strength in the hardened mortar. The powder is usually manufactured by spray drying of a PVA containing latex emulsion. In contrast to the well-investigated concrete applications, such tile adhesive mortars are prepared with a high w/c (water/cement ratio) of approximately 0.8 and characterised by high air void contents of more than 20 vol.%, and low degrees of cement hydration (less than 30%).

In the literature, the influence of storage conditions including water contact on the mechanical properties of polymer-modified cementitious products were studied extensively (reviewed in Ohama 1995, more recent studies e.g., Ball & Wackers 2001, Schulze 1999, Schulze & Killermann 2001). Some of these studies also investigated microstructural changes during wet storage. The investigations of Tubbesing 1993 include a microstructural characterisation of wet-stored polymer-modified mortars. Based on scanning electron microscopy (SEM) images of fracture surfaces, Schulze & Killermann 2001 concluded that latex morphology undergoes no structural changes, even after 10 years of

[wt.%] of Dry mix	Component	Details
35.0	Ordinary Portland cement	CEM I 52.5 R, Jura Cement Fabriken, Wildegg, CH
40.0	Quartz sand	0.1-0.3 mm, Zimmerli Mineralwerke AG, Zürich, CH
22.5	Carbonate powder	Durcal 65, average grain size 57.5 µm, Omya AG, Oftringen, CH
0.5	Cellulose ether	MHEC 15000 PFF, Aqualon GmbH, Düsseldorf, D
2.0	Redispersible powder	VC, SA, EVA: lab samples with different latex compositions, containing PVA, Elotex AG, Sempach Station, CH
25.5	Water	deionised

Table 1. Formulations used for ceramic tile adhesives. Note that the percentages relate to 100 wt.% of the dry mix.

outdoor exposure. Other studies focussed on changing pore size distributions due to water contact (e.g., Cook & Hover 1999, Silva et al. 2001, Su 1995). Water intrusion and shrinkage/expansion were extensively investigated, but only in the field of concrete (e.g., Koenders 1997, Krenkler 1980, Lunk 1997, Stark & Wicht 2000). Some general findings also apply to polymer-modified mortars, whereas additional aspects like hydrophobicity (Lu & Zhou 2000) and the increased importance of the mortar's interface (Bijen et al. 1999, Justnes et al. 1999) have to be considered.

The presence of several organic, polymeric additives in tile adhesives creates a complexity of possible polymer-polymer and polymer-cement composite microstructures (chapter 2). Compared to former studies, we tried to focus on these polymer-related microstructures and how they developed during wet storage. Mechanisms like water intrusion, polymer mobilisation and redistribution, cement hydration and mortar volume changes play an important role and were investigated. Only a thorough knowledge of these mechanisms and their influence on the microstructures and the physical properties allows improvements of the system and the components involved.

In this study, we apply a variety of different analytical techniques to investigate this highly complex system. First of all, the water resistance of the three polymer types (latex, PVA, and CE) was studied in model and in-situ experiments, followed by a quantitative investigation on their distribution within the real mortar before and after wet storage. Finally, with analysis of the microstructure on failure surfaces, it was possible to link the microstructural changes with the mechanical properties.

3.2 Materials and methods

3.2.1 Light microscopy

To investigate the water resistance of polymer films, experiments on the individual polymers were performed. For this purpose, polymer powders were redispersed (RP) or dissolved (CE/PVA) in water with an ionic composition representative of the pore water during early cement hydration. In this context, three different types of aqueous phases were used: (a) deionised water, (b) a filtered cement water, and (c) a synthetic cement water (Table 2). The filtered cement water derived from the cement paste used in all experiments of this study. This filtered water may deviate from the true pore solution in the fresh mortar and therefore synthetic cement water was used which is assumed to represent a more realistic pore solution chemistry (Odler & Strassinopoulus 1982). RP containing ethylene/vinyl-acetate latex (EVA) was also dispersed in water containing NaOH, CaO, and $CaCl_2$.

	Filtered cement water	Synthetic cement water
Pro-duction	Filtering of a 5 min old Portland cement paste (w/c=1)	Mixing of pure components
Na	540 mg/l	870 mg/l
K	7800 mg/l	9000 mg/l
Ca	400 mg/l	150 mg/l
SO_4	8400 mg/l	9700 mg/l
Cl	140 mg/l	0 mg/l
pH	13.1	12.7

Table 2. Composition and pH of filtered and synthetic cement waters used for synthesis of the polymer films in the model experiments.

The amount of NaOH and CaO corresponded to a pH value of 12.5, whereas the $CaCl_2$ concentration was adjusted to reach the same Ca^{2+} concentration as in the CaO solution. The RP concentration in these deionised or cementitious waters was 10%, the CE concentration2% and the PVA concentration 2.2%. Dispersion or dissolution of the polymers was achieved by ultrasonic treatment at 25 kHz/50 W for 2 minutes. A metal grid of 86 µm sized square voids was immediately dipped into the polymer solution or dispersion, before gravitational fractionation occurred (Fig. 1a). Evaporation of the water under room conditions increased the polymer concentration and caused the formation of polymer films. The amount of each polymer used was carefully evaluated in advance to promote the formation of polymer films with a hole in the centre. This situation is, in terms of film dimensions, similar to polymer films in real mortars (Fig. 2a). After storage for at least 2 weeks under room conditions, the films were exposed to deionised and synthetic cement water between two glass slides for time intervals ranging from 10 minutes up to 2 months (Fig. 1b). Water induced changes in the film structure were observed by transmitted light microscopy and qualitatively rated on a scale between 0 (complete disintegration, Figs. 2a and b) and 1 (no major changes of the film morphology, Figs. 2c and d).

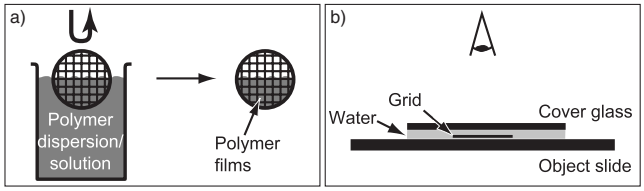

Fig. 1. (a) Polymer films with thicknesses of about 1 µm are generated by dipping a grid into polymer dispersions or solutions. The polymer films form in grid meshes by evaporation of the water. (b) Water resistance experiment: a grid with polymer films is placed between two glass slides and immersed in water. Morphological changes can be monitored by light microscopy.

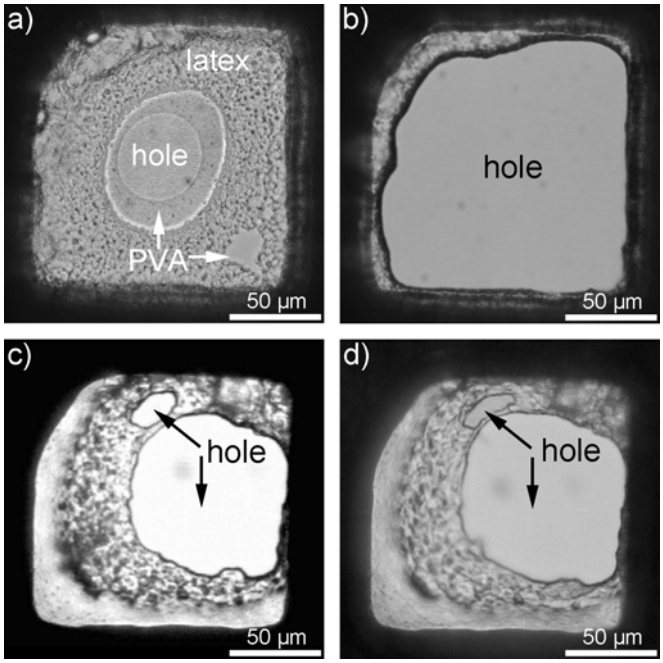

Fig. 2. (a) A composite polymer film consisting of PVA and latex formed from RP redispersed in deionised water. This structure is representative of all investigated RPs. (b) Decay of composite film due to water exposure. (c) Polymer film of the same redispersible powder, but redispersed in filtered cement water. Only one polymer film is developed that is water-resistant (d). Even after several weeks of water contact, only minor morphological changes are visible.

The size of these artificial polymer films corresponds to the polymer films in air voids (pores of >10 µm) of real mortars. However, care is required in extrapolation of these results from such model experiments to real mortar. Cement-polymer interaction is not restricted to the pore solution, but also occurs at various solid-liquid interfaces, which can lead to intergrowth of minerals and polymers. Therefore, we also performed

environmental scanning electron microscopy (ESEM) in-situ studies on polymer films in water stored mortars.

3.2.2 Environmental scanning electron microscopy

ESEM allowed in-situ observation of microstructures before and after water contact. The behaviour of the polymeric microstructures during such water immersion experiments revealed their water resistance.

First, the formulations of three lab mortars with a single polymer type (latex, PVA, or CE) were analysed. In a second step, real formulations with two or all three polymer types were investigated (formulation details see Table 1; in lab mortars with only one or two polymer types, mineral filler replaced the omitted polymers). This type of comparative study allowed the development of characteristic morphological criteria to identify each single polymer type before interpreting microstructures in real mortars containing all additives.

Based on standard EN1348, the mortars were applied in two steps on a concrete plate (10x40x3 cm, Gehwegplatte, Gebr. Müller AG, Triengen, Switzerland; water uptake is approximately 3.0 wt.%). (1) A first contact layer with a thickness corresponding to the coarsest grain size (approximately 0.3 mm) and (2) In a ripple and groove pattern induced by a toothed trowel (teeth 6x6x6 mm) on top of the first contact layer. After 5 min (Open Time), fully vitrified ceramic tiles (5x5x0.5 cm; Winkelmanns weiss unglasiert lose, SABAG Bauhandel AG, Rothenburg, Switzerland) were laid in. They were loaded with 2 kg for 30 seconds, creating a 1-2 mm thick mortar layer between concrete substrate and tile. A more detailed description is available in chapter 1. After 28 days of dry storage (23°C and 50% relative humidity), the sample was crushed, and a mortar fragment smaller than 3 mm was sampled. The fragment was attached to the sample holder and inserted into the sample chamber of a Philips ESEM-FEG XL30 equipped with a gaseous secondary electron detector and a Peltier cooling stage. Polymer domains were located, imaged and their coordinates were stored. By changing the sample temperature and the water gas pressure, water condensed on the sample, which was consequently wetted completely. After 30 minutes of water exposure, all water was evaporated by changing temperature and pressure conditions. During the whole experiment, the temperature was in the range of 1-10°C. The polymer domains were revisited, imaged and qualitatively compared with the microstructures documented before watering.

This method reveals no quantitative information about polymer redistribution in the mortar bed during wet storage. For this purpose, additional measurements on polished sections of the real mortar were carried out.

3.2.3 Quantitative scanning microscopy

Two specific methods were developed to quantify the latex, CE, and PVA distribution within mortars with compositions according to Table 1 and prepared as described above. The localisation and quantification of the latex from the RP containing vinyl-acetate/ethylene/vinyl-chloride (VC) bases on wavelength-dispersive spectrometric (WDX) Cl mappings, which were measured on impregnated and polished mortar sections by an electron microprobe (Cameca SX-50).

CE and PVA were stained with a fluorescent dye prior to mortar mixing. Their distribution in the mortar bed was measured with a laser scanning microscope (LSM) on impregnated and polished sections. The resulting distributions of the three polymers in the mortar bed were normalised to the cement-polymer matrix, revealing the polymer distribution in the matrix. Following Ohama 1987, we define the cement-polymer matrix as the sum of all cement phases including gel pores (<10 nm) and capillary pores (10 nm-10 µm), and all polymer phases. The whole mortar consists therefore of air voids, mineral fillers and the cement-polymer matrix. As many mechanisms fractionate the mortar components across the mortar bed, the distribution patterns were depicted in cross-sections perpendicular to the mortar bed and the trowelling direction. An extended description of sample preparation, image acquisition, analysis, and quantification of polymer-modified mortars is available in chapter 1. Microstructural quantification was applied

to samples with the formulations shown in Table 1. The samples were subjected either to dry storage (28 days at 23°C and 50% relative humidity) or wet storage (7 days at 23°C and 50% relative humidity + 21 days completely immersed in water, followed by at least 28 days under room conditions before impregnation). The obtained data provide the basis for (a) the detection of various microfabric modifying processes during wet storage, and for (b) a comparison between microstructures and physical tests.

3.2.4 Testing of mechanical properties

The adhesive strength was measured by a standard tensile test according to EN 1348. Shear strength and flexibility were evaluated by a test in which, in contrast to the tensile test, the deformation apparatus was run in compressive mode pushing the ceramic tile (50x50 mm), which overlapped the substrate plate by 10 mm. Both applied force and shear displacement were continuously monitored. In order to obtain the shear strength, the measured force was divided by the mortar-tile contact area (2000 mm^2). This simple method provides information about both, shear strength and flexibility (applied shear strain and maximum deformation at break, respectively). The average of five individual measurements of the same sample batch was calculated. In contrast to the sample preparation for microscopy, the mechanical properties of wet stored samples were measured immediately after withdrawal from the water tank.

Alternating storage consists of dry-wet cycles including 7 days of dry storage (23°C and 50% relative humidity) and 21 days of wet storage (completely immersed in water). The tests described above were performed immediately after each storage period.

Shrinkage and expansion were measured on 1x4x16 cm mortar prisms that were demoulded after 24 hours for a zero reference measurement. The prisms were then stored under conditions of dry or wet storage and prism length was measured at selected times.

3.2.5 Examination of failure surface

Illumination of mortar surfaces with ultraviolet light excites CE and PVA stained with a fluorescent dye, which emits green light. The intensity of the emission depends on the concentration of the dye, i.e. the polymer (Rost 1991; see also chapter 1). Using transparent glass tiles (similar material properties as the ceramic tiles), this method delivers qualitative information about the CE or PVA distribution on failure surfaces or at mortar-tile interfaces prior to the physical test.

In detail, an ultraviolet light bulb (VL-100F, 100 W, and 365 nm) irradiated the sample's surface from a distance of 20 cm and an angle of 75°, and a digital camera was placed perpendicularly. Images were acquired immediately after illumination to prevent bleaching artefacts (Song et al. 1995).

Furthermore, SEM was used to study the fracture morphology. For this purpose failure surfaces were coated with a 300 nm thick carbon layer (Balzers carbon coater) and examined in a CamScan CS4 SEM equipped with a Robinson backscattered electron (BSE) detector and a Voyager 4 digital image acquisition system.

3.3 Results

3.3.1 Model system

During water storage there is a significant loss in adhesion strength. In order to understand the role of the polymer during water contact, we performed model experiments where the behaviour of polymer films was microscopically investigated during water immersion (chapter 2.1).

Fig. 2a shows RP after film formation in a deionised water environment. The transparent PVA film in the centre is clearly distinguishable from the textured rim (Jenni et al. 2001a). The film identification is based on film morphology, which was compared with monophase latex or PVA systems and was also confirmed by element dispersive spectroscopy. Within minutes, both phases disintegrated (Fig. 2b) during

water exposure. In contrast, a monophase film formed from RP redispersed in cement water (Fig. 2c) was water-resistant even after several weeks of water immersion (Fig. 2d). Macroscopic polymer foils synthesised from deionised and cement water behaved in a similar manner when exposed to water.

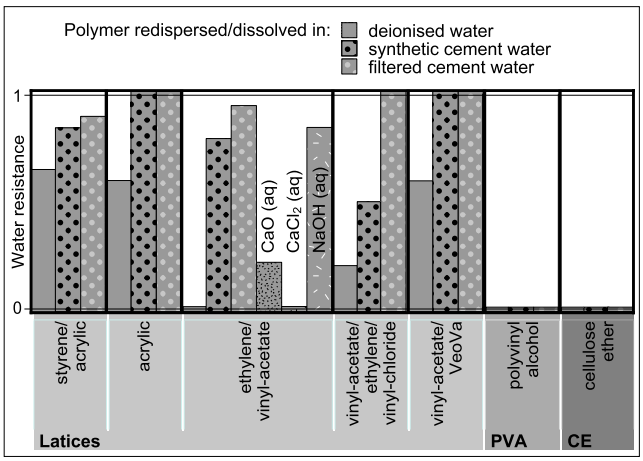

Fig. 3. Qualitative observation of the water resistance of different polymers synthesised from different types of cement waters. Vertical axis: 0 = virtually complete disintegration (shown in Fig. 2b), 1 = no changes during water contact (shown in Fig. 2d).

Different types of RP, CE, and PVA films synthesised from redispersions/solutions made of deionised, synthetic cement, and filtered cement water were rewetted by deionised water (Fig. 3). All RP films showed a remarkable increase in water resistance when synthesised from a redispersion made of cement water instead of deionised water. In particular, a large increase of EVA water resistance was observed in the presence of cementitious ions. In general, RP films synthesised from filtered cement water were more water-resistant than RP films synthesised from synthetic cement water. NaOH seems to have a more pronounced influence on water resistance than Ca salts. In contrast, CE and PVA redissolved instantaneously, independent of the composition of the aqueous phase used for film synthesis.

To check for a potential influence of cement water (a situation that is closer to a real wet-stored mortar system), all films were also exposed to cement water. However, no difference in polymer behaviour was observed with exposure to cement water, relative to deionised water.

3.3.2 In-situ watering

To investigate the behaviour of polymers in a real mortar exposed to water, mortar samples containing only one polymer type were monitored before and after wetting within the ESEM sample chamber (method description in chapter 2.2, data in Fig. 4). The images below represent typical examples from an extensive image database.

The latex film depicted in Fig. 4a survives the wetting period without major changes (Fig. 4b), and only the film surface tends to change from a smooth to a more structured morphology. In contrast, CE structures (arrows in Fig. 4c) dissolve completely during wet storage (Fig. 4d). Fig. 4e shows the base of an air void with no polymer microstructures. After water immersion, PVA films precipitated out of the evaporating water (Fig. 4f), clearly indicating the mobility of PVA.

These results are consistent with qualitative SEM investigations on fractured mortar samples after water storage. There, latex films are present and partly overgrown with cement hydrates, whereas the typical CE membranes of dry stored mortars are absent after water storage (Jenni et al. 2002).

3.3.3 Distribution patterns before and after wet storage

By combining WDX, fluorescence microscopy and the appropriate image analysis techniques, the spatial distributions of the polymer phases were determined. The comparison of the distribution diagrams before and after wet storage indicates which polymer type is mobilised, to what extent and in which direction.

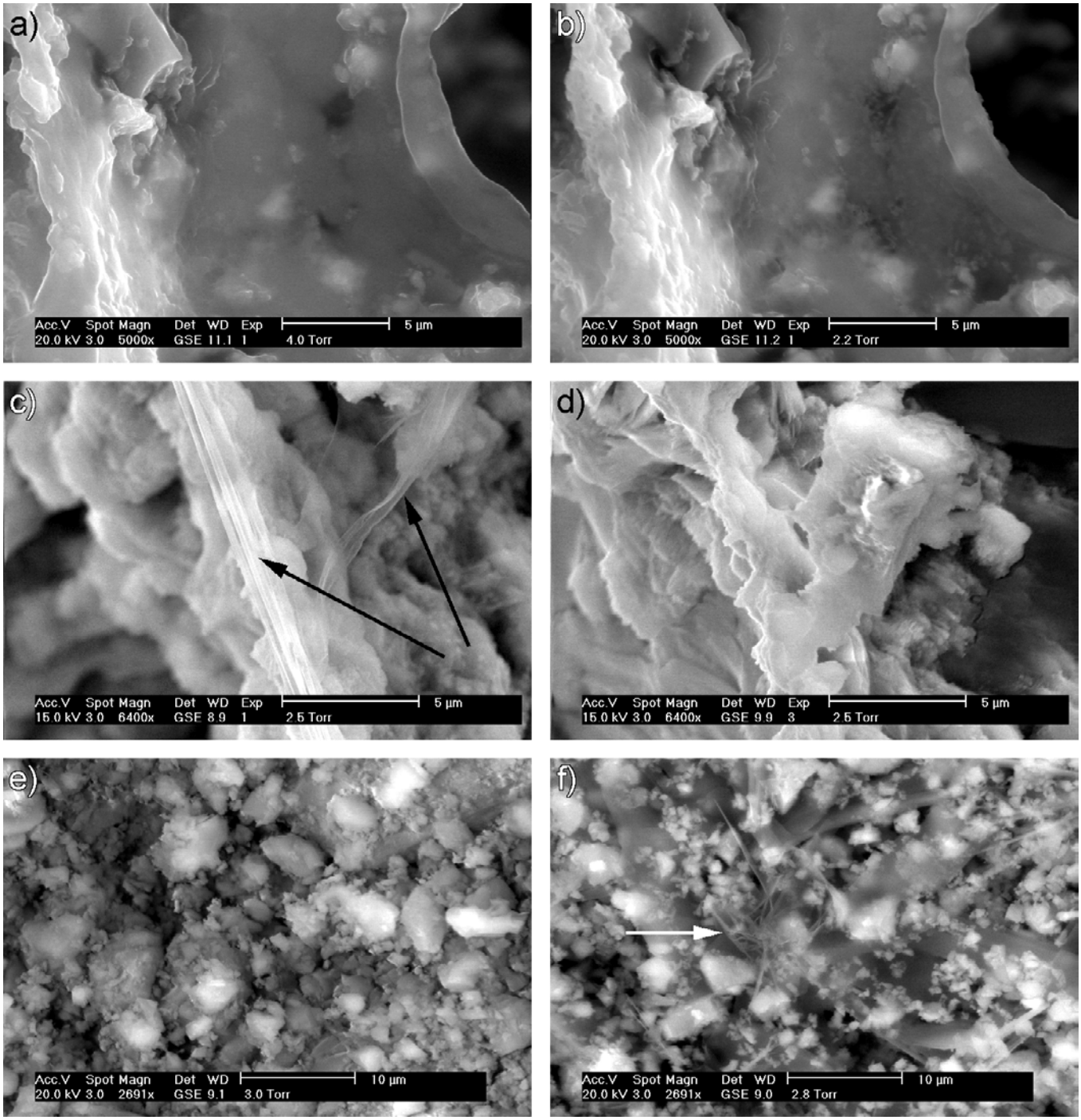

Fig. 4. In-situ polymeric microstructures in mortar before (left column) and after wetting experiment (right column) in the ESEM sample chamber. Each pair of pictures shows the same location in the microstructure. The VC latex film remains unchanged during wetting and redrying (a, b), whereas CE structures (marked in c) are completely dissolved (d). PVA structures could not be found in the mortar before wetting (e), but PVA films form as the water front retreats during redrying (f).

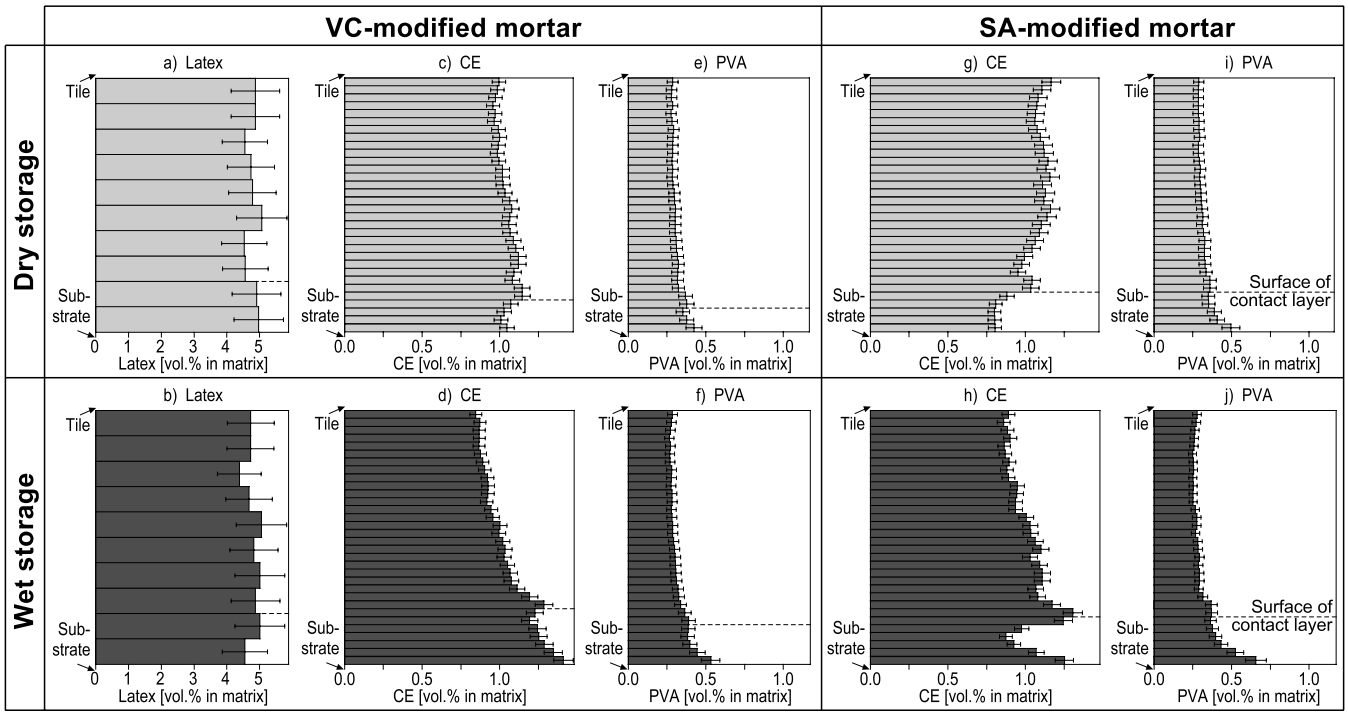

Fig. 5. Quantitative distribution diagrams of VC latex, CE and PVA across the mortar bed for dry and wet stored samples. VC distribution was measured by chlorine mapping of a 1.5 mm wide section in the centre of the mortar bed. CE and PVA were stained with a fluorescent dye and visualised by laser scanning microscopy across the half-length mortar bed. The polymer concentrations in horizontal stripes were stacked to generate vertical concentration profiles across the 1.1-1.4 mm thick mortar bed.

Due to large differences in grain size between the coarse sand fraction and the fines that comprise the cement-polymer matrix, the interstitial matrix phase is enriched at the relatively flat interfaces to tile and substrate. In order to remove this geometric effect on calculations of distributions within the matrix, and to investigate potential polymer fractionations within the matrix, all constituents are normalised to the volume percentage of the cement-polymer matrix.

Fig. 5 shows a representative VC latex distribution in the cement-polymer matrix before (a) and after (b) wet storage. The mortar bed is subdivided into layers parallel to the mortar-tile interface and for each layer, the latex concentration in the cement-polymer matrix is depicted. Apparently, there are no changes in latex concentration and distribution during wet storage. To date, no methods exist to visualise and quantify other latices within the microstructure.

Analogously, Figs. 5c and g show the CE distributions in a VC-/CE-modified and a SA-/CE-modified dry-stored mortar, respectively (SA: RP containing styrene/acrylic latex). After wet storage, the corresponding CE distributions are shown in Figs. 5d and h. Both wet stored mortars show a more pronounced CE increase from tile to first contact layer than before wet storage. The enrichment present at the contact layer surface after dry storage increased significantly, and there is also a strong enrichment right above the substrate.

The PVA distributions in the same two dry- and wet-stored mortars are depicted in Figs. 5e, f, i, and j. In both mortars, the PVA enrichment at the substrate surface is more intense after wet storage. Otherwise, the distribution patterns after dry and wet storage are identical.

3.3.4 Mechanical properties

Dry and wet stored mortar samples were subjected to adhesive strength tests to compare their mechanical properties (Fig. 6a, first cycle). Testing of the wet

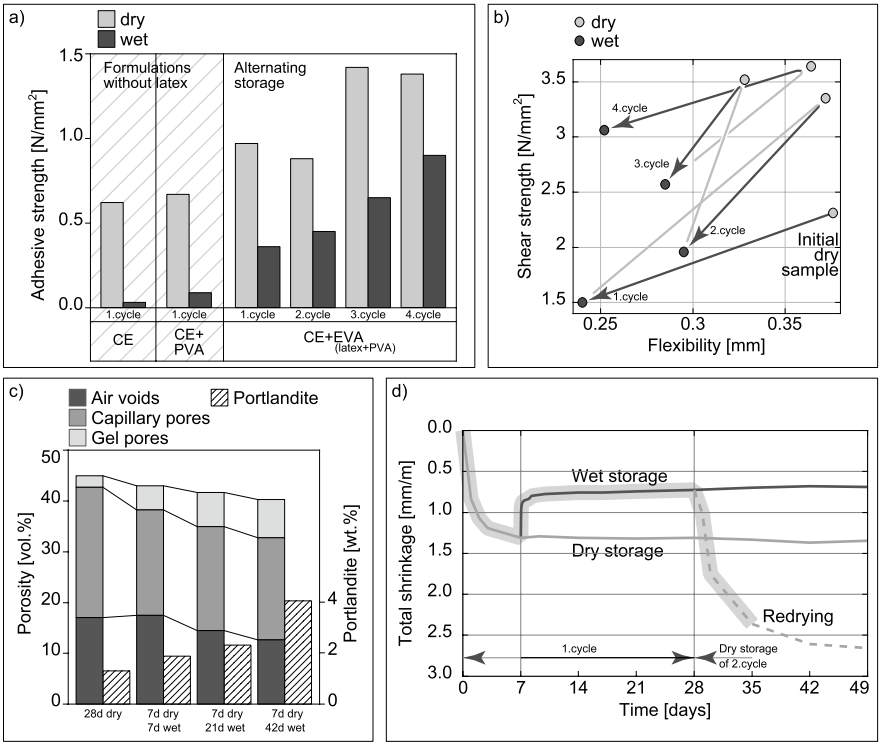

Fig. 6. (a) Adhesive strength of different mortar formulations (Table 1; in lab mortars with only one or two polymer type, mineral filler replaced the omitted polymers). The two formulations on the left (hatched area) contain no redispersible powder. On the right, a tile adhesive modified with CE and EVA underwent cycles of dry-wet storage ranging from one up to four cycles. (b) Evolution of shear strength and flexibility (deformation at break) during dry-wet cycling of the same EVA-modified mortar measured in a). (c) Pore size distribution after dry and wet storage. The amount of air voids (>10 µm), capillary pores (10 µm - 10 nm) and gel pores (<10 nm) were calculated from a continuous pore size curve measured by mercury intrusion porosimetry. The amount of portlandite, analysed by the method of Franke 1941, is an indicator for the degree of cement hydration. Data taken from Knöfel et al. 1998. Analogous changes in pore sizes and portlandite content are expected during alternating storage cycles depicted in a), b), and d). (d) Shrinkage and expansion during dry and wet storage, and during redrying of a mortar prism.

stored samples was carried out immediately after removal from the water tank. All wet stored formulations show a decrease in adhesive strength compared to their dry stored equivalents. Mortars without CE were not tested because they are not applicable as tile adhesives. However, modification of the mortar with RP reduces the strength decrease remarkably (Fig. 6a).

In addition, an alternating dry and wet storage was applied to a mortar modified with EVA and CE. Adhesive strength, flexibility and shear strength were measured immediately at the end of each storage period. In general, the measured adhesive strength increased with each new dry-wet cycle (Fig. 6a). Fig. 6b shows the corresponding flexibility and shear strength values. After the initial dry storage, the following wet storage provokes a decrease of both flexibility and shear strength. After the second dry storage period, the flexibility recovers and reaches the value of the initial sample, whereas the shear strength increases. In the following wet-dry storage cycles shear strength increases after each cycle. With respect to flexibility, a slight decrease occurs after each cycle.

Fig. 6c shows the evolution of pore distribution (mercury injection porosimetry) and portlandite content (measured after Franke 1941) as function of the wet storage duration. The total porosity decreases with ongoing wet storage and the pore size distributions shift towards smaller pore sizes (gel pores). Simultaneously, the portlandite content, which is an indicator for the degree of hydration, increases.

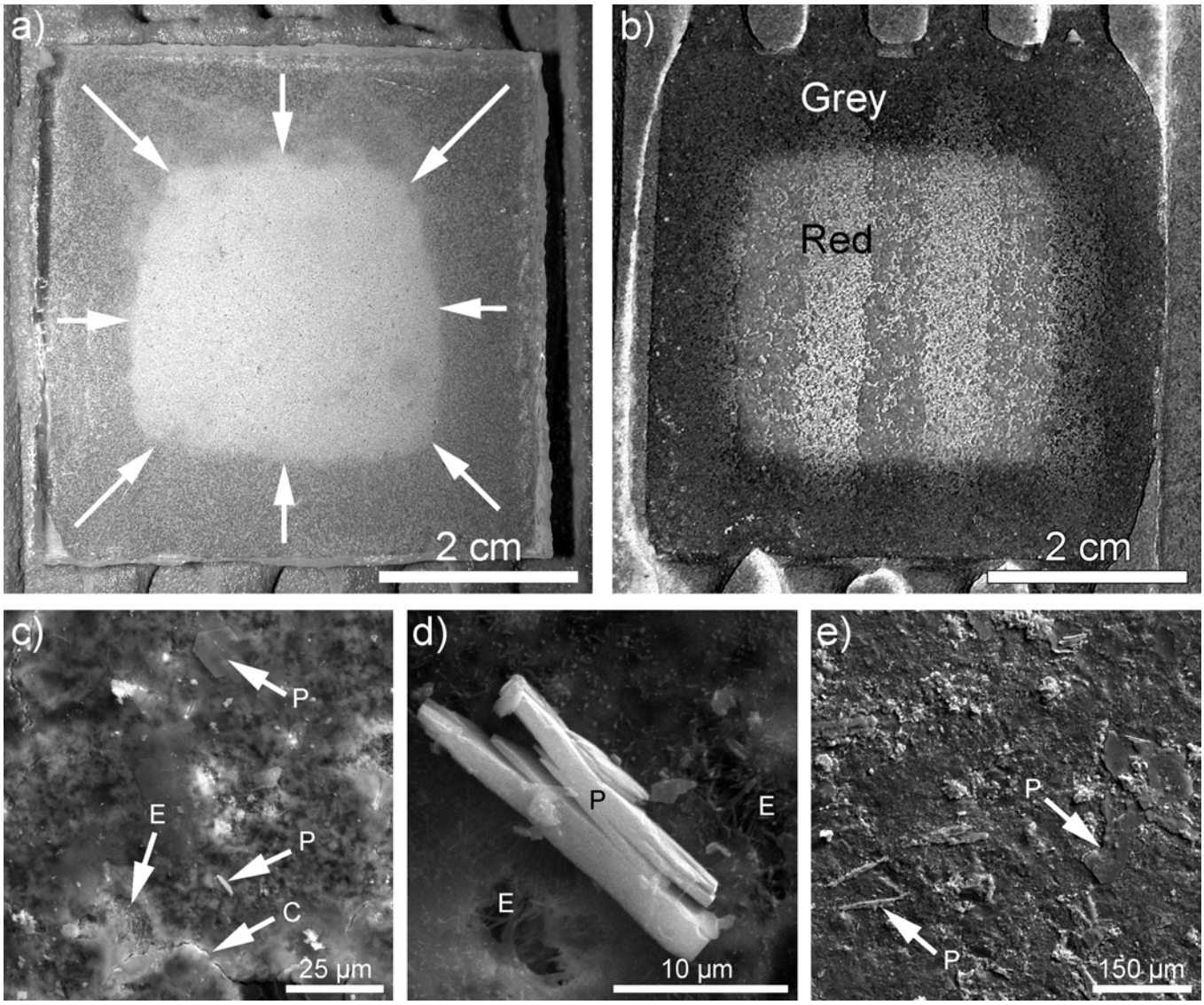

Fig. 7. Microstructures at the mortar-tile interface. (a) Glass tiles allow tracing of the intruding water front. Situation after 2 days of water immersion. (b) Mortar bed of dry stored mortar after tearing off the tile. The phenolphthalein test indicates that a rim of approximately 1 cm of the mortar bed is carbonated. SEM images: (c, d) Ettringite (E), micro-cracks (C), and portlandite (P) on the failure surface of a wet stored VC-modified mortar (Table 1). (e) Tile part of the mortar-tile interface after adhesive strength test, opposite side from sample shown in c).

Fig. 6d documents measurements of the mortar volume changes during wet and dry storage. Dry-stored mortars shrink within the first 7 days. The following wet storage induces a rapid expansion during the first 2 days. Surprisingly, redrying of this wet-stored sample induces shrinkage that is twice as intense as the initial drying shrinkage.

3.3.5 Failure mode and related microstructures

During adhesive strength tests, wet stored samples predominantly fail along the mortar-tile interface (adhesion failure). In this context, the mechanism of interfacial water intrusion and the consequences for mineral growth or lateral polymer redistribution are of special interest. Therefore, the migration of the waterfront at the mortar-tile interface was observed

through a transparent tile (Fig. 7a). The capillary waterfront can be recognised as an abrupt change in colour from bright (dry) to dark grey (wet). In terms of water migration the following points are observed by mapping the waterfront in time intervals: (a) The migration rate of the water front slows down in mortars with increasing amounts of latex, and also depends on its hydrophobicity. (b) Water intrusion in the mortar bed starts at the rim of the tile and progresses continuously towards the centre. Additional SEM investigations showed that in the rim regions, both portlandite and ettringite are found, whereas ettringite predominates towards the centre. This difference in mineralogy is attributed to the variable time interval during which water is present at the rim and at the centre, and occurs close to the tile-mortar interface as well as in the mortar bed itself. The minerals were identified by their morphology.

At the interface, ettringite grows in pores and in shrinkage/expansion cracks opened during water storage (Figs. 7c and d). Ettringite needles grown in these cracks rarely touch the opposite crack side and therefore do not induce cracking, but only fill the created cavity. It is important to note that these cracks do not occur in dry-stored mortars. No ettringite grows across interfacial cracks, e.g., between mortar and tile. In contrast, portlandite plates grow parallel and perpendicular to the interface, and even grow onto the ceramic tile (Fig. 7e).

Phenolphthalein applied to the failure surface of a dry stored mortar sample (after RILEM Committee CPC-18 1988) shows a carbonation front that advanced from the grout (peripheral part of mortar bed) towards the centre (Fig. 7b).

The failure surfaces and the mortar-tile interface observed through a glass tile were illuminated with ultraviolet light to excite the stained CE, providing a qualitative CE distribution in the plane of the interface. Note that the section in Fig. 8 is perpendicular to the vertical distribution profiles shown above. The mortar-tile interface of the dry stored mortar shows CE enrichment within a rim of 1 cm (Fig. 8a). Fig. 8b shows the same mortar after wet storage. The boundary of CE enrichment is more localised and curved towards the centre. These accumulations are confirmed by observations performed on failure surfaces after the adhesive strength test (Figs. 8c to f). As the stained CE is present in the whole cement-polymer matrix, the emitted green light traces this matrix on a macroscopic scale (chapter 1). Two types of failures can be distinguished: adhesion failure occurs at the mortar-tile interface, whereas cohesion failure is localised within the mortar bed. Comparing failure modes after dry and wet storage (Figs. 8c and e versus Figs. 8d and f) indicates that dry storage causes mixed failure (adhesive failure above ripples and cohesive failure above grooves), whereas wet storage predominantly induces pure adhesion failure. An exception is the central part where a tendency for cohesive failure exists. Besides studying the mortar-tile interface, the chosen set-up also allows the investigation of initial ripple and groove surfaces that remained uncovered by the tile. Here, CE concentration is higher compared to the mortar interior, but seems to decrease during wet storage, a fact that might be attributable to dissolution of superficial CE into the tank water. However, analysis of the tank water chemistry showed only low polymer concentrations. This implies that almost no polymers left the mortar system.

The enrichment of CE at the mortar surface is also documented by combined SE/BSE microscopy. The smoother surface of the SE compared to the BSE image reflects the existence of polymer films on top while the internal part of the mortar surface is documented by the BSE picture (Figs. 9a and b). Note the apparently larger cavities (framed) in the BSE image, which are covered by polymer films in the SE image.

Principally, PVA shows the same horizontal distribution patterns, but due to its lower concentration, the zones of enrichment are less obvious than is case for CE.

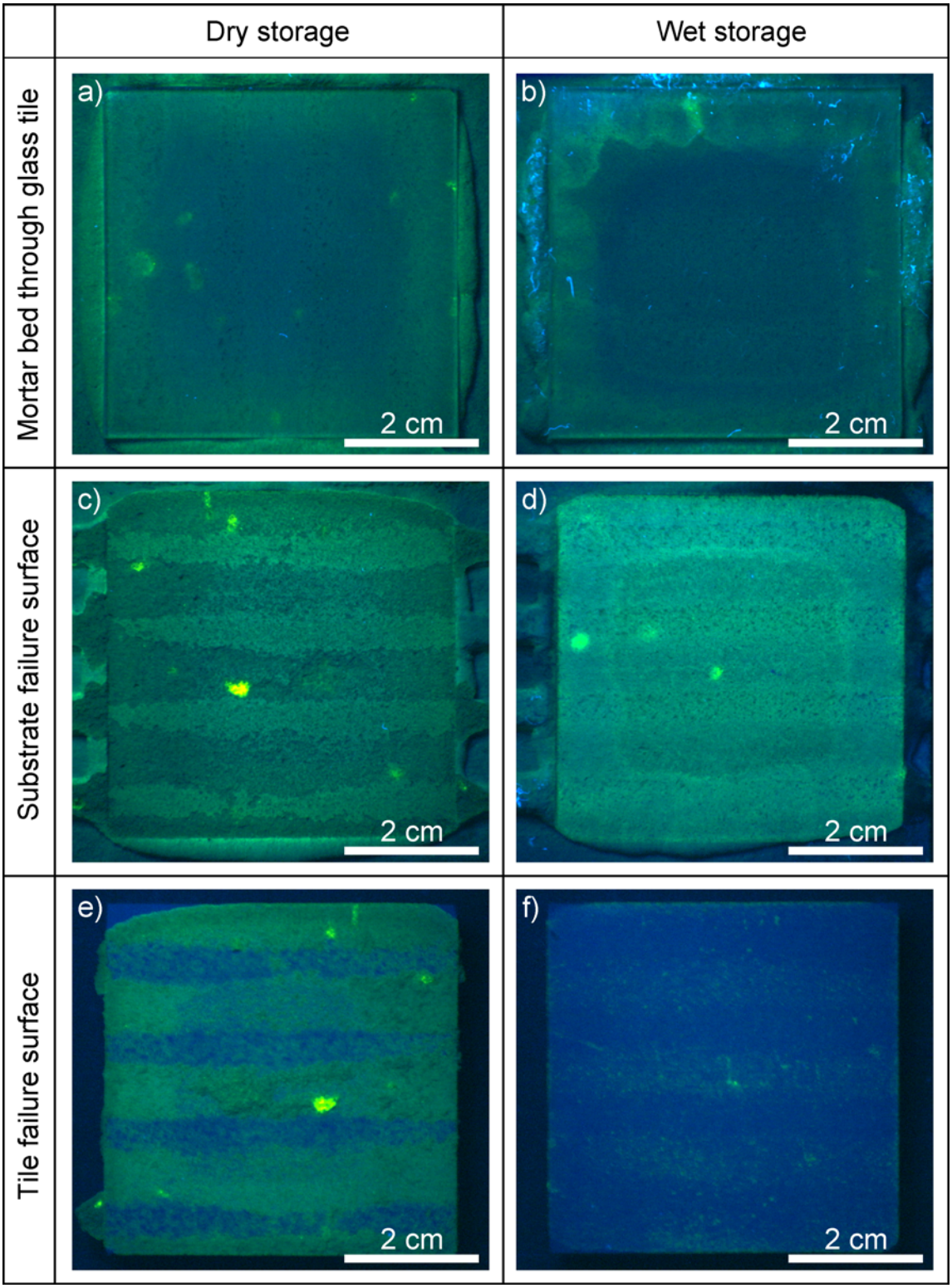

Fig. 8. SA-modified mortar samples (Table 1) illuminated with ultraviolet light to excite the stained CE (green) within the mortar. Dry stored samples in the left, wet stored in the right column. (a) and (b) show the mortar covered by a transparent glass tile, (c) and (d) the mortar failure surface, (e) and (f) the tile failure surface after adhesive strength test.

3.4 Discussion

The mechanisms that occur from the time the fresh mortar is mixed until hardening, and the resulting microstructures are extensively discussed in chapter 2. One of the major findings was that the migrating pore water causes several mortar components to segregate across the mortar bed. The resulting microstructural heterogeneities have a major influence on type of failure mode and bulk strength. As water intrusion during wet storage also induces water fluxes, further fractionation can be expected. In the following, we focus on the relationship between microstructural changes and related physical properties of tile adhesives during water immersion. The mechanisms detected are valid for the chosen mortar formulation and sample configuration (e.g., material and dimensions of substrate and tile), and may change for deviating set-ups. Three major themes are discussed: (1) the mobility of pore water and polymers, (2) volumetric changes, and (3) reinitiated hydration of the cement.

3.4.1 Influence of water intrusion and related mobilisation of polymers on mechanical properties

Water intrusion during wet storage is a 3D-problem as a result of the interconnected pore network. Based on sections parallel and perpendicular to the tile-mortar-substrate interfaces (Figs. 5, 7 and 8), we can detect the 3D water flow and study the related microstructural changes. In top view, the water front moves from the grout towards the centre of the mortar bed (Fig. 7a). Perpendicular to the mortar bed, the water usually first intrudes the mortar, and from there the underlying concrete plate, creating a water flux through the mortar towards the substrate. The more hydrophobic the redispersible powder is, and the higher its quantity, the lower the intrusion rate. As the polymers seal the pores, they reduce the degree of connectivity of the pores and also the intrusion rate. Such pore structure alterations also result in a reduced carbonation depth prior to water immersion (Fig. 7b). Ohama 1987 has already demonstrated that latex-modification decreases the total porosity and the carbonation depth.

In the case of wet storage, questions about the behaviour of the polymers during water exposure arise. Model experiments and ESEM investigations under wet conditions show a significant difference in water resistance between latex and solution polymers (CE and PVA; Figs. 3 and 4). Water dissolves CE and PVA films immediately, independent of the initial ion concentration of the polymer solution. In contrast, all tested latices show an increased water resistance if cementitious ions were present during film formation. In case of the EVA powder, enhanced water resistance in the presence of sodium ions suggests a close relationship between film properties and type of ion.

All investigated dispersions and redispersible powders contain PVA, which is assumed to form the shell of the latex particles or even exists as an interstitial phase between them. According to Larbi & Bijen 1990, saponification generally is enhanced by a higher alkali (Na^+ and K^+) concentration. Transferred to our system, saponification of PVA is promoted by the sodium ions. This hydrolysed PVA is supposed to hinder latex interdiffusion to a lesser extent. Consequently, sodium ions favour coalescence of latex particles resulting in an increase in water resistance. This assumption is in agreement with findings of Chevalier et al. 1992.

Du Chesne et al. 2000 describe the addition of ionic surfactants to improve the water resistance of latex films. In this case, interaction with the surfactant leads to imperfect PVA membranes that are no longer able to prevent latex interdiffusion. Presumably, cementitious ions might have a similar effect leading to PVA accumulations in interstitial pools and PVA immobilisation. Different ions might play different roles. While alkali and hydroxyl ions increase the degree of hydrolysis of the PVA, which in turn reduces its cold water solubility, divalent cations may cause a bridging of the accumulated PVA polymers.

Beside these inferences about the mechanisms that improve latex interdiffusion, we have microscopic evidence that the degree of film formation is more advanced in cementitious systems. An SEM morphology study (Jenni et al. 2001a) revealed that the

surfaces of latex films made from a cementitious redispersion are smoother, while latex films made from deionised water redispersions predominantly show particle structures. According to Huijs & Lang 2000 the film surface flattens with advanced film formation. Therefore, we interpret the reduced film relief as a progressed stage of film formation of these "cementitious" latex films. Latex films in real mortars rarely show relicts of the initial particle structure (Figs. 4 a and b; see also chapter 2). This suggests that latex film formation in mortars usually reaches the final stage of coalescence.

In the case of acrylic copolymers, divalent calcium ions might induce an additional mechanism to increase water resistance, called cross-linking (Chandra & Flodin 1987, Ohama 1995). But because carboxylate groups can also link onto cationic sites on mineral surfaces, this involves a latex-cement interaction mechanism. Often, such interactions occur too early in the fresh mortar stage and cause coagulation and bad workability properties, which in turn reduce proper wetting of the tiles and, thus, lower final adhesion properties.

Because latex structures in mortars are water resistant, they are also immobile during water storage. This is confirmed in Figs. 5a and b where a homogeneous latex distribution after dry storage and a similar distribution after wet storage are showed.

In contrast, CE and PVA films in the mortar dissolve during water exposure (Figs. 4c to f). Although the distribution patterns of CE prior to water immersion in mortars with different latices (VC versus SA) varies due to the different CE-latex interaction mechanisms (chapter 2), water intrusion changes the CE distribution in both mortars in a similar way and via the same mechanism (Figs. 5c, d, g, and h). Water intrusion from the grout induces water migration through the mortar bed towards the underlying concrete substrate. Simultaneously, the dissolved CE is transported downwards through the capillary pores, but accumulates at the contact layer and substrate surface, which act as micro filters (Figs. 5 d and h). This filtering is interpreted to result from a locally reduced pore size. The pore size reduction at the upper horizon (top of contact layer within the mortar bed) could be explained by a combined process of densification of the first contact layer surface and skinning (chapter 2). Fig. 9a illustrates an example of reduced porosity at the surface of the mortar versus the internal porosity (inset). The filtering effect at the mortar-substrate interface can be explained by a drastic change in porosity between the high-porous mortar and the dense concrete substrate. The carbonated surface of the concrete plate also helps to reduce the porosity. The few CE occurrences found in the substrate are all related to microcracks, which penetrate the concrete surface and therefore locally reduce the aforementioned filtering.

Although exactly the same segregation mechanisms as described above can be expected for PVA, the water flux during wet storage stage influences the PVA distribution to a much lower extent. This can be attributed to the reduced cold water solubility of a fully hydrolysed PVA, and to the fact that the smaller polymer size allows PVA to occur in smaller capillary pores. As a consequence, PVA is intergrown with cement hydrates on a smaller scale.

The CE and PVA distributions along the mortar-tile interface were investigated qualitatively by fluorescence imaging through transparent glass tiles. CE is accumulated towards the grout already after initial dry storage (Fig. 8a). This is due mainly to water flux from the centre towards the periphery of the tile during hardening. With the onset of water storage, CE in the vicinity of the mortar surface becomes transported either into the tank water or back into the mortar bed. The resulting CE distribution pattern can be seen in Fig. 8b. The distribution patterns of PVA are very similar, but less pronounced.

Even though redispersible powders increase tensile adhesion strength after both dry and wet storage, there is a significant loss in wet strength (difference between dry and wet strength in Fig. 6a). The same is observed for adhesive shear strength and flexibility (Fig. 6b). In spite of these reductions, however, further drying of the samples yields the same or even higher strengths than those of the initial sample. This reversible behaviour can be explained by water uptake and

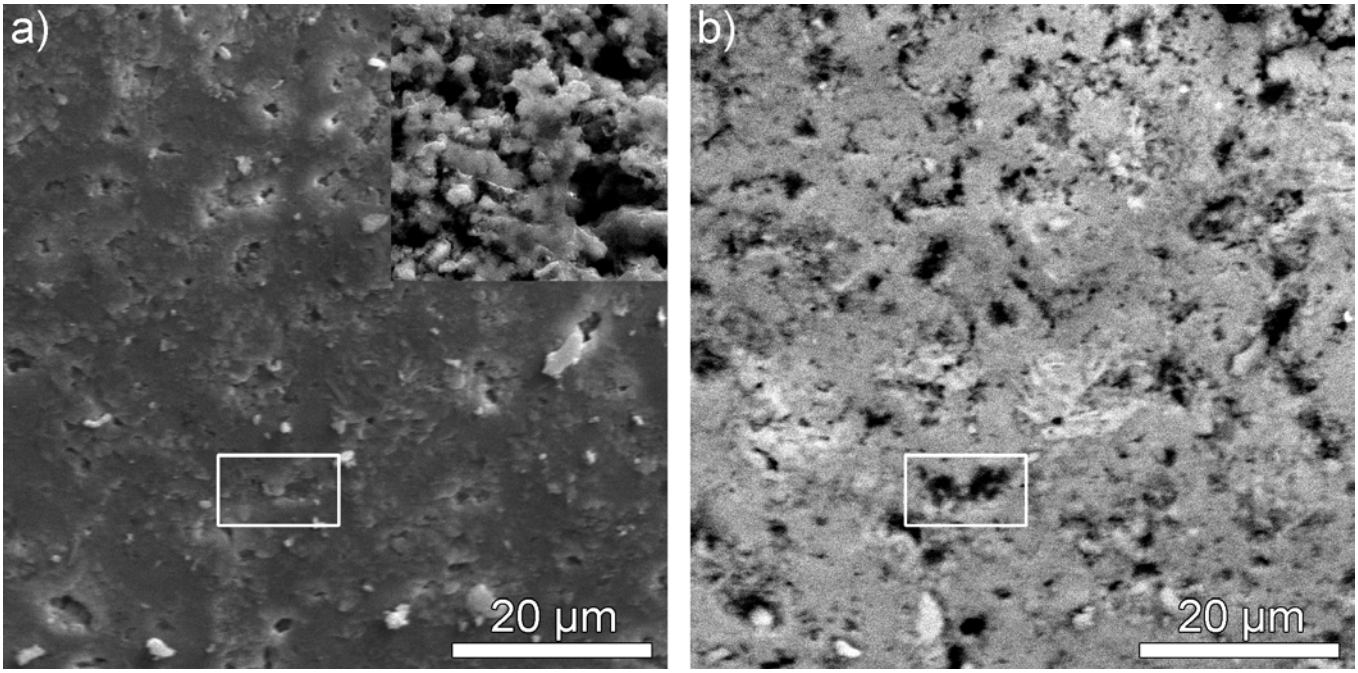

Fig. 9. (a) SEM secondary electron image of the uncovered mortar surface that underwent skinning (dry stored, EVA-modified according to Table 1). In contrast, the inset (same scale) shows the microstructure of a cohesive failure across the cement-polymer matrix. Note the difference in pore structures (b) The same mortar surface as in a) in back-scattered electron mode where polymers become transparent and only mineral structures are visible. Compare the boxes in a) and b).

softening of the latex microstructures during water immersion followed by redrying and related strengthening of the same microstructures. Enhanced latex interdiffusion, resulting in an increased coalescence of the latex film in a swollen stage of latex during water immersion, represents an explanation for the overstepping in strength compared to the initial dry stored sample (Jain 2002). Additional effects of water storage and their influence on the mortar strength are discussed below.

3.4.2 Volume changes and mechanical properties

Physical shrinkage and expansion depend mainly on the porosity, environmental conditions (humidity, e.g., Stark & Wicht 2000), and geometric aspects like body dimensions and restraining conditions of juxtaposed materials (tile, concrete substrate, grout). Stress gradients induced by these parameters can occur throughout the mortar layer, which may result in failure, and therefore can be critical. There is little known about the mutual interaction of all these parameters and the resulting internal stresses. In the following section, we will highlight some major findings of the shrinkage/expansion behaviour of tile adhesives.

The w/c of concretes is widely known to be a major factor for drying shrinkage. The higher the w/c, the higher is the capillary porosity, which enhances capillary drying shrinkage. Tile adhesives have a w/c around 0.8 and these mortars are only partly hydrated. Autogenous drying shrinkage for dense concrete and high-porous tile adhesive mortars fall within the same range of 1-2 mm/m (Krenkler 1980). This indicates that in case of tile adhesive mortars, a major part of drying shrinkage must be accommodated by so-called inner shrinkage (increasing bulk porosity including shrinkage cracks). During water storage of a previously dry-cured mortar, volume changes due to water intrusion and the reinitiated secondary cement hydration can induce cracking (Fig. 7c). In particular, the situation can be critical with respect to adhesion strength at the tile-mortar interface, where the highest material contrasts occur.

Of special interest are the irreversible volume changes occurring during alternating dry-wet storage cycles (Fig. 6d). For concrete it has been established that the irreversible part of the initial drying shrinkage increases with higher porosity (e.g., Krenkler 1980). In our mortar system, however, we face another complex situation of repeated, additional and irreversible drying shrinkage. In case of redrying of wet stored mortars, drying shrinkage is at least twice as intense as the expansion during the previous period of water storage. A second storage cycle (not shown here) revealed that the additional drying shrinkage of alternating wet and dry stored mortars has a dominant irreversible component. We interpret this behaviour as a consequence of the irreversible secondary cement hydration during water immersion. This is confirmed by the fact that both the irreversible drying shrinkage component and the degree of secondary cement hydration, are progressing at similar relative rates, and terminate as the mortar is close to complete hydration after 10 dry-wet cycles (Zurbriggen & D. 2000). The link between these two phenomena is interpreted to be the pore size distribution. Air voids, capillary and gel pores change their relative and absolute quantities during ongoing hydration and cause a general shift of pore size distribution towards smaller pores (Fig. 6c). Drying shrinkage is generated by retreating water films along the walls of capillary and gel pores. In this way, the negative capillary pressure causes the cement matrix to shrink (e.g., Stark & Wicht 2000). With an increasing number of small-sized pores, the area of pore walls increases as well, lowering the total capillary pressure in the system during retreat of the water films. Consequently, a more intense volume decrease occurs during redrying (Fig. 6d). The reason for the increased irreversible shrinkage during redrying is thus based on the initial low degree of hydration.

Comparing the highly porous mortar, the dense concrete and the ceramic tile, the most pronounced difference in volumetric changes during water intrusion and drying will occur at the mortar-tile interface. As this interface is progressively wetted and dried from rim to centre (Fig. 7a), the lateral variations in volume changes create strong gradients along the interface promoting crack formation. This is a potential explanation for the commonly observed failure localisation at the mortar-tile interface in wet stored mortars (Fig. 8d and f).

3.4.3 Influence of hydration on mechanical properties

As indicated by a strong and progressive increase in the amount of portlandite and gel pores (Fig. 6c), cement hydration, which virtually stopped after 7 days of dry storage, continues during wet storage. Besides polymer film formation, cement hydration is the other major strengthening mechanism. Particularly during water storage when the solution polymers dissolve and the latex films swell and soften, the degree of cement hydration dominates the bulk strength of the mortar. The reinitiated hydration during water immersion is the main reason for an enhanced dry and wet strength with further storage cycles (Figs. 6a and b). As this secondary hydration is considered to create rigid mineral structures, the flexibility, mainly given by latex, is constant or decreases slightly.

The aspect of hydration at the mortar-tile interface is of special interest, because this is the site of failure after wet storage (Figs. 8d and f). Figs. 7c to e are typical examples of portlandite crystals, which grew during water storage in a crack at the mortar-tile interface caused by differential volume changes. Because such relatively large portlandite crystals can hinder the reversible opening and closing of cracks during dry-wet cycling, they may induce stress concentration, promoting further crack propagation along the mortar-tile interface during the closing phase (shrinkage during drying). Crystallisation pressure of portlandite might represent an alternative explanation for interfacial cracking and related adhesion failure.

3.5 Conclusions

In light of polymer film formation, the chemical environment plays a crucial role controlling the final film properties. This is particularly important for experimental simulations of polymer film formation in cementitious systems. In this way, model experiments involving film formation on grids are only realistic

when performed under similar chemical conditions (ionic concentration) as present in the mortar. It is important to note that additional parameters like mineral interfaces do not influence the water resistance of the films. Therefore, this type of model experiment represents a fast and easy screening test for the water resistance of polymer films in cementitious environments.

In the context of tile adhesives, microstructural changes during wet storage and resulting material properties of tile adhesives can be divided into two principal groups: (a) irreversible changes, and (b) reversible changes.

a) Irreversible changes are mainly related to the low degree of initial cement hydration after dry storage. As the cement continues to hydrate during water immersion, the cement-derived strength component increases. Simultaneously, this secondary hydration during wet storage shifts the pore size distribution towards smaller pore sizes, a process that again increases drying shrinkage during the following redrying. In terms of adhesion strength, this additional component of drying shrinkage can be critical, because cracks preferentially form at the mortar-tile interface, where the material contrast is most pronounced. The formation of large portlandite crystals in these cracks is thought to further reduce strength.
   Once formed in the cementitious environment, the latex films at least partly reach the coalescence stage, which provides their water resistance. During water immersion, latex interdiffusion is reactivated promoting further coalescence. This improves the mortar properties after redrying. As a consequence of latex immobility, this phase cannot enter the newly formed shrinkage cracks to heal these microdefects.
   Solution polymers, like CE and PVA, do not form water resistant microstructures, and have therefore no influence on strength in the wet stage. They redissolve during each water immersion period, are transported by the migrating pore water phase and enriched due to filtering mechanisms. As PVA is fully hydrolysed with time, its solubility is decreased, which lowers the PVA mobility compared to CE.

b) Reversible changes during water storage can be followed in test series over multiple dry-wet cycles. Adhesion strength and flexibility are lost and regained as the sample is wetted and dried, respectively. This can be related mainly to reversible swelling and softening, followed by drying and strengthening of the latex films in the mortar.
   Shrinkage and expansion are also partly reversible. As RP enhances the flexibility of the bulk system, latex is thought to increase this reversible part of the volume changes.

This study demonstrates that the interplay of all endogenous (mortar components) and exogenous (environmental) parameters determines the evolution of the microstructure and therefore the material properties of polymer-modified mortars during wet storage. The relationships of the various interaction mechanisms have to be taken into account for future research and product development.

Appendix A

4.1 Agglomeration in latex dispersions

4.1.1 Introduction

The well-known latex film formation is mainly driven by evaporation. More recent studies (Routh & Russel 1999) propose also wet sintering, where film formation can already start in the dispersion. As shown in chapter 3, cementitious ions in the latex dispersion are supposed to increase film formation. In this experiment, we compared latex dispersions with and without cement ions in order to investigate the influence of the ions already in the wet environment.

4.1.2 Methods

- Preparation of EVA redispersible powder dispersions with deionised, synthetic cement, and filtered cement water according to chapter 3
- Already dispersed experimental EVA (before spray drying) is further diluted with the same water types to reach the same polymer content used above. Thus, ionic strength is weaker in these dispersions.
- Storage for one month in waterproof sealed containers under room conditions
- Stirring of the dispersions
- Pipetting of one drop onto a glass slide
- Immediate investigation of the dispersions with transmitted light microscopy, before pronounced evaporation can take place

4.1.3 Results

The dispersions without cement ions show individual particles with sizes of the latex particles (0.4-2 µm), which are migrating with water fluxes. Agglomeration is rare.

The dispersions containing cement ions show agglomerates with average sizes of 20-40 µm, but they can range from 5 µm to 200 µm. Individual particles are present between the agglomerations. In general, the agglomerations are structured and the individual latex particles are visible. An exception are the experimental EVA dispersions, because they contain few agglomerates with a size of >100 µm, which are completely transparent in their centre. Dispersions with synthetic and with filtered cement water do not differ.

4.1.4 Implications

Already in the wet environment, cement ions induce latex particle agglomeration, which can be considered as the very first step of film formation. In few cases, transparent agglomerations indicate an advanced stage of film formation, but do not necessarily suggest coalescence (Keddie 1997).

4.2 Ion composition of cementitious waters before and after polymer addition

4.2.1 Introduction

Cementitious ions can influence the film formation of latex films (chapter 3), which can already occur in the wet environment (page 69). Also CE shows different film structures in the presence of cement ions (Jenni et al. 2001a). The following experiment investigates, which ions build complexes with the latex in water.

4.2.2 Methods

- Different RPs, an experimental EVA dispersion (before spray drying), CE, and PVA were mixed with synthetic cement water, concentrations according to chapter 3.
- Waterproof sealing
- 5 min. ultrasonic treatment according to chapter 3
- Storage for one hour under room conditions
- Stirring
- Filtering (pore size 0.2 µm)
- Dilution 1:100
- Filling into sample containers, sealing under nitric atmosphere
- Measurement of total organic anions, CH_3COO^-, Cl^-, SO_4^{2-}, Na^+, K^+, Ca^{2+} concentrations with ion chromatography
- A blank (synthetic cement water without polymers) was additionally subjected to the aforementioned treatment.
- Normalisation of the ion concentrations in the polymer dispersions/solutions to the concentrations in the blank (except Cl^-, organic anions and CH_3COO^-, which are not present in the synthetic cement water)

4.2.3 Results

- organic anions: constant for all samples, except PVA (elevated) and CE (no anions)
- CH_3COO^-: very high content in case of PVA, very low for the experimental EVA dispersion; not present in CE sample
- Cl^-: high for VC and very high for CE
- SO_4^{2-}, Na^+, K^+: same concentration as the blank
- Ca^{2+}: generally lower than the blank

4.2.4 Implications

CH_3COO^- is supposed to be released by saponification, which seems to be strongest for PVA. As the CH_3COO^- content is very low for the experimental EVA dispersion that contains no free PVA, PVA present in the RPs is supposed to release CH_3COO^-. It unclear what the contribution of latex to the increased CH_3COO^- content is. It is also possible that PVA passed the filter and was able to saponify during the whole period between filtering and measuring. In contrast, CE does not saponify.

The high Cl^- content for CE is explained by its presence during initial CE production; in contrast, VC releases chlorine ions.

Ca^{2+}: is caught by all polymers. At least in case of CE, cross-linking as described in Chandra & Flodin 1987, Ohama 1995 is not expected because of the unsuitable polymer structure of CE.

4.3 Latex film formation on grids in the environmental scanning electron microscope

4.3.1 Introduction

ESEM allows the observation of evaporation induced latex film formation on metal grids. As the mesh size approximately corresponds with the size of the air voids in the mortar, this model experiment simulates the situation between two juxtaposed air voids in the fresh mortar paste that undergoes drying.

4.3.2 Methods

Already dispersed experimental VC (before spray drying) was prepared on grids as described in chapter 3. Deionised water was used exclusively. Immediately after dipping the grid into the dispersion, the sample was inserted into the ESEM sample chamber (see chapter 3) and imaged under water atmosphere. Temperature and pressure changes allow the controlled evaporation of water and simultaneous imaging of the forming latex structures.

4.3.3 Results

The spherical latex particles are covered with or embedded in PVA and/or water. With ongoing evaporation, the volume of this PVA/water phase decreases, which leads to a contraction of the whole structure and opening of holes in the forming film. Latex particle ordering occurs, and the PVA/water phase seems to be pushed away, forming a smooth PVA film. In the completely dried state, PVA films with an even surface are separated from a film with a particle structure (chapter 2). These latex particles are often deformed and show hexagonal cross-sections, according to stage II of latex film formation (particle deformation). Long-time storage under room conditions does not change these film structures.

4.3.4 Implications

VC undergoes step I and II of latex film formation, which consist of particle ordering and deformation. Step III (coalescence), which leads to smooth planar latex film surfaces, does not take place in this experimental set-up. The presence of PVA in the latex film can not be excluded.

4.4 Polymer microstructure investigations with transmission electron microscopy

4.4.1 Introduction

The polymer films prepared on metal grids can be investigated with transmission electron microscopy without further preparation effort.

4.4.2 Methods

VC with and without anti-blocking agent is prepared as described in chapter 3. using tap water. After drying during at least one week under room conditions, the grids carrying the polymer films were inserted into a Hitachi H-600 transmission electron microscope. Investigation of latex film microstructure is restricted to areas around holes in the films, where only one layer of latex particles is present (film thickness of approximately 0.4-2 µm). PVA films are thin enough to resolve their microstructure.

4.4.3 Results

The latex particle structure is clearly visible and is partly deformed to hexagonal shapes. Depending on the local stress regime, the particles can be elongated. A dark phase is present at particle triple points. Mineral anti-blocking agent is visible as dark, hexagonal plates, which are integrated in the film and coated with PVA. Larger areas between the particles (1-3 µm) or at the film border show no particle structure and are therefore supposed to represent PVA.

Film areas without 1 µm sized particle structures (PVA) show isolated round inclusions with sizes of approximately 200 nm. Apart from that, the film shows no structure. Indistinct lines parallel to nearby elongated latex particles seem to indicate film stretching during drying.

4.4.4 Implications

The latex particles are partly separated by a dark phase, which can be interpreted as very fine mineral substance (anti-blocking agent) in PVA. The inclusions in the PVA film are supposed to derive from the tap water.

The microstructures indicate that the latex particles did not coalesce in this experimental set-up, but underwent stage II of latex film formation (particle deformation). Non-latex phases between the particles are supposed to hinder coalescence.

4.5 Latex coalescence: investigations on film surfaces with scanning electron microscopy

4.5.1 Introduction

According to Huijs & Lang 2000, coalescence provokes flattening of the latex film surfaces. As shown above, latex films do not coalesce from deionised water dispersions dried under room conditions. In contrast, latex films in mortars show smooth planar surfaces, which indicate particle coalescence. Therefore, the latex was exposed during or after film formation to different conditions and the resulting film surface was examined.

4.5.2 Methods

- VC preparation on grids as described in chapter 3, using deionised and cement water
- Exposure of the deionised water dispersion on the grid to relative humidity of 100% for 4 days at approximately 20°C, in order to simulate the conditions in a fresh mortar air void
- The dry films synthesised from deionised water were exposed to 70°C or 120°C for 2 hours
- Examination of the film surfaces with ESEM at about 1 Torr water gas pressure by secondary electron imaging

4.5.3 Results

- Latex films synthesised from deionised water under room conditions show latex particle structures
- Latex films synthesised from filtered and synthetic cement water under room conditions show mostly flat surfaces, covered with a bright phase that forms chicken-wire structures. Partly, transformations into a columnar habitus can be observed, suggesting that the chicken-wire structure is built up by a mineralic phase (page 74). PVA films are not present any more or can not be distinguished from the latex film.
- Films from dispersions on grids exposed to high humidity show latex particle structures
- Films exposed to 70°C show relic latex particle structures. PVA films are still present.
- Films exposed to 110°C show no latex particle structures. PVA films can not be observed any more.

4.5.4 Implications

Coalescence is mainly driven by high temperatures and by ions from the cement water, which are present during film formation. The latter also increases water resistance (chapter 3).

4.6 Latex coalescence: investigations on film surfaces with atomic force microscopy (AFM)

4.6.1 Introduction

According to Huijs & Lang 2000, coalescence provokes flattening of the latex film surfaces. To consolidate the results from SEM investigations, additional surface measurements were performed using AFM.

4.6.2 Methods

- Preparation of EVA and VC, with and without anti-blocking agent, on grids as described in chapter 3, using deionised and cement water
- Pipetting of the dispersions onto glass slides, where a polymer foil forms during drying under room conditions
- Examination of films on grids and of polymer foils with an AFM Autoprobe CP (Park Scientific Instruments) in contact mode with a scan rate of 2 Hz
- Quantification of the film topography by determination of the average valley depths between the latex particles

4.6.3 Results

All resulting micrographs show latex particles. The latex films synthesised from deionised water have the same topography as cement water films.

4.6.4 Implications

These results contradict the results of the ESEM surface investigations (above). Both, coalesced and uncoalesced film surfaces can be observed in the ESEM, therefore, the electron beam does not induce coalescence. The preparation of the films for AFM and ESEM was identical, but not at the same time. As the ESEM-results are in accordance with the findings in chapter 3, the only explanation found for this contradiction is an error in AFM sample preparation. Thus, the entire AFM experiment should be repeated.

4.7 Mineral formation on polymer films synthesised from cementitious waters

4.7.1 Introduction

The ESEM investigations on film surfaces suggested the presence of a mineral phase on the latex film surface, which form the negative of the particle structure before coalescence. In this investigation we identify the type of mineral.

4.7.2 Methods

EVA and VC preparation on grids as described in chapter 3, using synthetic and filtered cement water. Minerals were investigated by their habitus and chemical composition in the ESEM combined with energy dispersive spectroscopy. In addition, x-ray diffractometry was carried out (x-ray Powder Diffractometer PW1800).

4.7.3 Results

The chicken-wire structures with partly columnar habitus are formed by arcanite (K_2SO_4). In addition, sylvine (KCl) is present. Both minerals occur on the film surfaces of films synthesised from synthetic and filtered cement water.

4.7.4 Implications

Minerals form on the isolated latex films from the ions present in the cement water. In order to generate sylvine (KCl), a Cl source is required. Because of lacking Cl in synthetic cement water, VC represents the only Cl source available. In other words, Cl had to be separated from VC to become integrated into the sylvine structure. Sylvine occurs rarely and its quantity present on the film is just above the detection limit of the powder diffractometer.

4.8 Polymer film resistance to impregnation resins and polishing liquids

4.8.1 Introduction

As shown in chapter 3, the polymer films can be destroyed during water contact. Similar experiments were carried out to evaluate impregnation resins and polishing liquids, which do not harm the films.

4.8.2 Methods

- Preparation of CE, VC, and partly other RPs on grids as described in chapter 3, using deionised water
- Exposure of the dried films as described in chapter 3
    - to the following liquids: water, cement water, lamp oil (technical product kerosene, boiling point 150-280°C), glycerine, hexane, heptane
    - to the following resins: epoxy-based resin, Epotek 301, Epofix, sodium silicate (soluble glass), cellulose lacquer, Leica Historesin, wax BASF AH3, paraffin wax (Wintershall 58/60D fully refined), Polyfin
- Investigation of changes in film morphology with transmitted light microscopy

4.8.3 Results

- Water, cement water, and glycerine destroy all polymer films
- Lamp oil attacks latex films, but does not destroy CE and PVA films
- Hexane and heptane do not destroy latex, PVA, and CE films
- The standard epoxy-based resin does not destroy the CE films
- Latex and PVA films resist only wax, paraffin, and Polyfin impregnation

4.8.4 Implications

The substances were tested on films synthesised from deionised water. (Chapter 3, water resistance and ESEM in-situ watering) showed that latex films in the mortar are generally more resistant. Thus, the above experiments test weaker films than present in the mortar.

Polyfin is recommended for latex- and PVA-conserving impregnation, whereby the other waxes show considerable hardening shrinkage. Standard epoxy-based resin is recommended for impregnation of samples used for CE investigation; those samples are easier to handle for further preparation. Note that for chlorine distribution mappings, no Cl-containing resins can be used.

Heptane, less volatile than hexane, is recommended for polishing and cleaning of sample surfaces. As heptane can dissolve the impregnation resin, polishing was performed with water. The impregnation stabilises the polymer structures, which therefore resist polishing, as verified on the polished sample surface.

4.9 Localisation of polymers containing chlorine in mortar with energy dispersive spectroscopy (EDX)

4.9.1 Introduction

Similar to the description of WDX mappings in chapter 1, element distribution maps can be acquired by EDX. As in general, this method is less elaborate in use and sample preparation. EDX was applied to VC-modified mortars in order to obtain the spatial distribution of this chlorine containing latex.

4.9.2 Methods

The sample preparation followed the techniques described in chapter 1. In contrast to the used microprobe, which requires samples with a thickness of <1 cm, samples with almost any dimensions can be inserted into the CamScan CS4 SEM equipped with a Voyager 4 digital image acquisition system for EDX. The easier sample preparation reduces possible artefacts.

Chlorine mappings were acquired with different parameters, which were increased up to 30 keV acceleration voltage, 200 µA filament current, spot size/resolution 1, 0.2 seconds dwell time.

4.9.3 Results

In all measurements, the chlorine-containing cement-polymer matrix did not show significant higher chlorine concentrations than phases virtually without chlorine (e.g., quartz, Polyfin impregnation resin, tile).

4.9.4 Implications

The chlorine concentration in mortars modified with 2 wt.% of VC is too low to be measured within EDX element mappings. We therefore recommend the use of WDX (chapter 1).

4.10 Localisation of polymers in mortar with Raman spectroscopy

4.10.1 Introduction

Raman spectroscopy allows detection and discrimination of the used polymers due to specific covalent bond properties. Theoretically, the micro-Raman option enables the acquisition of spatial distributions with a maximum resolution of 1 µm.

4.10.2 Methods

Polymer powder, films prepared as described in chapter 3, and mortars (fracture surfaces) were measured in non-confocal and confocal mode of a Renishaw Ramascope 2000 (HeNe 633 nm) combined with a Leica DML light microscope. In confocal mode, which is used for mappings with a resolution of less than 10 µm, the laser beam is not only more focussed, but also strongly attenuated by an aperture.

4.10.3 Results

Measurements on the films with an acquisition time of 20 seconds in non-confocal mode result in characteristic spectra in case of several latices and PVA, whereas the thinner CE films show no suitable spectrum. Only the CE powder showed a characteristic spectrum.

In the mortar, peaks corresponding to latex could be found after acquisition times of 1 minute or more, measured in non-confocal mode.

In confocal mode, no characteristic polymer peaks were measured on any sample.

4.10.4 Implications

Raman can be used to distinguish the polymer powders. The polymer content in the studied tile adhesives is too low to map the polymer distribution in the mortar with reasonable resolutions and within realistic acquisition times.

4.11 Localisation of polymers in mortar with fluorescence microscopy after staining with microspheres

4.11.1 Introduction

Reagent microspheres consist of a reagent part bonded to a dye. Hydrophobic microspheres are supposed to physically adsorb on latex surfaces. The fluorescent dye can then be excited. Hence, the emitted light allows mapping the latex distribution on polished mortar surfaces with LSM.

4.11.2 Methods

- Preparation of a SA-modified mortar sample as described for WDX mappings (chapter 1), resulting in a Polyfin-impregnated, polished section
- Diluting of the carboxyl (hydrophobic) microsphere dispersion 1:1 with deionised water (FR2040HA, polystyrene particles with surface carboxyl groups for charge stabilisation, Brookhaven international ltd, www.brookhaven.co.uk)
- Sample immersion for 2 hours
- Careful rinsing of the sample surface for 5 minutes with 0.4 l deionised water
- Exposure of the sample surface to ultrasonic water bath of 50 kHz/50 W for 2 minutes
- Measurement of the sample surface with LSM

4.11.3 Results

Also phases containing no latex were stained (e.g., substrate, unhydrated cement grains). The dye was adsorbed to sample surface areas with high relief, but the cement-polymer matrix showed more adsorbed microspheres. Perfectly polished Polyfin surfaces were not stained.

4.11.4 Implications

Further experiments are needed to improve the selective microsphere adsorption to SA latex. In addition, perfectly polished surfaces are recommended. Due to strong material contrasts between the soft Polyfin and the hard mineral phases, it was impossible to further reduce the surface relief of our samples. As there are different reagent microspheres with several adsorption or covalent coupling properties, this method can probably be applied to products containing other polymer types.

4.12 3d-imaging of polymer films on fracture surfaces with LSM

4.12.1 Introduction

LSM allows 3d-imaging of fluorescent polymer structures like stained CE or PVA, which was carried out in order to investigate polymer morphology.

4.12.2 Methods

- Preparation of fracture surfaces of mortars containing CE or PVA stained with a fluorescent dye according to chapter 2 (qualitative SEM investigations)
- 3d-imaging of the surfaces with LSM

4.12.3 Results

The whole cement-polymer matrix is fluorescent and imaged in case of both, stained CE or PVA, showing that CE and PVA are distributed in the cement-polymer matrix. In case of CE, thin sail-like structures can be interpreted as CE films (chapter 2) or as thin cement-polymer composite walls. Due to the maximum LSM resolution of 1 µm, a differentiation is impossible. In case of stained PVA present in the mortar, such thin structures are rarely observed.

4.12.4 Implications

CE and PVA are present in the whole cement-polymer matrix. Compared to the frequent thin CE structures, thin PVA structures are rare, which suggests that these structures are thin cement-polymer composite walls, as also observed by SEM. Therefore, PVA is supposed to form no sail-like structures or is not present within CE structures (no CE-PVA composites).

Appendix B

5.1 Extended abstract of the oral presentation at the "8th Euroseminar on Microscopy Applied to Building Materials", September 4-7, 2001, Athens, Greece

SAMPLE PREPARATION OF POLYMER-MODIFIED HIGH-POROUS MORTARS FOR QUANTITATIVE MICROFABRIC ANALYSIS

Jenni A., Herwegh M., University of Bern, Switzerland

Zurbriggen R., Elotex AG, Sempach Station, Switzerland

Holzer L., EMPA, D□bendorf, Switzerland

Abstract

Polymer-modified cement mortars, namely, tile adhesives, can be described and classified either by their compositions, working parameters (e.g., application, workability, storage conditions) or final physical properties. All of these parameters are closely related to the time-dependent interaction of the individual components (polymers, cement phases, mineral fillers, pores). From initial mixing to the hardened endproduct the microfabric evolution in this complex polyphase system links all the different stages and their physicochemical aspects. Therefore, detailed electron microscopy of polymer-modified mortars is regarded as a key tool for an integral understanding of such composite materials.

Preparation techniques for scanning electron microscopy (SEM) investigations on fracture surfaces are straightforward. However, fractures preferentially evolve along initial zones of weaknesses and side fractures can be misinterpreted as shrinkage cracks. Additionally, topography, high porosity and the very thin polymer membranes only allow for qualitative observations.

Consequently, planar and polished sections are required for quantitative microfabric analysis. Unfortunately, conventional impregnation and polishing techniques often affect the polymer phase causing severe artifacts by dissolution and redispersion followed by redistribution and leaching, as well as mechanical damaging. In order to prevent these artifacts various impregnation resins, polishing and cleaning aids were evaluated by their dissolving effect on the polymer phases (latices, polyvinyl alcohol, cellulose ether). In a second step, selective staining of the polymers allows their discrimination in the mortar by element mapping.

Also, coating artifacts were studied by comparing differently treated and untreated environmental scanning electron microscope (ESEM) samples, thereby showing that evaporation coating techniques preserve the thin polymer membranes much better than Ar sputtering does.

The authors discuss preparation procedures for such composite materials with extremely contrasting organic and inorganic components and their delicate structures.

Keywords: electron microscopy, sample preparation, staining, polymer-modified cement mortar, ceramic tile adhesive, latex

1 Introduction

Common tile adhesives are commercially available as premixed dry compounds. At the construction site only a predifined amount of water must be added and mixed to gain a ready-to-use fresh mortar. The components of such an instant dry mortar can basically be grouped into binders, fillers and additives. Ordinary Portland cement (OPC) is the most typical binder, which is added in the amount of 20-40˚wt%. Other types of cement, hemihydrate, natural and industrial puzzolana can be combined with OPC or even replace it completely. 60-80˚wt% are composed of filler materials, typically siliceous and/or carbonate sand and finer grained fractions (<100˚□m), but also various light weight fillers can be contained. Typical additives are cellulose ether (CE) and redispersible powder (RP). In order to achieve a good workability and water retention, approx. 0.5˚wt% CE is added. RP (0.5-5˚wt%) further improves the workability of the fresh mortar and finally provides an increased adhesive strength of the hardened end product (Ohama [1]).

For the purpose of this research study the mortars investigated only contain OPC, quartz sand, CE and RP: 30˚wt% OPC (CEM I 52.5 R), 63.6-69.6˚wt% quartz sand (0.1-0.3 mm), 0.4˚wt% CE (MHEC15000PFF, Aqualon), and 0-6˚wt% RP (two types of ELOTEX redispersible latex powders were chosen: (a) vinyl-acetate/ethylene/vinyl-chloride and (b) styrene acrylate). The amount of added water was adjusted to gain optimal workability characteristics (approx. 25˚wt% of the dry mix).

In between the predefined staring composition and the measurable final physical properties (e.g., adhesive strength), the mortar microfabric evolves. Up to know, this evolution and the involved processes are only weakly known. Air entrainment, dissolution and redispersion of the polymers produce an early protofabric during the mixing procedure of the fresh mortar. During application of the mortar these early structures can change depending on working tools and techniques. Cement hydration and the formation of polymer films (both strongly influenced by environmental conditions) finally lead to a solid state microstructure. This microfabric defines the physical properties of the hardened mortar. For that reason, a proper description and understanding of microstructure and involved processes, respectively, is required to understand the evolution of a mortar and its material properties.
In this sense, microscopic investigations on fracture surfaces represent the first approach. Fracture surfaces are easy in preparation and resulting images are widespread in literature (e.g. Zurbriggen [2]). However, the high porosity of these composite materials (bulk porosity of up to 40˚vol.%) create fractures with intense topography allowing only qualitative investigations. In order to detect the evolution of the microfabric, quantitative analysis of the microstructural elements on planar sections are required. For this aim, conventional preparation techniques have to be modified such that original polymer distribution patterns can be preserved. This is challenging because sizes and distributions of microstructural elements range over several orders of magnitudes (nm-cm). As will be shown below, a combination of light and electron microscopy is the most promising approach to cover most of this range.

2 Fracture surfaces

Typically, tile adhesives are applied in a 1-5˚mm thick layer in between a substrate (e.g., concrete) and a tile (Figure 1 a). To produce a fresh sample surface across the tile-mortar-substrate layers, the samples cannot be sawed because the microstructures are destroyed and the air voids become filled with sawing residues. The cleaning of the air voids in a ultrasonic bath can also destroy the polymer structures. Therefore, the only way to produce a fresh surface is to break up the sample along pre-cut notches within the ceramic tile and the concrete substrate. These fracture surfaces can be analysed by reflected light and electron microscopy (Fig. 1).

Except for environmental scanning electron microscopy (ESEM) common electron scanning microscopy (SEM) methods require a coating of the non-conducting mortar surfaces. Most suitable coating materials are C and Au. Both materials were coated by evaporation, the distance between the target and the sample was around 25˚cm.

Evaporation coatings with smaller distances heat up the sample considerably and may destroy the polymer structures. Clear evidence for destruction of polymer structures was found after gold sputtering in an Ar plasma (Figure 1d).

By these techniques different phases in the mortar can only be distinguished by their morphology, a fact that is useful for qualitative descriptions. To obtain quantitative results, however, it is necessary to measure planar surfaces representing real distribution patterns of all components.

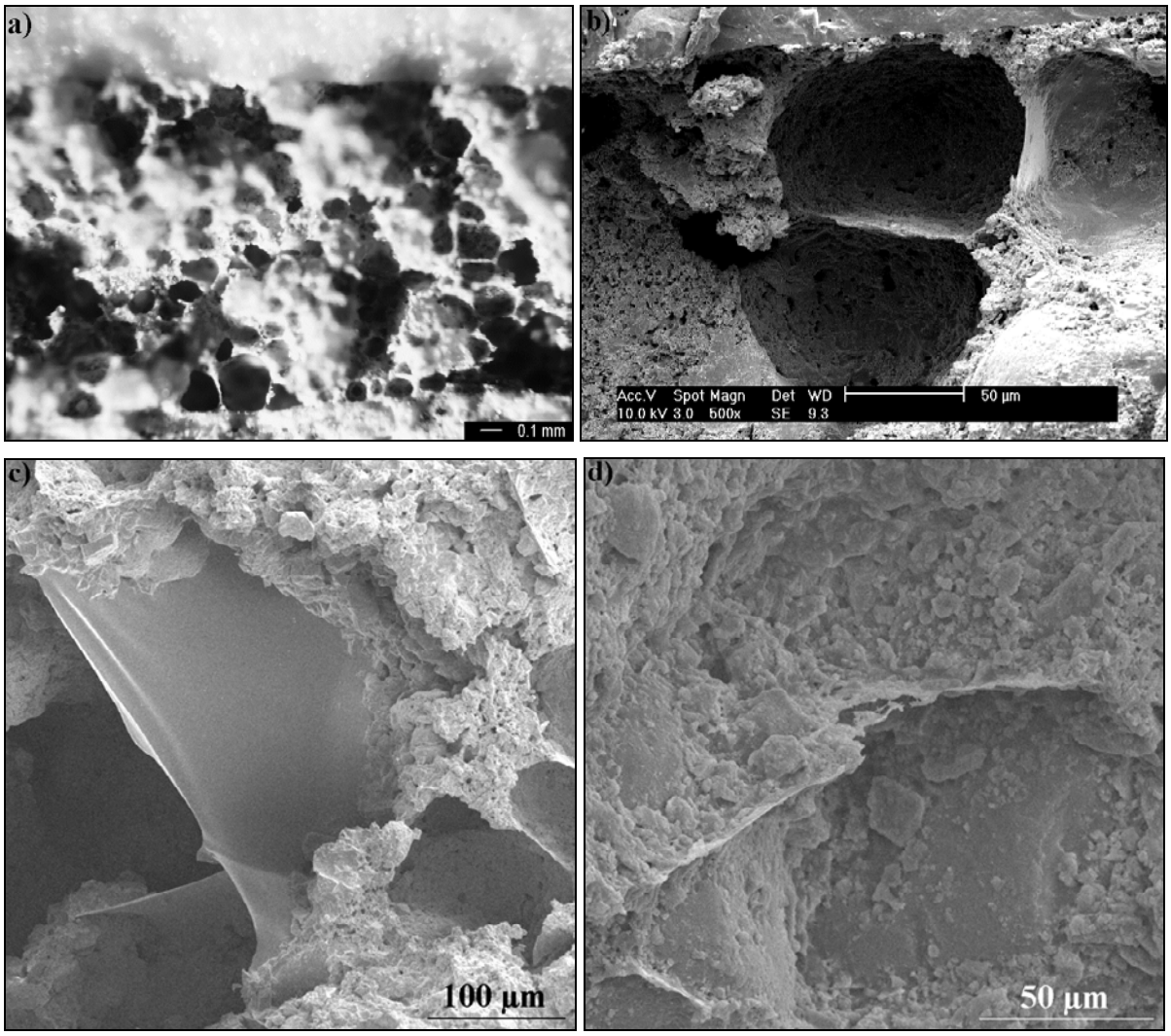

Figure 1: a) Reflected light microscope image of a polymer-modified mortar. Fracture surface from tile (top) through highly porous mortar to concrete substrate (bottom); b) ESEM image of an uncoated fracture surface. Three air voids are separated by a polymer film (vertical) and a cement-polymer composite wall (horizontal); c) SEM image of an intact polymer film (Au evaporation coating); d) SEM image of a destroyed polymer film (Au sputtered in Ar plasma)

3 Conventional preparation of polished sections

For this preparation method, (a) the samples usually are exposed to a vacuum of 0.05˚mbar, (b) penetrated by a liquid coloured resin (mixture of epoxy based resins) in the vacuum, (c) put then under pressure where (d) the resin hardened. The advantage of this approach is an excellent penetration of the mortar fabric by the resin.

Unfortunately, all tested resins attack the polymer structures by redispersion or dissolution (Figure 2). In addition, the intruding resin damages mechanically fragile cement and polymer structures. Therefore this vacuum-pressure epoxy impregnation is only suitable for investigation of supra-micron structures, i.e. for the preparation of thin sections for optical microscopy.

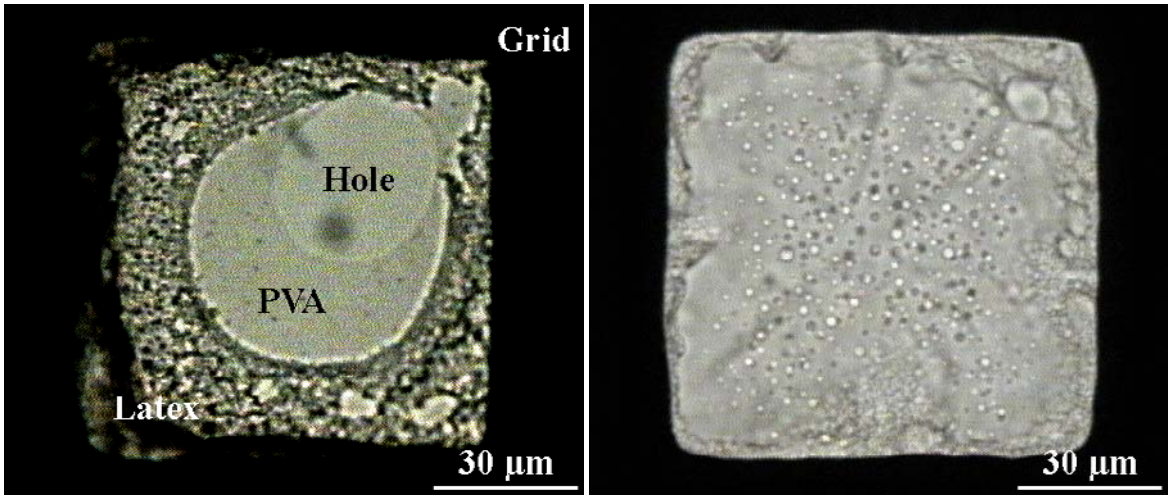

Figure 2: Structured latex- and unstructured polyvinyl alcohol (PVA)-films in a void of a nickel grid, before (left) and after (right) embedding in a epoxy based resin (transmitted light microscopy). Obviously, the resin destroys the original polymer structures.

Digital images of planar sections either taken with the light or electron microscope can be quantified using appropriate software (Image SXM by Rasband [3]). Figure 3 shows the distribution of the cement-polymer matrix, quartz (filler) and air voids in a tile adhesive from the ceramic tile (top) to the concrete substrate (base). A mortar with 0.4˚wt% cellulose ether is compared to a mortar containing no cellulose ether. It becomes obvious that the cellulose ether acts as an air entraining agent. The general decrease of air voids with a complementary increase of the cement-polymer matrix are due to (a) application techniques and (b) water migration towards the porous concrete substrate by capillary forces.

- During application of the tile adhesive, the working tool presses the mortar onto the substrate creating a contact layer that is enriched in cement and water.
- Within the first 20 minutes a tile adhesive looses approx. 40˚wt% of its water content towards the porous substrate. This water migration may lead to a gradual enrichment in water and fine-grained cement particles towards the substrate.

Modification by cellulose ether increases water demand. This higher water content generates a higher content of capillary pores, which are contained within the cement-polymer matrix. Therefore, the cement-polymer matrix/quartz ratio is larger in the cellulose ether-modified mortar.

The sum of the three phases is a controlling for the image processing: the difference from 100% indicates the error arising from the phase discrimination.

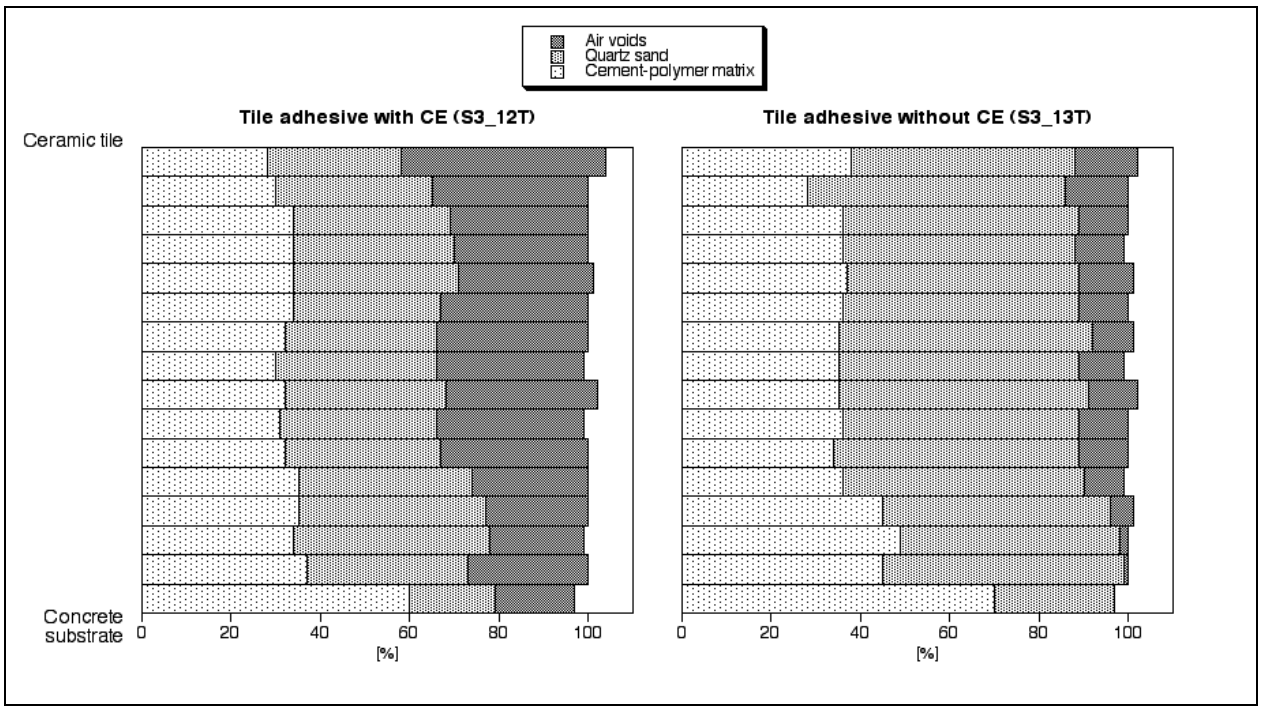

Figure 3: Profile across the mortar ranging from the concrete substrate to the ceramic tile. The diagrams show the distribution of the cement-polymer matrix, quartz filler and air pores in a mortar containing cement, quartz, latex and cellulose ether (on the left), and without cellulose ether (on the right).

4 Polymer-preserving preparation of polished sections

In order to avoid the destruction of fragile polymer and cement structures in (sub-)micron dimensions, an initially liquid impregnation substance had to be found which does not dissolve or disperse the various polymer films. Additionally, the appropriate physical impregnation parameters had to be evaluated to avoid any kind of physical damaging. Experimental tests on isolated polymer films, showed that common impregnation resins attack the films. However, Polyfin (a mixture of different paraffins which is commonly used for the preparation of biological sections) proved to preserved original polymer films (Figure 4, compare with Figure 2). Polyfin has to be heated up to 75¡C to achieve suitable viscosity penetration. In this manner, the samples and Polyfin resin chips were exposed to a vacuum of 16˚mbar and heated. The resin penetrates only several mm into the sample, but fragile structures are not destroyed. Some caution is still required because the elevated temperatures can provoke an improved film formation, but, the original distribution patterns are not changed and can be analysed as such.

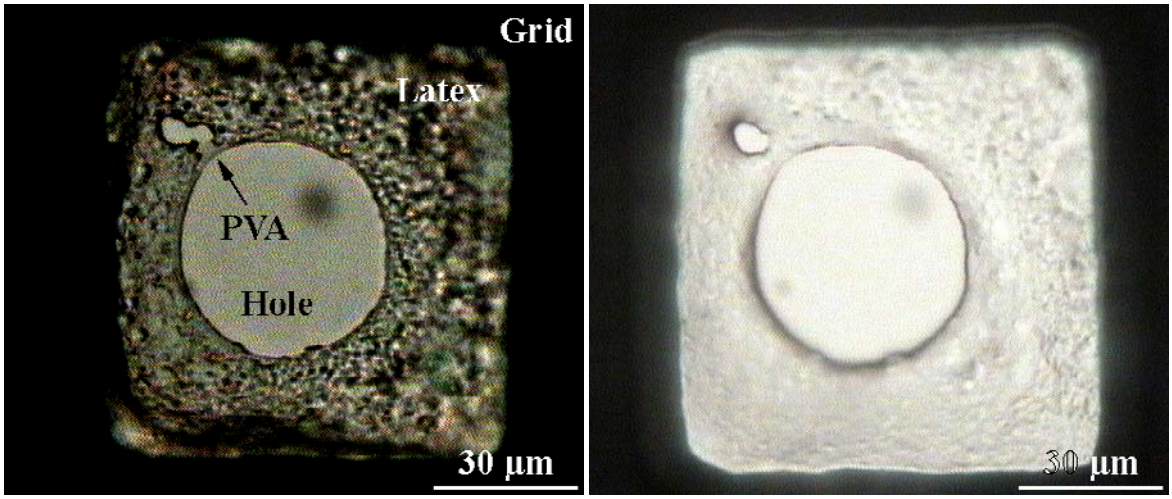

Figure 4: Latex- and polyvinyl alcohol (PVA)-films in a void of a nickel grid, before (left) and after (right) treatment with Polyfin. It does not attack any polymer structure

The hardened resin is not transparent and mechanically rather soft. Therefore it is unfortunately not suitable for the preparation of thin sections. Due to significant material contrasts between the different phases (Polyfin, mineral filler, cement, polymers), common polishing methods create topography which is unfavourable for quantitative approaches using electron microscopy. Best results were achieved with very fine sandpaper and water.

In case of the vinyl-acetate/ethylene/vinylchloride terpolymer (VA/E/VC), a mapping of Cl by element dispersive spectroscopy (EDS) can be used to visualise the polymer□s distribution. Many polymers contain no specific element or have any property that can be contrasted and imaged by any microscopical method. Therefore, different staining methods were tested.
Polyvinyl alcohol can be stained by exposition to iodine gas for 10 minutes. The iodine is caught in helix structures of the polyvinyl alcohol and can be mapped by the help of wavelength dispersive spectroscopy (WDS). The iodine distribution corresponds to the distribution of the polyvinyl alcohol.
Osmium tetroxide stains polymers containing double bonds, e.g. styrene acrylates. The polymer has to be exposed to the gas for 10 days.
As an example, element distribution maps are presented of a mortar containing cement, quartz, cellulose ether and latex (VA/E/VC) with polyvinyl alcohol as redispersion aid (Figure 5). The sample was stained with iodine. As shown by the binary images of Cl (latex) and I (polyvinyl alcohol) distribution maps, the Cl and I distribution is not identical, indicating that the polyvinyl alcohol is mobilised independently from the latex. Interestingly, the original Ca mapping showed a bimodal grey value distribution. Additional quantitative point analyses on the specific locations revealed a Ca content of about 10 and 30˚wt%. Both the bimodal grey value distribution and the differences in Ca content indicate the occurrence of two different Ca phases, interpreted as cement hydrates (10˚wt% Ca) surrounding relicts of unhydrated clinker phases (30˚wt% Ca). These facts allowed the segmentation of the two Ca phases and their visualisation as ternary image (Ca in Figure 5). Black regions containing no Ca are either air voids (marked with □V□) or quartz. Quartz grains (filler) are reflected by the Si element mapping and are shown as binary image.

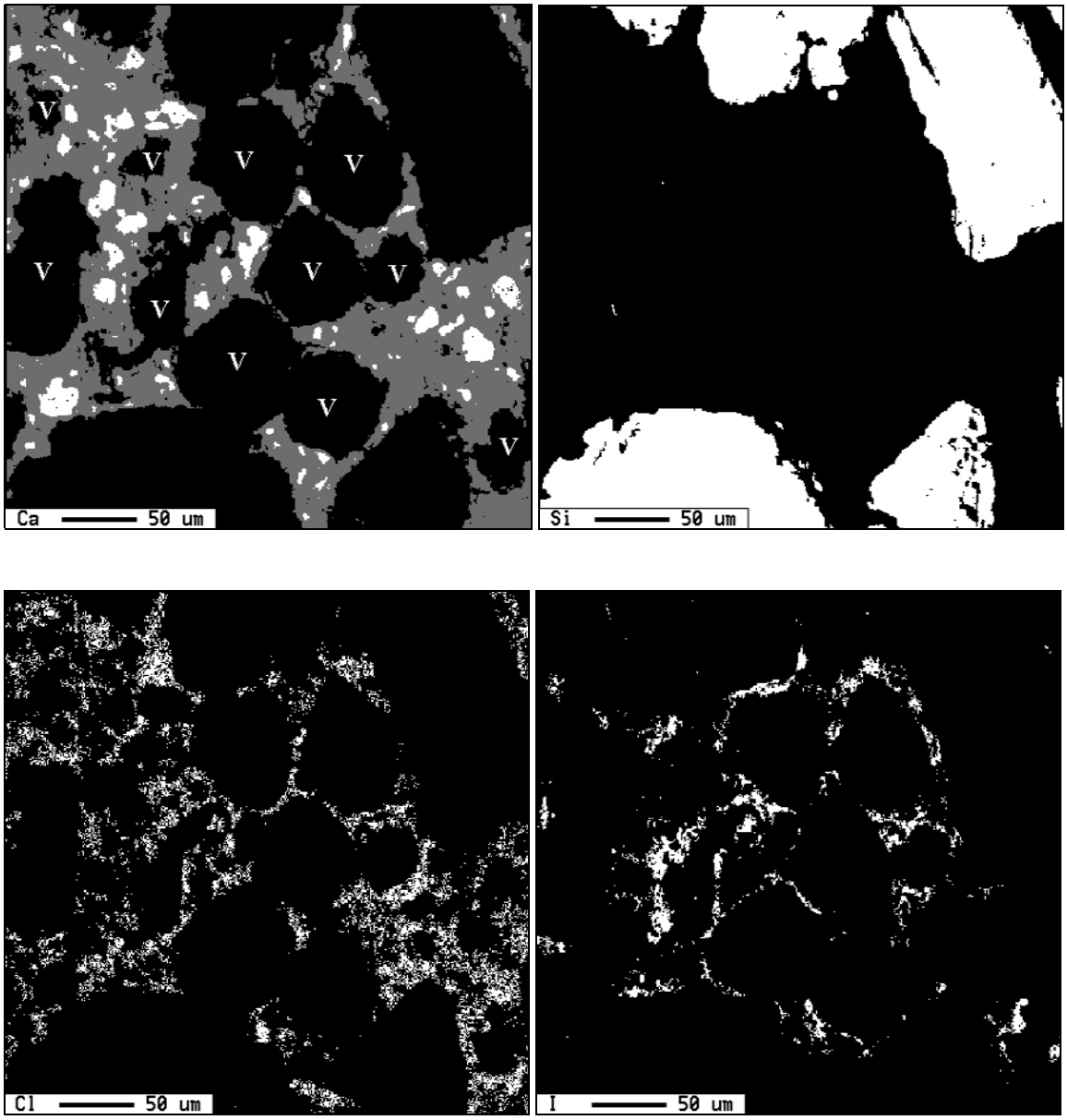

Figure 5: Electron microprobe analysis (EMPA) WDS element mappings of a polymer-modified mortar containing 6˚wt% redispersible powder (VA/E/VC) after processing to a binary (Si, Cl, I) or ternary (Ca) image. Ca: white: more than approx. 30˚wt% calcium, grey: more than approx. 10˚wt% calcium, V: air voids; Si: white: more than approx. 30˚wt% silicon; Cl: white: more than approx. 1˚wt% chlorine; I: white: more than approx. 6˚wt% iodine

5 Conclusions

We presented a method to detect, map, discriminate, and quantify the organic and inorganic phases present in a polymer-modified cement mortar. To differentiate original structures from preparation artifacts, micrographs from differentially prepared samples were compared qualitatively to microstructures of untreated specimens.

The described method combined with other staining and imaging techniques will be applied to a wider range of mortar types stored differently (dry vs wet storage). Problematic will be the long running times of SEM EDS and

EMPA WDS element mappings: a mapping with the highest possible resolution (around 1˚□m) takes up to 10˚hours.

In order to understand the physical properties, and to develop new products with specific performance profiles, the quantitative microscopy of polymer structures is regarded as an important step in the study of the entire evolution of the microfabric of such composite materials. But, quantitative microfabric analysis in submicron scale is still a challenge and holds great potential for future projects.

6 References

1 Ohama Y., □Handbook of polymer-modified concrete and mortars□, Noyes Publications, Park Ridge, New Jersey, U.S.A., 1995.

2 Zurbriggen R., □Einfluss von Dispersionspulver auf das Schwund- und Abbindeverhalten und die Gef□geentwicklung von Fliesenklebern□, 2.Seminar □Beschichtungen und Bauchemie□, Kassel, Germany, 1998, p.p. 47-62.

3 Rasband W., □Image SXM v1.6.1□, National Institutes of Health, USA, FTP:zippy.nimh.nih.gov/pub/nih-image, 1997.

5.2 Extended abstract of the oral presentation at the "3. Tagung Bauchemie", September 27/28, 2001, Würzburg, Germany

Polymerverfilmung in zementären Systemen

A. Jenni, M. Herwegh

Universität Bern, Schweiz

R. Zurbriggen

Elotex AG, Schweiz

L. Holzer

EMPA Dübendorf, Schweiz

Zusammenfassung

Verschiedene, als Additive in Zementmörteln (insbesondere Fliesenklebern) gebräuchliche Polymere wurden ausserhalb des Mörtels verfilmt. Ein Vergleich von aus deionisiertem und aus Zementwasser gezüchteten Latexfilmen hat gezeigt, dass letztere besser verfilmen. Ausserdem erwiesen sich die Zementwasser-Filme als wesentlich wasserbeständiger. Die Resultate dieser Studie konnten durch simultan durchgeführte in situ ESEM-Experimente bestätigt werden (Holzer et al. /1/).

1. Einführung

Zwecks Verbesserung der Verarbeitbarkeit und der physikalischen Endeigenschaften werden Mörtel mit Polymeren vergütet. Dabei spielt die Art und Menge des Polymers (z.B. Latex, Polyvinylalkohol, Celluloseether) sowie der Grad der Verfilmung eine massgebliche Rolle.

Das an sich schon komplexe zementäre System wird somit durch solche Polymere erweitert, die gegenseitig und mit den Zementphasen wechselwirken. Die dynamische Entwicklung solcher reaktiven Kompositmaterialien vom Zeitpunkt des Mischens bis hin zum ausgehärteten Mörtel verursacht eine Vielfalt von Mikrostrukturen. Da in diesen polyphasen Systemen die unterschiedlichen Polymerfilme und deren Bildung nur schwer untersuchbar sind (Fig. 1), wurde in einer ersten Stufe die Filmbildung in Modellexperimenten ausserhalb des Mörtels als Funktion der Zusammensetzung der wässrigen Phase studiert. Insbesondere wurden die Filme im Hinblick auf die Nasslagerung polymermodifizierter Mörtel auf ihre Wasserbeständigkeit untersucht.

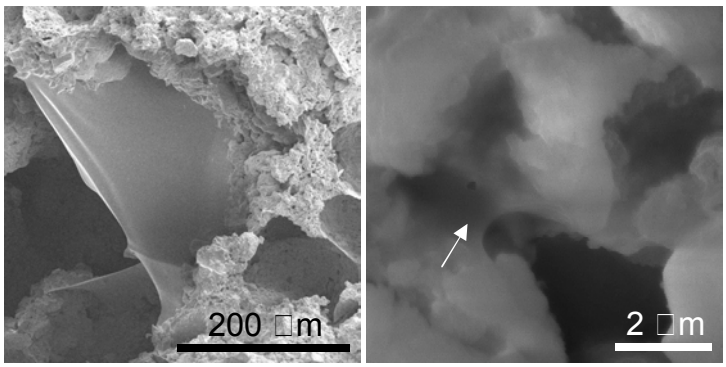

Fig. 1: Ein Polymerfilm im hoch porösen Mörtelgefüge als Trennwand zweier Luftporen (links) und in kleinerem Massstab in der Zementmatrix (rechts, Pfeil).

2. Experimentelle Anordnung

Die verschiedenen Polymere wie Latex, Polyvinylalkohol (PVA) und Celluloseether (CE) sind einerseits in deionisiertem Wasser, andererseits in Zementwasser redispergiert, bzw. gelöst (5 Minuten Ultraschall) worden. Zwei unterschiedliche Zementwässer wurden verwendet: ein synthetisch hergestelltes und ein aus einer Portlandzement-Suspension (w/z=1) abgefiltertes Zementwasser. Aus diesen Dispersionen bzw. Lösungen konnten zweierlei Proben hergestellt werden: a) Durch Aufbringen auf ein Objektglas entstehen beim Eintrocknen makroskopische Polymerfolien, welche im Vergleich zum Polymerfilm im Mörtel dicker ausfallen; b) Durch Eintauchen eines feinmaschigen Trägernetzchens (Maschengrösse ca. 100 µm) entstehen in den Maschen beim Eintrocknen dünne, gespannte, mikroskopische Polymerfilme. Die Konzentrationen wurden bewusst so gewählt, dass sich in den Filmen im Maschenzentrum beim Eintrocknen ein Loch ausbildet: dies stellt sicher, dass die Filme eine kleinstmögliche Dicke besitzen und somit in ihren Dimensionen und ihrer Entstehung am ehesten mit den Filmen im Mörtelgefüge vergleichbar sind. Die dicken Polymerfolien sind sehr einfach in ihrer Präparation und eignen sich für Labortests.

Untersuchungen der Filmstrukturen und deren zeitliche Entwicklung wurden mittels einem ESEM (Environmental Scanning Electron Microscope) durchgeführt, was ein weitgehend artefaktfreies Arbeiten ermöglichte.

Die trockenen Polymerfilme wurden auf ihre Wasserbeständigkeit hin untersucht: a) durch Eintauchen der Polymerfolien in deionisiertes Wasser und makroskopisches Beobachten, b) durch Lagern der Trägernetzchen in deionisiertem Wasser zwischen Träger- und Objektglas und Beobachten mit einem Durchlichtmikroskop. Die Wasserlagerung ist in einigen Fällen auf bis zu einen Monat ausgedehnt worden.

3. Resultate

Die Wasserbeständigkeit der makroskopischen Polymerfolien unterscheidet sich im Wesentlichen nicht von derjenigen der mikroskopischen Polymerfilme. Der Faktor Zeit ist ebenfalls von geringer Bedeutung; zeigt sich ein Film innerhalb der ersten 10 Minuten als wasserbeständig, ändert sich dies auch nach einem Monat nicht. Der Film kann aber stärker aufquellen, was seine mechanischen Eigenschaften beeinflusst.

Exemplarisch zeigt Fig. 2 a einen mikroskopischen Latexfilm (Dispersionspulver redispergiert in *deionisiertem* Wasser, verfilmt) vor Wasserkontakt und nach 10 Minuten Wasserkontakt. Der Film zerfällt beinahe vollständig. Im Gegensatz dazu bleibt der Latexfilm in Fig. 2 b (dasselbe Dispersionspulver redispergiert in *Zementwasser*, verfilmt) während der Nasslagerung unverändert.

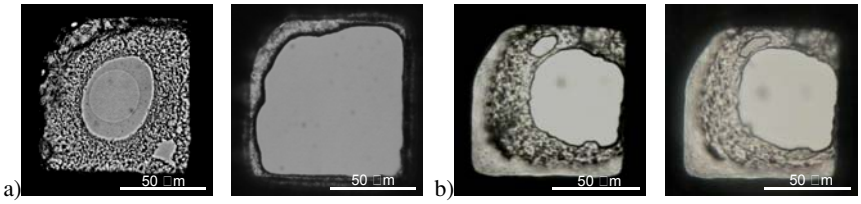

Fig. 2: a) Dispersionspulver (Latex: Ethylen/Vinylacetat/Vinylchlorid, PVA) in *deionisiertem* Wasser redispergiert und verfilmt: links vor Wasserkontakt, rechts nach 10 Minuten in deionisiertem Wasser; b) Dasselbe Dispersionspulver in *Zementwasser* redispergiert und verfilmt: links vor Wasserkontakt, rechts nach 10 Minuten in deionisiertem Wasser.

Verschiedene Latex-Typen sowie PVA und CE wurden in deionisiertem Wasser und in beiden Zementwässern redispergiert bzw. gelöst, verfilmt ("gezüchtet") und auf ihre Wasserbeständigkeit überprüft. Die Ergebnisse sind in Fig. 3 dargestellt. Die vertikale Achse zeigt eine qualitative Wasserbeständigkeit, wobei der Wert 0 einer Situation analog Fig. 2 a und der Wert 1 Fig. 2 b entspricht. Sowohl Latizes mit niedriger, als auch solche mit bereits hoher Wasserbeständigkeit (aus deionisiertem Wasser gezüchtet), werden äusserst wasserbeständig, wenn sie im zementären Milieu gebildet wurden. Das abgefilterte Zementwasser bewirkt generell eine höhere Wasserbeständigkeit als das synthetische. PVA und CE zeigen unabhängig von der Zusammensetzung der wässrigen Phase kaum eine Wasserbeständigkeit.

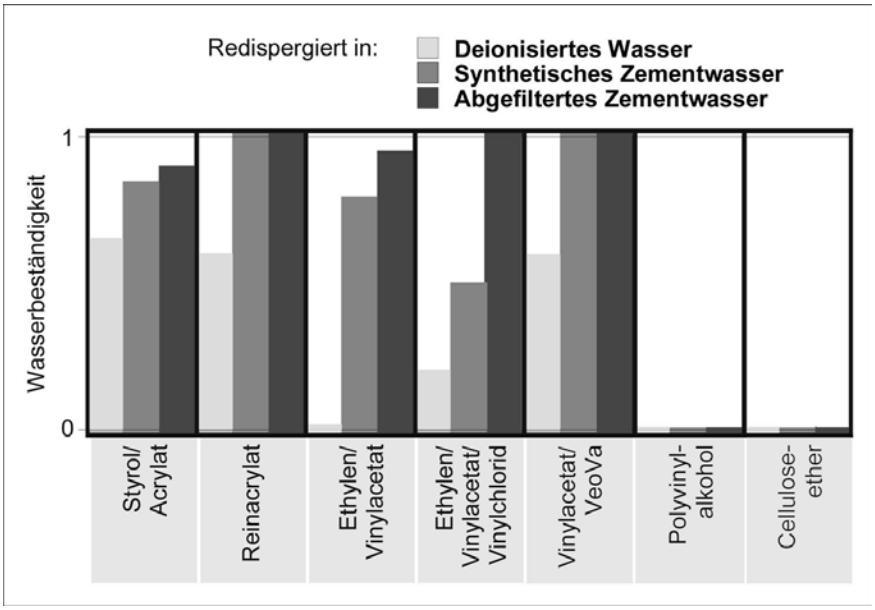

Fig. 3: Wasserbeständigkeit verschiedener Latex-Typen, sowie von PVA und CE, als Funktion der Zusammensetzung der wässrigen Phase.

4. Interpretation

Um die unterschiedliche Wasserbeständigkeit der Latexfilme erklären zu können, wurden die Mikrostrukturen der Oberfläche von Zementwasser-Filmen mit der Oberfläche von aus deionisiertem Wasser gezüchteten Filmen verglichen. Auf beiden Oberflächen sind deutlich die Kugelstrukturen der Latexpartikel erkennbar (Fig. 4), auf den Zementwasser-Filmen befinden sich zusätzlich zwischen den Partikeln zementäre Ausfällungen. In einigen Bereichen scheint sich aber das Relief der Kugeloberflächen reduziert zu haben (Fig. 5, links), was auf eine bessere Filmbildung hinweisen könnte.

Die Oberflächen von PVA-Filmen ist unabhängig vom Lösungsmittel planar. Mit dem ESEM ist keine Oberflächenstruktur ersichtlich. Oberflächen von CE-Filmen, die aus deionisiertem Wasser gezüchtet wurden, sind ebenfalls planar. Zementwasser-CE-Filme liegen

hingegen in Form eines schwammartigen Netzwerks vor (Fig. 5, rechts), diese Ausbildung kann teilweise auch an CE-Filmen direkt im Mörtelgefüge beobachtet werden.

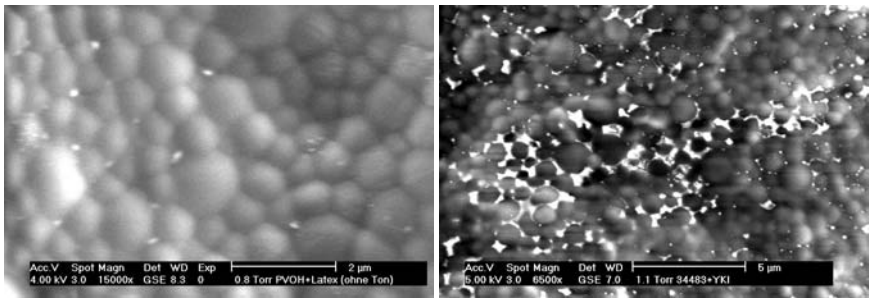

Fig. 4: ESEM-Aufnahmen (Sekundärelektronen) von Latexfilmen (Ethylen/Vinylacetat/Vinylchlorid) gezüchtet aus deionisiertem Wasser (links) und aus Zementwasser (rechts).

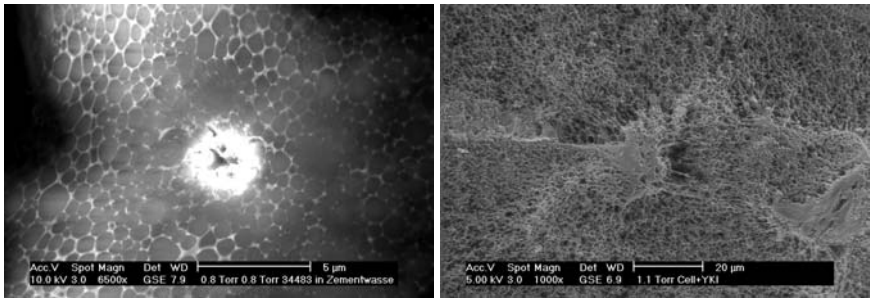

Fig. 5: ESEM-Aufnahmen (Sekundärelektronen) eines Latexfilms (Ethylen/Vinylacetat/Vinylchlorid) gezüchtet aus Zementwasser (links) und eines CE-Films, ebenfalls aus Zementwasser gezüchtet (rechts). Links im Zentrum eine Schädigung durch den Elektronenstrahl.

5. Diskussion

Zementwasserionen fördern die Filmbildung und erhöhen die Wasserbeständigkeit von Latexfilmen. Im Mörtelgefüge gebildete Latexfilme sind deshalb stationär und können nicht ausgewaschen werden. Die genaueren Wirkungsmechanismen sind noch nicht geklärt. Im Hinblick auf zukünftige Studien an Polymeren für Zementmörtel sollte berücksichtigt werden, dass Labortests an Polymerfilmen ausserhalb des Mörtelgefüges nur in "mörtelnahen" chemischen Umgebungen sinnvoll sind.

Verdankung

Mitfinanzierung durch die Kommission für Innovation und Technologie, Schweiz.

Literatur

/1/ L. Holzer, A. Jenni & R. Zurbriggen: dieser Band.

5.3 Extended abstract of the oral presentation at the "Tagung Bauchemie", September/October 30/1, 2002, Weimar, Germany

Morphologie und Innenleben von Polymer-Phasen in Zementmörteln

A. Jenni, M. Herwegh

Universität Bern, Schweiz

R. Zurbriggen

Elotex AG, Sempach Station, Schweiz

Zusammenfassung

Die Polymerstrukturen in Fliesenklebern wurden mittels Rasterelektronen-mikroskopie untersucht. In Modelmörtelsystemen modifiziert mit jeweils einem Polymerzusatz konnten charakteristische Morphologien der Polymerfilme von Latex, Polyvinylalkohol und Celluloseether beobachtet werden. Diese Kriterien können nun im realen Mörtelsystem angewandt werden, um die unterschiedlichen Poylmertypen zu unterscheiden. Zusätzlich zeigt sich, dass in diesen komplexen Systemen Latex-Zempentphasen- und Latex-Celluloseether-Kompositfilme ausgebildet werden.

1. Einführung

Seit rund 50 Jahren werden Mörtel und Beton zwecks Verbesserung der Verarbeitbarkeit und Endfestigkeit mittels Polymeren vergütet. Die dadurch hervorgerufenen Gefügeveränderungen wurden ausgiebig untersucht. Einige Arbeiten befassten sich unter anderem mit der Ausbildung der Polymerfilme /1/, /2/.

Derartige Studien, einschliesslich der Vorliegenden, wurden auf Bruchflächen durchgeführt. Ein Bruch durch ein inhomogenes Material folgt stets den vorgegebenen Schwächezonen, die z.B. besonders porenreich oder arm an Latex sind (Fig. 1). Dies führt zu einem nicht repräsentativen Erscheinungsbild der Bruchfläche, bei welchem gewisse Gefügeelmente gar verborgen bleiben können.

2. Methodik

Die Unterscheidung zwischen Polymer- und Zementphasen wurde bisher aufgrund der Oberflächenmorphologie durchgeführt, was bei gewissen Zementgelen oder bei starker Vergrösserung problematisch werden kann. In dieser Studie diente zusätzlich die unterschiedliche Elektronenstrahlresistenz im Rasterelektronenmikroskop (REM) sowie der grosse Materialkontrast zwischen Polymer und Zement als Unterscheidungskriterium.

Die untersuchten Mörtelrezepturen enthalten bis zu drei Polymertypen: Latex, Polyvinylalkohol und Celluloseether. In einem ersten Schritt wurden Mörtel mit jeweils nur einem Polymertyp untersucht. Die dabei gewonnenen Erkenntnisse dienten danach zur Diskriminierung der einzelnen Polymerphasen in komplexen Mörtelrezepturen mit allen drei Polymeren.

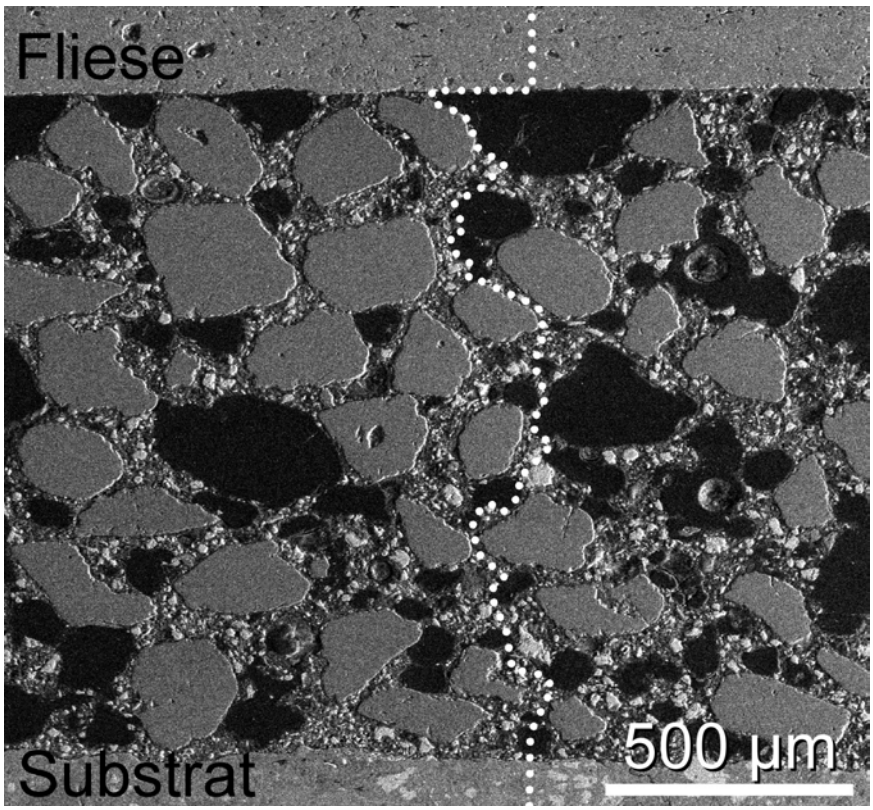

Fig. 1: Ein Bruch (punktiert) durch den inhomogenen Mörtel folgt Schwächezonen wie Poren (schwarz) und bricht beispielsweise die Zementmatrix nicht bei kohäsiven Latexstrukturen auf.

3. Resultate und Interpretation

Die Latex-, Polyvinylalkohol- und Celluloseetherstrukturen sind in Fig. 2-4 abgebildet. Insbesondere Latexfilme (homogene Oberfläche im Sekundärelektronenbild, Fig. 6) bestehen in ihrem Inneren zu einem beachtlichen Teil aus Zementphasen, welche im Rückstreuelektronenbild klar ersichtlich sind (Fig. 7). Ebenso neigen verschiedene Polymere dazu, untereinander Polymer-Kompositfilme auszubilden (Fig. 5).

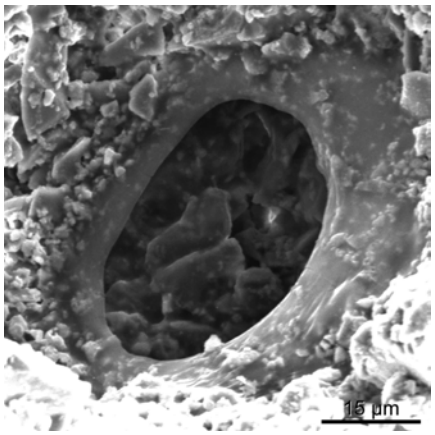

Fig. 2: Massiger Latexfilm (REM Sekundärelektronenbild)

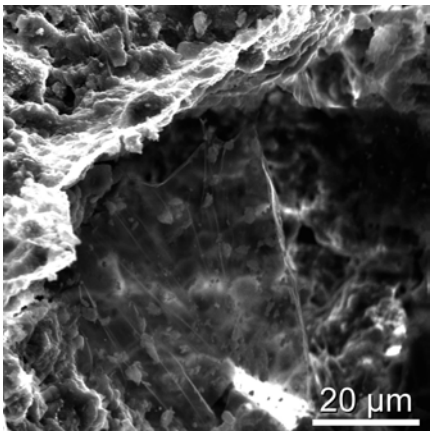

Fig. 3: Segelartiger Celluloseetherfilm (REM Sekundärelektronenbild)

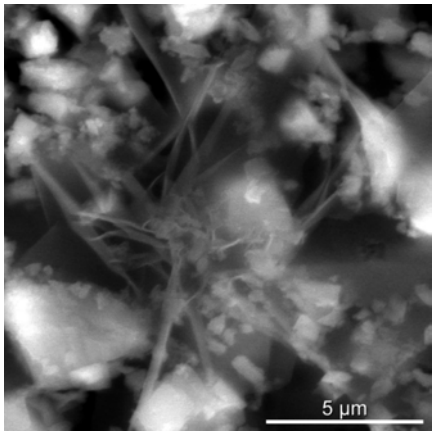

Fig. 4: Polyvinylalkoholfilm (REM Sekundärelektronenbild)

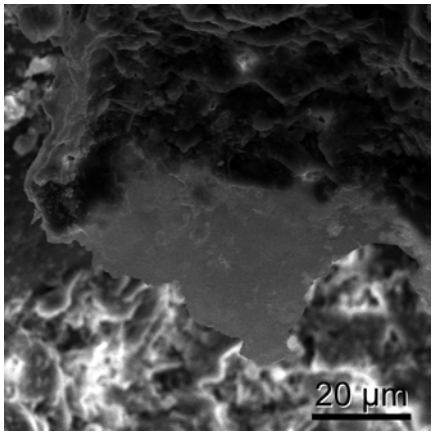

Fig. 5: Latex-Celluluseether-Kompositfilm (REM Sekundärelektronenbild)

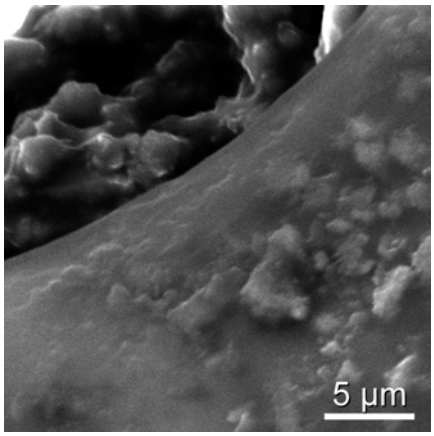

Fig. 6: Vergrösserter Ausschnitt aus Fig. 2 (REM Sekundärelektronenbild)

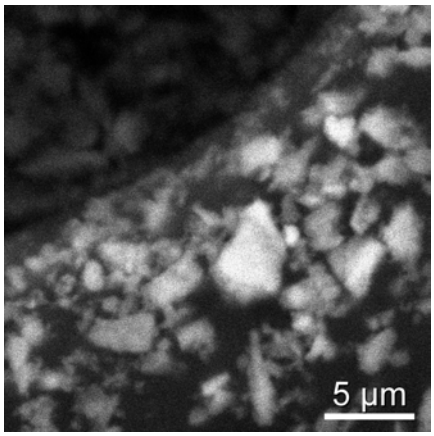

Fig. 7: Gleicher Ausschnitt wie Fig. 6 (REM Rückstreuelektronenbild)

4. Diskussion

Die neuen Erkenntnisse helfen einerseits, verschiedene Polymere in Mörteln zu differenzieren (REM), andererseits liefern sie Rückschlüsse über die Entstehung und zeitliche Entwicklung der Polymerphasen /3/ sowie ihre Interaktion mit den Zementmineralen.

Verdankung

Wir verdanken die finanzielle Unterstützung durch die Kommission für Innovation und Technologie (Schweiz).

Literatur

/1/ Z. Su: Diss. Univ. Delft (1995)

/2/ K. Tubbesing: Diss. Tech. Univ. Hamburg-Harburg (1993)

/3/ R. Zurbriggen, A. Jenni: dieser Band

References

Afridi, M.U.K., Ohama, Y., Iqbal, M.Z. & Demura, K. 1995. Water Retention and Adhesion of Powdered and Aqueous Polymer-Modified Mortars. *Cement and Concrete Composites* **17**, 113-118.

Ball, H. & Wackers, M. 2001. Long-term durability of naturally aged GFRC mixes containing Forton polymer. *GRC congress*, Dublin, 83-97.

Bijen, J., Schlangen, E. & Salet, T. 1999. Modelling of effects of schrinkage on the performance of adhesives. *Adhesion between Polymers and Concrete. 2nd International RILEM Symposium ISAP '99* PRO **9**. RILEM, Cachan Cedex, France, 299-310.

Chandra, S. & Flodin, P. 1987. Interactions of polymers and organic admixtures on portland cement hydration. *Cement and Concrete Research* **17**, 875-890.

Chen, J.J., Zampini, D. & Walliser, A. 2002. High-pressure epoxy-impregnated cementitious materials for microstructure characterization. *Cement and Concrete Research* **32**, 1-7.

Chevalier, Y., Pichot, C., Graillat, C., Joanicot, M., Wong, K., Maquet, J., Lindner, O. & Cabane, B. 1992. Film formation with latex particles. *Colloid Polymer Science* **270**, 806-821.

Cook, R.A. & Hover, K.C. 1999. Mercury porosimetry of hardened cement pastes. *Cement and Concrete Research* **29**, 933-943.

De Belder, A.N. & Granath, K. 1973. Preparation and properties of fluorescein-labelled dextrans. *Carbohydrate Research* **30**, 375-378.

Du Chesne, A., Bojkova, A., Gapinski, J., Seip, D. & Fischer, P. 2000. Film formation and redispersion of waterborne latex coatings. *Journal of Colloid and Interface Science* **224**, 91-98.

Franke, B. 1941. Bestimmung von Calciumoxid und Calciumhydroxid nebem wasserfreiem und wasserhaltigem Calciumsilicat. *Zeitschrift für anorganische und allgemeine Chemie* **241**, 180-184.

Goldstein, J.I., Newbury, D.E., Echlin, P., Joy, D.C., Romig, A.D., Lyman, C.E., Fiori, C. & Lifshin, E. 1992. *Scanning Electron Microscopy and X-Ray Microanalysis*. Plenum Press, New York.

Hayat, M.A. 1993. *Stains and Cytochemical Methods*. Plenum Press, New York, London.

Holzer, L., Jenni, A. & Zurbriggen, R. 2001. Eine in-situ ESEM-Studie über mikrostrukturelle Veränderungen polymervergüteter Mörtel während der Wasserlagerung. *3. Tagung Bauchemie* (edited by Hiller, W. & Jovovic, N.). *Bauchemie von der Forschung bis zur Praxis* **24**. GDCh-Fachgruppe Bauchemie, Würzburg, 156-159.

Holzer, L., Winnefeld, F., Kägi, R. & Zampini, D. 2003. Towards an integral understanding of the early cement hydration - a multi-method approach. *11th International Congress on the Chemistry of Cement ICCC*, Durban, Rep. of South Africa.

Huijs, F. & Lang, J. 2000. Morphology and film formation of poly(butyl methacrylate)-polypyrrole core-shell latex particle. *Colloid Polymer Science* **278**, 746-756.

Jain, N. 2002. Influence of spray drying onto powder performance. Elotex AG, Sempach Station, Switzerland.

Jenni, A., Herwegh, M. & Zurbriggen, R. 2002. Morphologie und Innenleben von Polymer-Phasen in Zementmörteln. *Tagung Bauchemie*. GDCh-Fachgruppe Bauchemie, Weimar.

Jenni, A., Herwegh, M., Zurbriggen, R. & Holzer, L. 2001a. Polymerverfilmung in zementären Systemen. *3. Tagung Bauchemie* (edited by Hiller, W. & Jovovic, N.). *Bauchemie von der Forschung bis zur Praxis* **24**. GDCh-Fachgruppe Bauchemie, Würzburg, 92-97.

Jenni, A., Herwegh, M., Zurbriggen, R. & Holzer, L. 2001b. Sample Preparation of Polymer-Modified High-Porous Mortars for Quantitative Microfabric Analysis. *8th Euroseminar on Microscopy Applied to Buildings Materials* (edited by Georgali, B.), Athens, Greece, 571-578.

Justnes, H., Reynaers, T. & Van Zundert, W. 1999. Dimensional changes of polymer cement mortars based on latices and redispersible polymer powders due to moisture transport. *Adhesion between Polymers and Concrete. 2nd International RILEM Symposium ISAP '99* **PRO 9**. RILEM, Cachan Cedex, France, 475-483.

Keddie, J.L. 1997. Film formation of latex. *Materials Science & Engineering R: Reports* **21**. Elsevier, 101-170.

Kim, J.H. & Robertson, R.E. 1998. Effects of Polyvinyl Alcohol on Aggregate-Paste Bond Strength and the Interfacial Transition Zone. *Advances in Cement Based Materials* **8**, 66-76.

Kjellsen, K.O. & Detwiler, R.J. 1992. A quantitative S.E.M. image analysis of cement paste microstructure. *Microscopy and image analysis of building materials* (edited by Raivio, P.). *VTT SSymposium* **136**. Technical Research Centre of Finland (VTT), Building Materials Laboratory, Espoo, Finland, 28-40.

Knöfel, D., Stephan, D. & Zurbriggen, R. 1998. Hydratationsverhalten polymermodifizierter Mörtel. Elotex AG, Sempach Station, Switzerland

Koenders, E.A.B. 1997. Simulation of volume changes in hardening cement-based materials. Thesis, Technische Universiteit Delft.

Krenkler, K. 1980. *Chemie des Bauwesens*. Springer Verlag, Berlin, Heidelberg.

Larbi, J.A. & Bijen, J.M.J.M. 1990. Interaction of polymers with portland cement during hydration: a study of the chemistry of the pore solution of polymer-modified cement systems. *Cement and Concrete Research* **20**, 139-147.

Lefebure, V. 1924. British Patent No. 217, **279**, Great Britain.

Lu, Z. & Zhou, X. 2000. The waterproofing characteristics of polymer sodium carboxymethyl-cellulose. *Cement and Concrete Research* **30**, 227-231.

Lunk, P.T.H.G. 1997. Kapillares Eindringen von Wasser und Salzlösungen in Beton. Thesis, ETH.

Odler, I. & Strassinopoulus, E.N. 1982. Über die Zusammensetzung der Porenflüssigkeit hydratisierter Zementpasten. *TZI-Fachberichte* **106**, 394-401.

Ohama, Y. 1987. Principle of Latex Modification and Some Typical Properties of Latex-Modified Mortars and Concretes. *ACI Materials Journal* **84**, Detroit, 511-518.

Ohama, Y. 1995. *Handbook of polymer-modified concrete and mortars, properties and process technology*. Noyes Publications, Park Ridge, New Jersey, USA.

Rasband, W. & Barret, S. 1997. Image SXM. National Institutes of Health, USA, http://rsb.info.nih.gov/nih-image/, Liverpool, UK.

RILEM Committee CPC-18. 1988. Measurement of hardened concrete carbonation depth. *Mater. Struct.* **18**, 453-455.

Rodger, S.A., Brooks, S.A., Sinclair, W., Groves, G.W. & Double, D.D. 1985. High strength cement pastes. Part2: Reactions during setting. **20**, 2853-2860.

Rost, F.W.D. 1991. *Quantitative fluorescence microscopy*. University Press, Cambridge, Great Britain.

Routh, A.F. & Russel, B.R. 1999. A Process Model for Latex Film Formation: Limiting Regimes for Individual Driving Forces. *Langmuir* **15**. American Chemical Society, 7762-7773.

Schulze, J. 1985. Redispersionspulver in Zement. *Tonindustrie-Zeitung* **109**, 698-703.

Schulze, J. 1999. Influence of water-cement ratio and cement content on the properties of polymer-modified mortars. *Cement and Concrete Research* **29**, 909-915.

Schulze, J. & Killermann, O. 2001. Long-term performance of redispersible powders in mortars. *Cement and Concrete Research* **31**, 357-362.

Schweizer, D. 1997. The role of cellulose ethers in gypsum machine plaster. *ConChem*, Düsseldorf, 227-234.

Scrivener, K.L., Patel, H.H., Pratt, P.L. & Parrott, L.J. 1986. Analysis of phases in cement paste using backscattered electron images, methanol adsorption and thermogravimetric analysis. *Microstructural Development During Hydration of Cement* (edited by Struble, L. J. & Brown, P. W.). *Materials Research Society Symposium Proceedings* **85**. Materials Research Society, Boston, USA, 67-76.

Silva, D.A., John, V.M., Ribeiro, J.L.D. & Roman, H.R. 2001. Pore size distribution of hydrated cement pastes modified with polymers. *Cement and Concrete Research* **31**, 1177-1184.

Silva, D.A., Roman, H.R. & Gleize, P.J.P. 2002. Evidences of chemical interaction between EVA and hydrating Portland cement. *Cement and Concrete Research* **32**, 1383-1390.

Simmons, S. & Thomas, E.L. 1998. The use of transmission electron microscopy to study the blend morphology of starch/ poly(ethylene-co-vinyl alcohol) thermoplastics. *Polymer* **39**. Elsevier Science Ltd., Great Britain, 5587-5599.

Song, L., Hennink, E.J., Young, I.T. & Tanke, H.J. 1995. Photobleaching Kinetics of Fluorescein in Quantitative Fluorescence Microscopy. *Biophysical Journal* **68**, 2588-2600.

Stark, J., Dimmig, A. & Müller, S. 2001. Interactions between polymer and cement. *Beton und Fertigteil-Technik*, 40-49.

Stark, J., Möser, B. & Eckart, A. 2000. Neue Aspekte der Zementhydratation. *14. Internationale Baustofftagung ibausil* (edited by Fischer, H.-B.) **1**. Stark, J., Weimar, Deutschland, 1093-1109.

Stark, J. & Wicht, B. 2000. *Zement und Kalk: der Baustoff als Werkstoff*. Birkhäuser, Basel.

Su, Z. 1995. Microstructure of polymer cement concrete. Thesis, Delft University of Technology.

Su, Z., Sujata, K., Bijen, J.M.J.M., Jennings, H.M. & Fraaij, A.L.A. 1996. The Evolution of the Microstructure in Styrene Acrylate Polymer-Modified Cement Pastes at the Early Stage of Cement Hydration. *Advances in Cement Based Materials* **3**, 87-93.

Taylor, H.F.W. 1997. *Cement chemistry*. Thomas Telford Publishing, London.

Tubbesing, K. 1993. Mikrostruktur von PCC : Gefügeuntersuchungen an polymermodifizierten Zementsteinen. Thesis, Technische Universität Hamburg-Harburg.

West, C.D. 1948. Structure-Optical Studies. II. Aqueous Dispersion of Polyvinyl Borate-Iodine and Its Heat of Formation. *The Journal of Chemical Physics* **17**. American Institute of Pyhsics, Melville, New York, 219-220.

Yang, R. & Buenfeld, N.R. 2001. Binary segmentation of aggregate in SEM image analysis of concrete. *Cement and Concrete Research* **31**, 437-441.

Zurbriggen, R. 1998a. Einfluss von Dispersionspulver auf das Schwund- und Abbindeverhalten und die Gefügeentwicklung von Fliesenklebern, Kassel, Deutschland, 47-62.

Zurbriggen, R. 1998b. Influence of redespersible powders on shrinkage, hydration behavior and micro-structure of tile adhesives. *2. Seminar: Beschichtung und Bauchemie*, Kassel, Germany, 47-62.

Zurbriggen, R. 2001. Investigation of the segragation behavior of different mortar constituents with TGA/SDTA. *UserCom (Information for users of METTLER TOLEDO thermal analysis systems)* **13**, 9-11.

Zurbriggen, R. & D., S. 2000. Flexibilität, Scherfestigkeit, Schwund, Hydratationsgrad und Porenverteilung nach 10 Trocken/Nass-Zyklen. Elotex AG, Sempach Station, Switzerland.

Zurbriggen, R. & Jenni, A. 2002. Lichtmikroskopische in-situ Experimente zur Filmbildung von Polymeren in zementären Systemen. *Tagung Bauchemie*. GDCh-Fachgruppe Bauchemie, Weimar.

Curriculum Vitae

ANDREAS JENNI

WINTERMATTWEG 11 - 3018 BERN • SWITZERLAND

PHONE +41 31 991 27 40 • E-MAIL: ANDREAS.JENNI@GEO.UNIBE.CH

- Marital status: single
- Nationality: Swiss
- Date of Birth: 30/01/1973
- Place of Origin: Escholmatt (CH)
- Parents: Ute and Eugen Jenni

EDUCATION

1980 - 1984	Primary School	Bern (CH)
1984 - 1986	Secondary School	Bern (CH)
1986 - 1993	High School (Gymnasium Neufeld)	Bern (CH)
1994 - 1999	University of Bern	Bern (CH)

lic. phil. nat.

- Structural Geology
- Diploma: „Geologie der Doldenhorn-Decke und des Bergsturzes im Gebiet Gspaltenhorn-Spitzhorn (BE)“

2000 – 2003 University of Bern Bern (CH)

Ph.D.

- Thesis: „Microstructural evolution and physical properties of polymer-modified mortars“

LANGUAGES

- Native language: German
- Foreign Languages: English, French

PROFESSIONAL EXPERIENCE

1997 - 1999 Junior Assistant University of Bern (CH)

Institute of Geology

- Teaching

1998 Junior Assistant University of Bern (CH)

Institute of Mineralogy

- Lithological characterisation of the Piora-Mulde (AlpTransit)

1999 Programmer University of Bern (CH)
Deanery of the phil.nat. Faculty
- Database programming

1999 – 2000 Assistant University of Bern (CH)
Institute of Geology
- Scanning electron microscope maintenance

2000 - 2002 Assistant University of Bern (CH)
Institute of Geology
- Teaching

STAY ABROAD

1993 - 1994 Informative Trip Australia

1999 - 2000 Informative Trip Spain, Marocco, Mali